

AD-A166 086

12

DNA-TR-84-379

DEVELOPMENT AND TESTING OF ADAPTIVE HF RADIO TECHNIQUES

**John W. Ames
Norman J. F. Chang
Thomas D. Magill
SRI International
333 Ravenswood Avenue
Menlo Park, CA 94025-3434**

1 October 1984

Technical Report

CONTRACT No. DNA 001-80-C-0253

Approved for public release;
distribution is unlimited.

THIS WORK WAS SPONSORED BY THE DEFENSE NUCLEAR AGENCY
UNDER RDT&E RMSS CODES B322080464 S99QAXHB05313 H2590D
AND B322083466 S99QMXBB00021 H2590D.

**Prepared for
Director
DEFENSE NUCLEAR AGENCY
Washington, DC 20305-1000**

**DTIC
ELECTE
APR 10 1986
E**

DTIC FILE COPY

86 1 24 001

UNCLASSIFIED
SECURITY CLASSIFICATION OF THIS PAGE

AR-066086

Form Approved
OMB No. 0704-0183
Exp. Date: Jun 30, 1986

REPORT DOCUMENTATION PAGE

1a. REPORT SECURITY CLASSIFICATION UNCLASSIFIED			1b. RESTRICTIVE MARKINGS			
2a. SECURITY CLASSIFICATION AUTHORITY N/A since Unclassified			3. DISTRIBUTION/AVAILABILITY OF REPORT Approved for public release; distribution is unlimited.			
2b. DECLASSIFICATION/DOWNGRADING SCHEDULE N/A since Unclassified						
4. PERFORMING ORGANIZATION REPORT NUMBER(S) SRI Project 1856			5. MONITORING ORGANIZATION REPORT NUMBER(S) DNA-TR-84-379			
6a. NAME OF PERFORMING ORGANIZATION SRI International	6b. OFFICE SYMBOL (if applicable)		7a. NAME OF MONITORING ORGANIZATION Director Defense Nuclear Agency			
6c. ADDRESS (City, State, and ZIP Code) 333 Ravenswood Avenue Menlo Park, CA 94025-3434			7b. ADDRESS (City, State, and ZIP Code) Washington, DC 20305-1000			
8a. NAME OF FUNDING/SPONSORING ORGANIZATION	8b. OFFICE SYMBOL (if applicable)		9. PROCUREMENT INSTRUMENT IDENTIFICATION NUMBER DNA 001-80-C-0253			
8c. ADDRESS (City, State, and ZIP Code)			10. SOURCE OF FUNDING NUMBERS			
			PROGRAM ELEMENT NO. 62715H	PROJECT NO. S99QAXH S99QMXB	TASK NO. B B	WORK UNIT ACCESSION NO. DH004887
11. TITLE (Include Security Classification) DEVELOPMENT AND TESTING OF ADAPTIVE HF RADIO TECHNIQUES						
12. PERSONAL AUTHOR(S) Ames, John W. Chang, Norman J. F. Magill, Thomas D.						
13a. TYPE OF REPORT Technical Report	13b. TIME COVERED FROM 800701 TO 840930		14. DATE OF REPORT (Year, Month, Day) 841001		15. PAGE COUNT 120	
16. SUPPLEMENTARY NOTATION This work was sponsored by the Defense Nuclear Agency under RDT&E RMSS Codes B322080464 S99QAXHB05313 H2590D and B322083466 S99QMXBB00021 H2590D.						
17. COSATI CODES			18. SUBJECT TERMS (Continue on reverse if necessary and identify by block number)			
FIELD 17	GROUP 2.1	SUB-GROUP	Adaptive High-Frequency Radio, Oblique Ionograms, HF Radio Communications, SELSCAN, AHF.			
19. ABSTRACT (Continue on reverse if necessary and identify by block number) <p>→ The Rockwell Collins SELSCAN adaptive high-frequency (HF) radio system, using an Air Force AN/ARC-190 transceiver, was operated over a 2615-km temperate latitude path for 24 hours. Propagation was monitored by an FMCW chirp oblique sounder. Voice and data transmissions were used to assess the quality of the selected channels. The SELSCAN always found a usable channel, and usually a very good one, even when propagation was limited to a small range of frequencies. A parallel effort to develop a test bed for experimentation with alternative probing waveforms is described. Results are incomplete because of difficulties with equipment and software. A theoretical analysis of probing waveforms for use with adaptive HF systems is presented. Finally, some recommendations are made for the application of adaptive HF.</p>						
20. DISTRIBUTION/AVAILABILITY OF ABSTRACT <input type="checkbox"/> UNCLASSIFIED/UNLIMITED <input checked="" type="checkbox"/> SAME AS RPT. <input type="checkbox"/> DTIC USERS			21. ABSTRACT SECURITY CLASSIFICATION UNCLASSIFIED			
22a. NAME OF RESPONSIBLE INDIVIDUAL Betty L. Fox			22b. TELEPHONE (Include Area Code) (202) 325-7042		22c. OFFICE SYMBOL DNA/STTI	

DD FORM 1473, 84 MAR

83 APR edition may be used until exhausted.
All other editions are obsolete.

SECURITY CLASSIFICATION OF THIS PAGE

UNCLASSIFIED

PREFACE

Permission to use the Churchill site was arranged by D. R. Tindall and K. E. Hooley of the Canadian Government Department of Communications, Communications Research Center. Assistance at the site was provided by Bob Cameron.

The SELSCAN equipment was provided by Rockwell/Collins Defense Communications Division in Cedar Rapids, Iowa. Arrangements for use of the SELSCAN equipment were made by several people at Collins, including Robert Sternowski, James Harmon, and Daniel Hawthorne. Richard Forrester operated the equipment. David Bliss, who is responsible for much of the SELSCAN design, helped make the experiment work.

The AN/ARC-190 transceivers were provided by the Air Force Logistics Command.

Archibald McKinley integrated the SELSCAN experimental equipment, including the ARC-190, the antenna, the SELSCAN, and the ionogram and recording equipment.

Most of the test operations at SRI were conducted by Charles Code, with help from John Buonocore.

Steven Ohriner did most of the detailed design and testing of the AHF test-bed hardware and software, along with Norman Chang.

Accession For	
NTIS GRA&I	<input checked="checked" type="checkbox"/>
DTIC TAB	<input type="checkbox"/>
Unannounced	<input type="checkbox"/>
Justification	
By	
Distribution/	
Availability Codes	
Dist	Avail and/or Special
A-1	



TABLE OF CONTENTS

<u>Section</u>	<u>Page</u>
PREFACE.	1
LIST OF ILLUSTRATIONS	4
LIST OF TABLES	6
1 INTRODUCTION	7
2 SIGNALING APPROACH IN THE EXPERIMENTAL (TEST-BED) EQUIPMENT	9
3 EARLY MEASUREMENTS	14
3.1 Short Path.	14
3.2 Long Auroral Path	14
4 SELSCAN MEASUREMENTS.	17
4.1 Objectives	17
4.2 Experimental Arrangements.	17
4.2.1 Sounder	17
4.2.2 SELSCAN	22
5 OBSERVATIONS.	26
6 CONCLUSIONS FROM THE EXPERIMENT	46
7 APPROACHES TO MITIGATING PROPAGATION DISTURBANCES . . .	48
8 CONCLUSIONS	51
REFERENCES.	52
 <u>Appendix</u>	
A ENCODER-DECODER-CONTROLLER DESIGN FOR THE ADAPTIVE AUTOMATIC HF RADIO	A-1
B CURRENT STATUS OF THE HARDWARE AND SOFTWARE OF THE AHF TEST BED	B-1

TABLE OF CONTENTS (Concluded)

Appendix

C	THEORETICAL ANALYSIS OF PROBING SIGNAL.	C-1
D	RELATIVE SENSITIVITY OF BFSK AND BDPSK TO FREQUENCY SPREAD	D-1
E	BER MEASUREMENT	E-1

LIST OF ILLUSTRATIONS

<u>Figure</u>		<u>Page</u>
1	Selective Call Detection Functional Diagram.	11
2	Compressed Calling Signal.	12
3	Churchill-Los Banos Oblique Ionogram for 23 September 1983 at 2312 UT	15
4	Menlo Park Antenna	19
5	CHIRP Receiver and Recorder.	21
6	SELSCAN/ARC-90 Experimental System	23
7	Summary of Propagation and SELSCAN Channel Selection.	27
8	Data for 1930 UT (1230-hr Midpath), 26 June 1984	29
9	Data for 2100 UT (1400-hr Midpath), 25 June 1984	32
10	Data for 0000 UT (1700-hr Midpath), 15 June 1984	33
11	Data for 0330 UT (2030-hr Midpath), 15 June 1984	34
12	Data for 0530 UT (2230-hr Midpath), 20 June 1984	36
13	Data for 0700 UT (Midnight Midpath), 20 June 1984. . . .	37
14	Data for 0930 UT (0230-hr Midpath), 20 June 1984	38
15	Data for 1000 UT (0300-hr Midpath), 20 June 1984	39
16	Data for 1140 UT (0440-hr Midpath), 14 June 1984	41
17	Data for 1330 UT (0630-hr Midpath), 14 June 1984	42
18	Data for 1600 UT (0900-hr Midpath), 26 June 1984	43
19	Data for 1730 UT (1030-hr Midpath), 26 June 1984	45
A-1	System Block Diagram of Three Adaptive HF Radio.	A-2
A-2	Timing for Call Sequence Showing Transmission of N ID Word Groups in Two Channels.	A-6
A-3	Flowchart for LISTEN Mode.	A-7
A-4	SCC Functional Block Diagram	A-9
A-5	PSK Modulator.	A-10
A-6	Synchronous Demodulator.	A-12

LIST OF ILLUSTRATIONS (Concluded)

<u>Section</u>		<u>Page</u>
A-7	Chip Synchronizer.	A-14
A-8	Functional Block Diagram	A-16
B-1	Block Diagram of the Adaptive Radio System	B-2
B-2	Block Diagram of the Adaptive Radio Controller	B-3
B-3	Bench Test Connections	B-8
C-1	Autocorrelation Functions of (a) Ideal PN Sequence and (b) Ideal Band-Limited White Noise	C-13
C-2	Autocorrelation Function for Four-Level PN Sequence with Delay of Three-Quarter Chip for Weighting Factors of (a) 0.5 and (b) 0.25	C-16
C-3	Autocorrelation Function for Four-Level PN Sequence with Delay of One-Half Chip for Weighting Factors of (a) 0.5 and (b) 0.25	C-17
C-4	Autocorrelation Function for Four-Level PN Sequence with Delay of One-Quarter Chip for Weighting Factors of (a) 0.5 and (b) 0.25	C-18
C-5	Block Diagram of Quasi-Coherent Multipath Phase- Reference Reconstruction System and Detector.	C-21
C-6	Block Diagram of Phase-Comparison Detection System.	C-22
C-7	Block Diagram of Digitally Implemented Phase- Comparison Detection System	C-24

LIST OF TABLES

<u>Table</u>	<u>Page</u>
1 Overall Rating for Telephony.	30
C-1 Present System Sounding Characteristics	C-8
C-2 Known Barker Sequences and Their Characteristics.	C-10
C-3 Auto Correlation Characteristics of Six Four-Level PN Sequences.	C-19
D-1 Power Loss (dB) as a Function of Frequency Offset for BKPSK and PFSK.	D-1
D-2 Relative Power Requirements (dB) for a Given Bit Error Rate for BDPSK and BFSK as a Function of Frequency Offset Error.	D-2

SECTION 1

INTRODUCTION

The concept of an adaptive automatic high-frequency (HF) radio was proposed in 1980 by Chang, Ames, and Smith.^{1*} The objective was to provide an HF radio link that could be operated by relatively untrained personnel with good reliability (connectivity) in the presence of propagation uncertainty and lack of precise timing or prearrangement. The sense in which such a system is adaptive is that an operating frequency is selected so that it is at least adequate for each exchange of traffic, which is assumed to last not more than a few minutes or tens of minutes. This may be contrasted with a system that adapts other parameters such as modulation or data rate or that spreads a signal over the entire HF spectrum redundantly so that the message can be reconstructed if there is any propagation. The specific manner in which the link adapts is that idle receivers scan continually through a set of defined channels listening for a coded call, and that calling stations transmit such a call while scanning through the same channels at a rate that is slow enough so that a receiver can be expected to scan through all the channels while the transmitter is on one.

The Chang et al.¹ report outlined a design of hardware and software to perform the adaptive radio function, a design for an experiment to test the concept, and some of the details for signal design for the selective calling function. At about the time that tasking was approved to proceed with this work, the Collins Radio Company announced a new developmental product that they termed SELSCAN, for SElective SCANning, which incorporates the same basic ideas, with at least one significant improvement. The DNA program was to include tests using SELSCAN in combination with the newly available Air Force AN/ARC-190 HF transceiver, which is also made by Collins.

*References are listed at the end of this report.

This report describes the experimental equipment developed at SRI International, termed the AHF Test Bed; on-the-air tests using it and the SELSCAN; and a general analysis of the factors influencing the performance of calling signals. The results and conclusions reported here are expected to be useful in planning for and designing adaptive HF radio links for use at times of poor or disturbed propagation caused by natural or man-made phenomena.

Section 2 provides a brief description of the basic principles of the test-bed hardware and software. A more complete description of the operation of the hardware is contained in Appendices A and B, and in the Chang et al.¹ reference.

Section 3 briefly summarizes the results of the development and on-the-air operation of the test-bed equipment. Unexpected delays in developing both the hardware and software prevented these tests from yielding practical results. The test program also used the Air Force/Collins ARC-190 SELSCAN combination, with results as described in Sections 4 and 5.

Conclusions and approaches to mitigating propagation disturbances complete the body of the report in Sections 6 through 8.

SECTION 2

SIGNALING APPROACH IN THE EXPERIMENTAL (TEST-BED) EQUIPMENT

The technical work on this project concentrated on the problems of signaling and of detecting probing signals. The logic of scanning through potential channels, being a more straightforward problem with less need for development, received less attention, although we implemented a simple scanning process for practical on-the-air experiments.

The heart of an adaptive radio system that automatically finds a workable propagating channel is the probing waveform and the means by which it is detected. This process must be efficient in order for the calling procedure to complete a scan through the available channels in a reasonable time. Because the calling station must transmit on each channel long enough for receivers to sample all channels, the time to establish contact is proportional to the square of the number of channels and to the time that a receiver must dwell on each channel. The detection process, therefore, should not depend on long synchronizing sequences or on time diversity to operate through multipath fading. To gain freedom from these factors, our test bed transmits a phase-coded probe signal that is intended to resist fading and suppress moderate interference.

In the test bed, the signal is transmitted as a Barker code that is detected in a continuously operating digital/analog delay line (shift register) that constitutes a filter matched to the code. In the first implementation of the test bed, the phase transitions were first detected in a Costas phase-locked loop. The phase transitions were encoded such that marks and spaces were of the opposite polarity after the signals were decoded. Because the transmitter and the receiver operated asynchronously, each information code group was preceded by a preamble to establish the sense and the start of the code. The present implementation dispenses with the polarity requirement by using off-on keying. The compressed pulses, after being detected in in-phase and

quadrature channels (I and Q) are combined to yield magnitude (Figure 1). The combined pulses represent the impulse response of the channel to a resolution permitted by the bandwidth of the phase code, which is about 3 kHz in the present implementation.

The combined Barker decoder output is examined for approximately 20 ms (the duration of two coded bits) to determine if any coded signal is being received. If no signal is present, the receiver is stepped to the next channel. If a signal is evidently present, the receiver remains on the channel long enough to store at least two full station identification (ID) transmissions, which requires 450 ms. If coded signals continue to appear, which will generally be the case if a signal is actually being transmitted, the receiver remains on the channel as long as the signal lasts, or until it has decoded the ID and determined that the call is not for itself.

The stored compressed signals are examined to determine a noise threshold, the time framing of bits, and the content of the ID symbols. With these processes all being performed on stored data, no time is lost in synchronizing or setting the threshold. The detector can, in effect, look forward and backward in time. The signal detection process is aided by the fact that the receiver, although it does not know the absolute time to expect an ID group to appear, does know the time extent of such groups, and can arrange the stored data in a sequence that allows exploiting the repetition of the probe calls to detect an ID. An example of a sequence of compressed pulses received in Menlo Park, California, from Churchill, Canada, is shown in Figure 2. This is typical of the data that are examined by the "smart detector" in recognizing an ID call. Each pulse is the result of correlation of the 13-element Barker code. The framing is arbitrary with respect to start time but makes the repetitive signal obvious by virtue of being matched to the duration of the call. Two frames, or ID groups, are examined by a sliding digital matched pattern to detect the ID, and thence to determine the absolute framing time. In a typical detection event, several ID groups would be detected because the originating station will transmit long enough to assure that the scans of unsynchronized receivers have an opportunity to intersect the scan of the calling station.

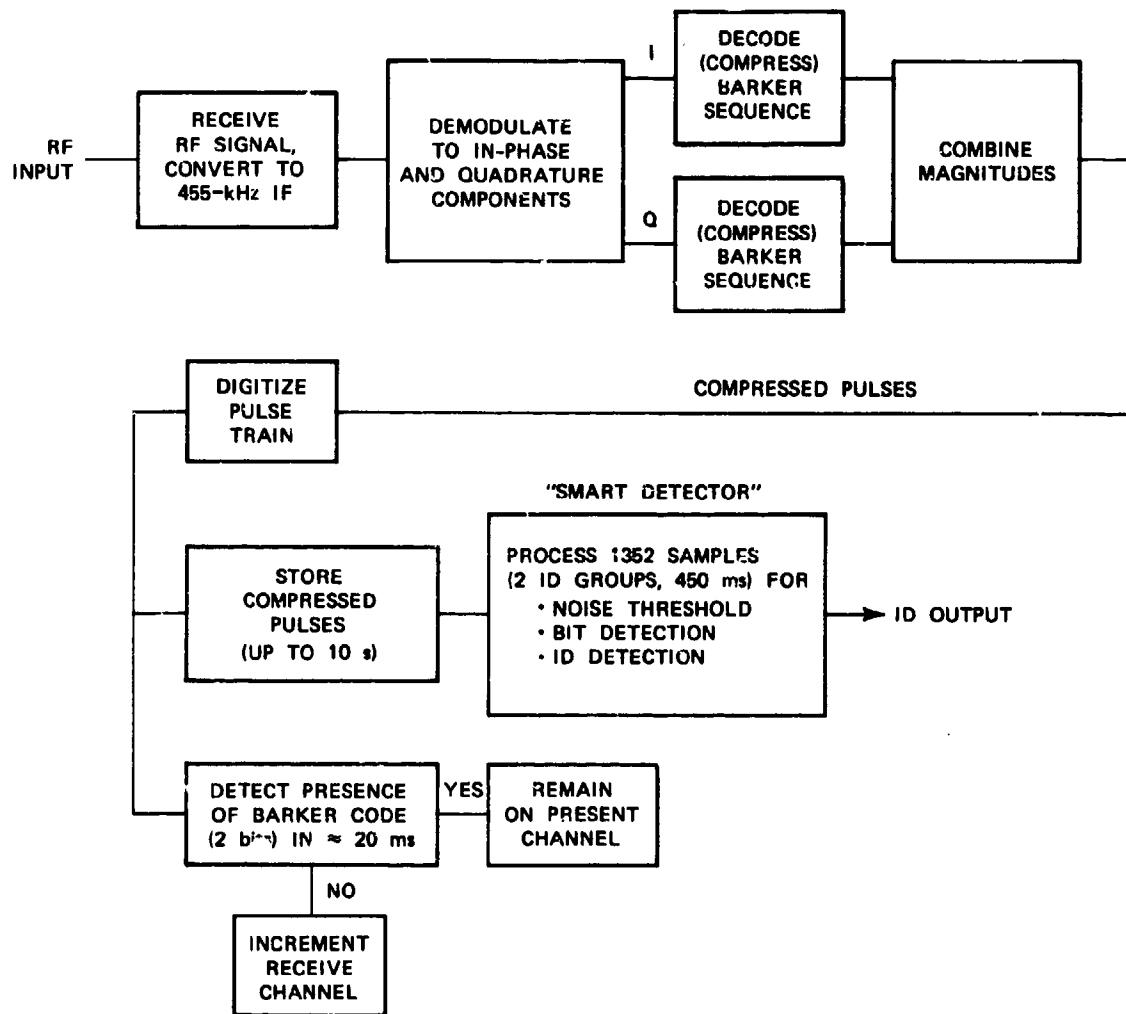


FIGURE 1 SELECTIVE CALL DETECTION FUNCTION DIAGRAM

CHURCHILL — LOS BANOS
2320 UT
SEPTEMBER 23, 1983

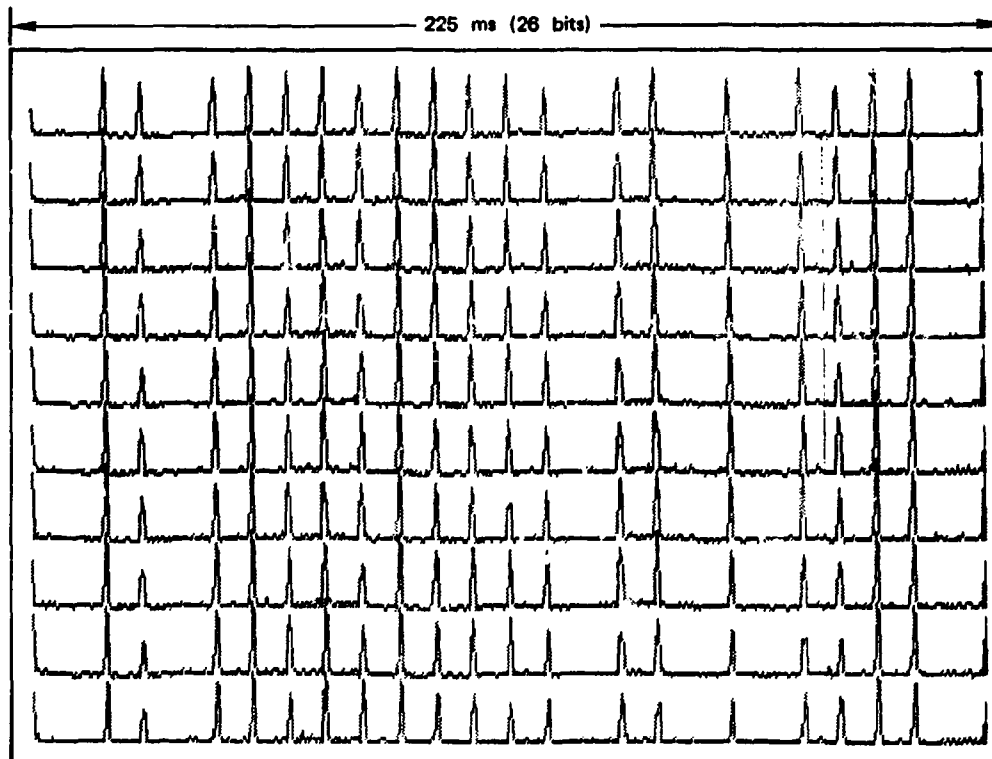


FIGURE 2 COMPRESSED CALLING SIGNAL

Close examination of the compressed signals reveals a certain amount of residual fading, even though the process of combining the I and Q components reduces it considerably. This fading is caused by interference between ray paths that are not resolved by the phase code. Our initial intent was to use a somewhat wider bandwidth, permitting better resolution of modes, and therefore, to experience less fading. The smart detector would process the compressed pulses in groups, corresponding to the impulse response of the channel. Although individual pulses of the groups would fade, the ensemble would be expected to provide a powerful form of antimultipath diversity. Implementation

problems prevented using the bandwidth necessary for this, which must remain as a future goal.

The test-bed probing signal was originally designed¹ to satisfy only a fairly general concept, i.e., to resolve modes, thereby reducing fading, and to be able to be rapidly synchronized. Appendix C contains an analysis of the test-bed probing signal to determine its adequacy for its task, and to recommend improvements. The conclusion of the theoretical analysis in Appendix C is that the present AHF Test-Bed sounding system is fairly well matched to the problem of evaluating HF channels for voice and data. Nevertheless, there is room for improvement in the existing design. Perhaps the principal improvement is the replacement of on-off keying (OOK) data modulation with phase-reversal-keying (PRK) data modulation. There are several substantial advantages in using PRK: (1) the noise performance is improved by 3 dB, (2) it is not necessary to set threshold levels and interact with the AGC system, and (3) the sounding signal is transmitted each bit, thereby guaranteeing a more frequent measurement of the channel impulse response.

The 13-chip Barker code presently implemented is desirable because it is the longest Barker code and offers the lowest side-lobe level. However, owing to its inequality of positive and negative elements, it suffers a loss of processing gain against a line component, such as a CW signal. The 10-chip Barker code may be preferable in this regard.

SECTION 3

EARLY MEASUREMENTS

3.1 Short Path

The test-bed equipment was completed in October of 1982 and operated over a 100-km path that included a range of mountains about 3000-ft high between the end points (Los Banos, California, and Stanford, California). Horizontally polarized antennas were used. Ground-wave transmission was thus effectively prevented and was not observed. The practical results were most encouraging in that the system linked reliably in a fully automatic mode with only 1 W of transmitter power. Observation of the signal structure, however, showed that this good performance was obtained when multipath fading was not present. The Costas loop demodulator in use at the time was recognized as being a potential liability in the presence of the greater multipath expected on longer paths. Replacing the Costas loop with the dual-channel demodulator described above was believed to be a routine matter, so the system was taken out of service for reconfiguration without performing a systematic series of on-the-air measurements, a course of action seen in hindsight as a mistake because the change took a full year.

3.2 Long Auroral Path

In September of 1983, the new detector and new software to perform the "smart detection" process were completed and installed in the test-bed units. One set of equipment was installed at Churchill, Canada, on the Western shore of Hudson's Bay in a small building that the Canadian government Department of Communications, Communications Research Center generously provided. The other end of the link was at the SRI field site at Los Banos, California, a distance of 3100 km. Signals such as those shown in Figure 2 were digitally recorded in a data-taking mode for several hours over a period of several days. An oblique ionogram recorded over the same path at that time is shown in Figure 3.

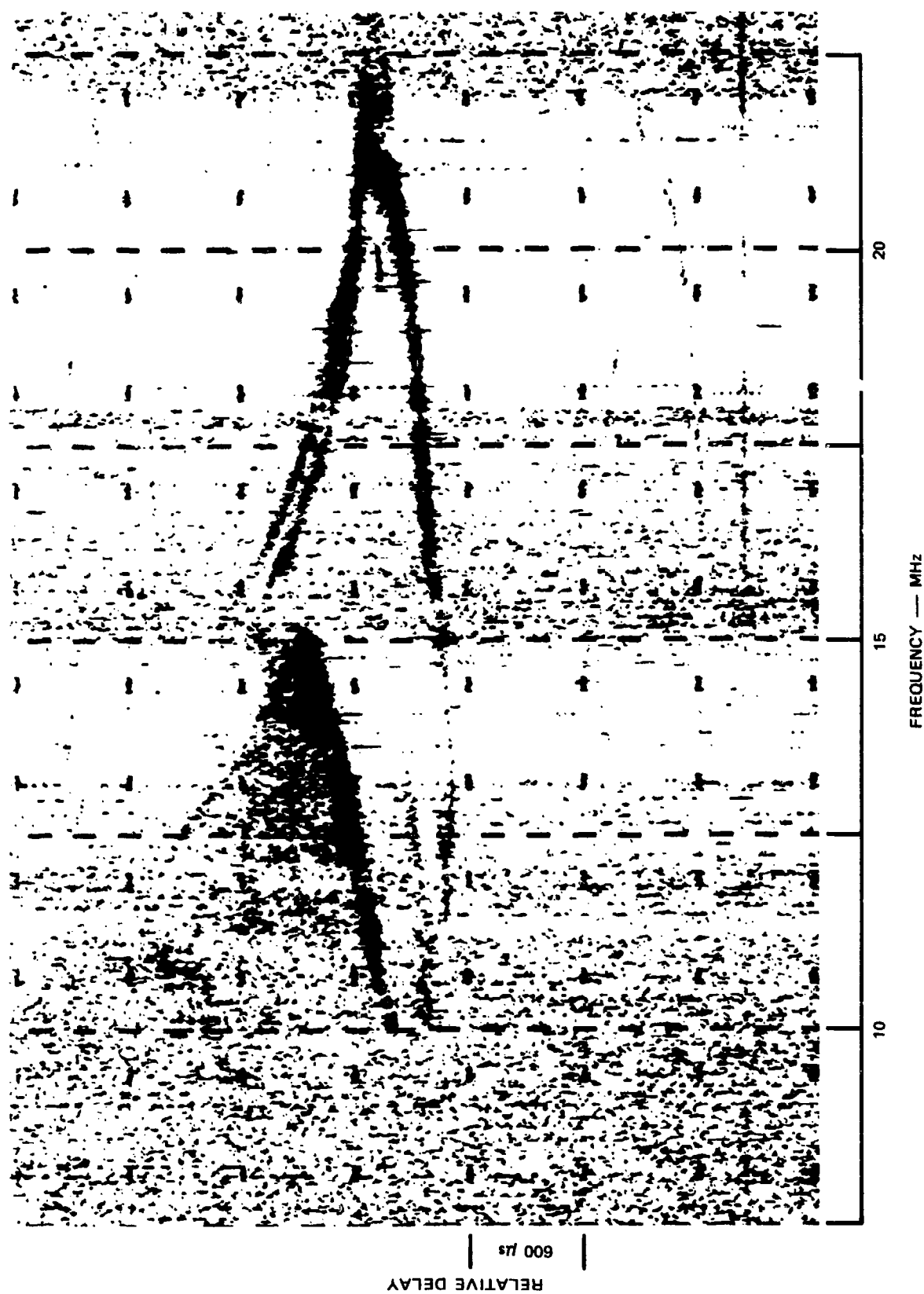


FIGURE 3 CHURCHILL-LOS BANOS OBLIQUE IONOGRAM FOR 23 SEPTEMBER 1983 AT 2312 UT

The new dual-channel Barker decoder worked as expected, showing only moderate fading, as indicated in Figure 2. Unfortunately, the "smart detector," which was to process the output of the Barker detector, failed to perform as intended with the result that automatic linking was not accomplished. The thresholding algorithm used to determine whether marks or spaces were received was found to be the cause of the problem. Field modifications to the software were made to change the threshold levels, and one-way link-up was achieved on several occasions. Because it was not possible to redo the threshold algorithm in the field in the time available, subsequent efforts were directed to digitally record the signals transmitted over the path for later use in testing modifications of the software.

Figure 2 is an example of the data collected at Los Banos at 19.010 MHz at 2320 UT. An oblique ionogram taken at 2312 UT over the same path is shown in Figure 3. The ionogram shows that at 19 MHz both a high- and a low-ray mode were supported. Because the two modes were separated in time by only 350 μ s, they were not resolved by the adaptive radio. Thus, the two modes were at least partly responsible for the slow fading evident in Figure 2.

The original intent was to operate the SELSCAN/ARC-190 over the auroral path at the same time as the DNA AHF test-bed, but delays in obtaining the hardware, and in constructing a necessary special power supply for the ARC-190, prevented this. The next section describes a series of successful tests that were conducted when these problems were overcome.

SECTION 4

SELSCAN MEASUREMENTS

4.1 Objectives

The primary objective of the SELSCAN tests was to determine specifically how well the SELSCAN technique finds operating frequencies and establishes links in poor and or changing propagation conditions. To the extent that these conditions are similar to those occurring during or after a nuclear attack, the tests will indicate the performance that can be expected at such times. Operating an oblique sounder over the same path is an important part of the objective in order that the propagation available to SELSCAN be known accurately. Ultimately, our objective was to test the SELSCAN over auroral and possibly equatorial paths that have substantial Doppler spread as well as off-great-circle multipath. The present tests, however, have been limited to operation over a temperate path in which the primary propagation problem was a limited and changing propagation spectrum and normal ionospheric multipath.

4.2 Experimental Arrangements

4.2.1 Sounder

The original plan for the present task was to operate SELSCAN over the Churchill-to-Menlo Park path to obtain some auroral propagation, but problems in obtaining various components of the system caused this objective to be missed. Instead, the tests were run between Cedar Rapids, Iowa, and Menlo Park, California, a temperate East-West path of 2615 km. Facilities at Cedar Rapids were provided by Rockwell Collins Company under subcontract to SRI International. Propagation on this path is expected to be primarily 1-hop F_2 at take-off angles of from

6 to 10 degrees. Two-hop F_2 rays at approximately 25° , as well as F_1 rays and some two-hop E, are also expected.

The equipment at Cedar Rapids was installed at the Collins manufacturing test facility. At Menlo Park, the equipment was installed in the shop of the Radio Physics Laboratory. Neither the Menlo Park nor Cedar Rapids facilities is an ideal, low-noise radio location. Both are part of active light industrial complexes.

The antenna at Cedar Rapids was a Collins model 237B log-periodic mounted on a nominally 100-ft (30-m) tower. This antenna is horizontally polarized and was rotated to the azimuth of Menlo Park (270°). This antenna has an elevation pattern the maximum of which varies from about 7° at 20 MHz up to about 15° at 9 MHz, the frequency range over which most of the operations were conducted. The antenna gain at its maximum is approximately 12 dBi.

The Menlo Park antenna was an SRI-built, broad-band sloping dipole with a feed point elevated 40 ft (12 m) and three wires forming dipole arms sloping to the ground, at which point they terminate in grounded resistors (Figure 4). This antenna has a broad response in elevation and azimuth with approximately 0 dBi directive gain and a loss of from 2 to 5 dB in the terminating resistors over the band of our operations.

The radio equipment at Menlo Park was an unmodified AN/ARC-190(V) furnished by the Air Force. The output power was measured at 200 W during most of the tests. The radiated power is estimated at approximately 100 W because of the loss in the antenna loading resistors.

At Cedar Rapids, the radio equipment was an HF-80 system operating at 400-W output power. Because of the efficient antenna, essentially all this power was radiated.

The path propagation was measured by an SRI-built, synchronized, oblique FMCW "chirp" sounder. The sounder receiving system, which was located in Menlo Park, is shown in Figure 5. The sounder transmitter, located at Cedar Rapids, is similar, except that the sweep generator operates from 2 to 32 MHz and is fed directly to a broad-band amplifier

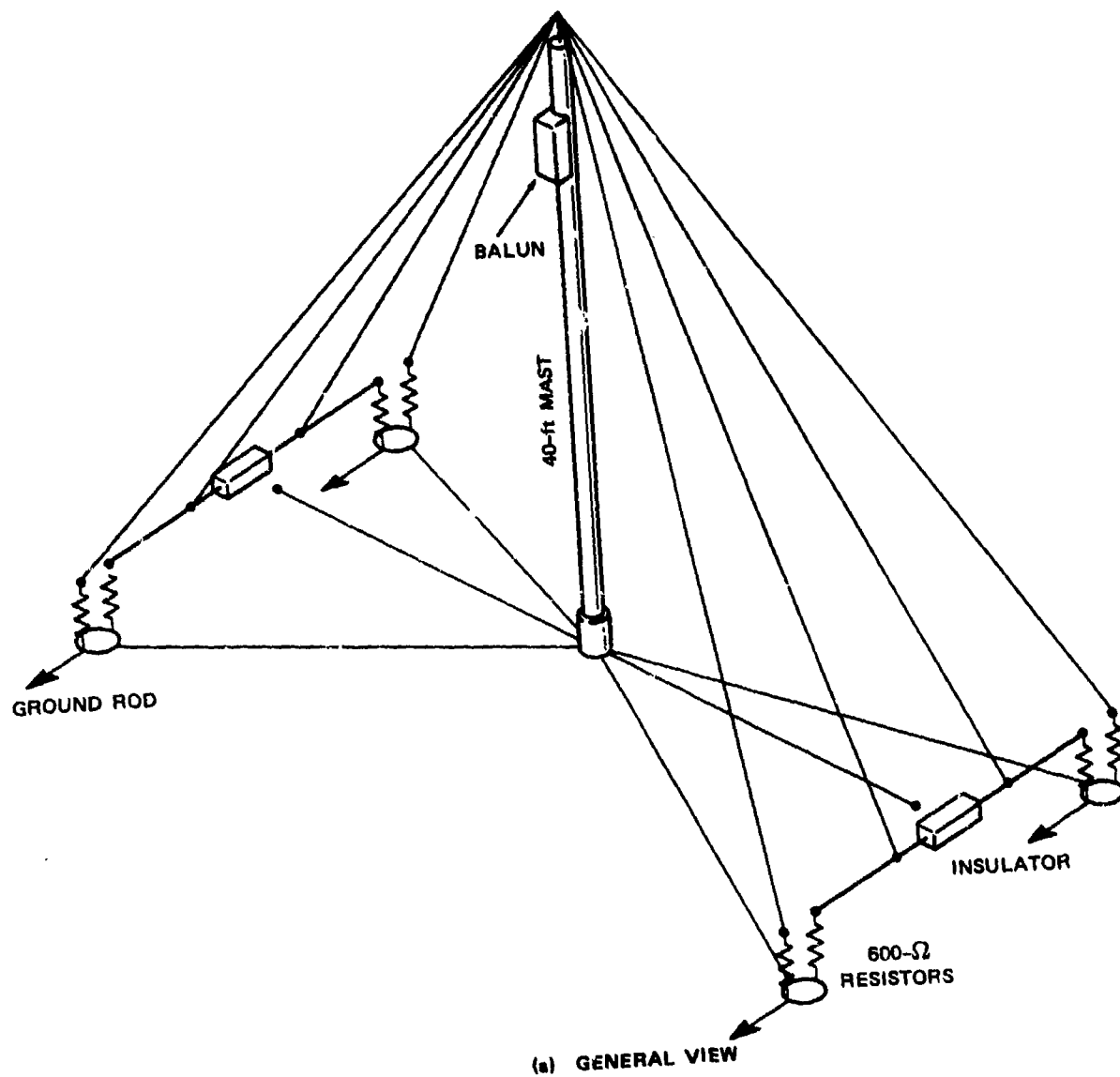


FIGURE 4 MENLO PARK ANTENNA

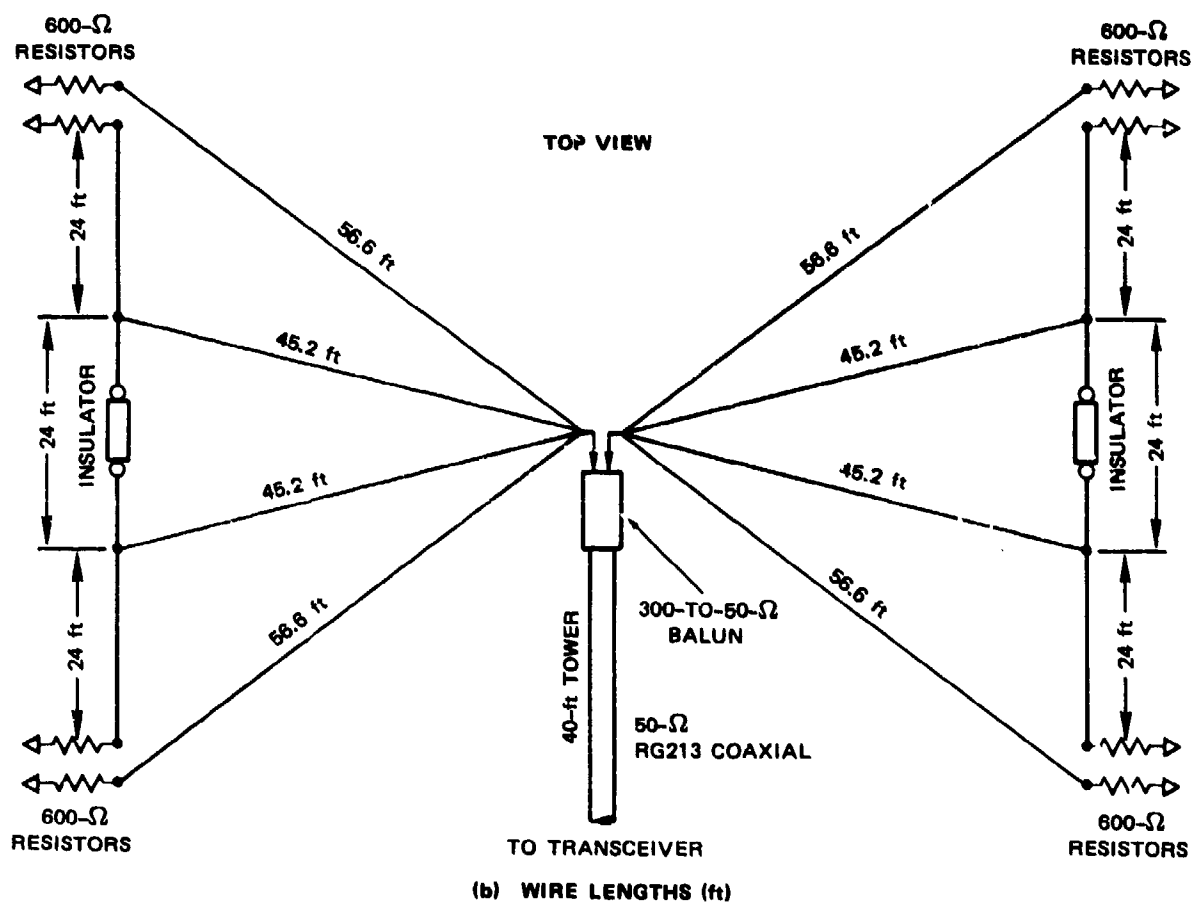


FIGURE 4 (concluded)

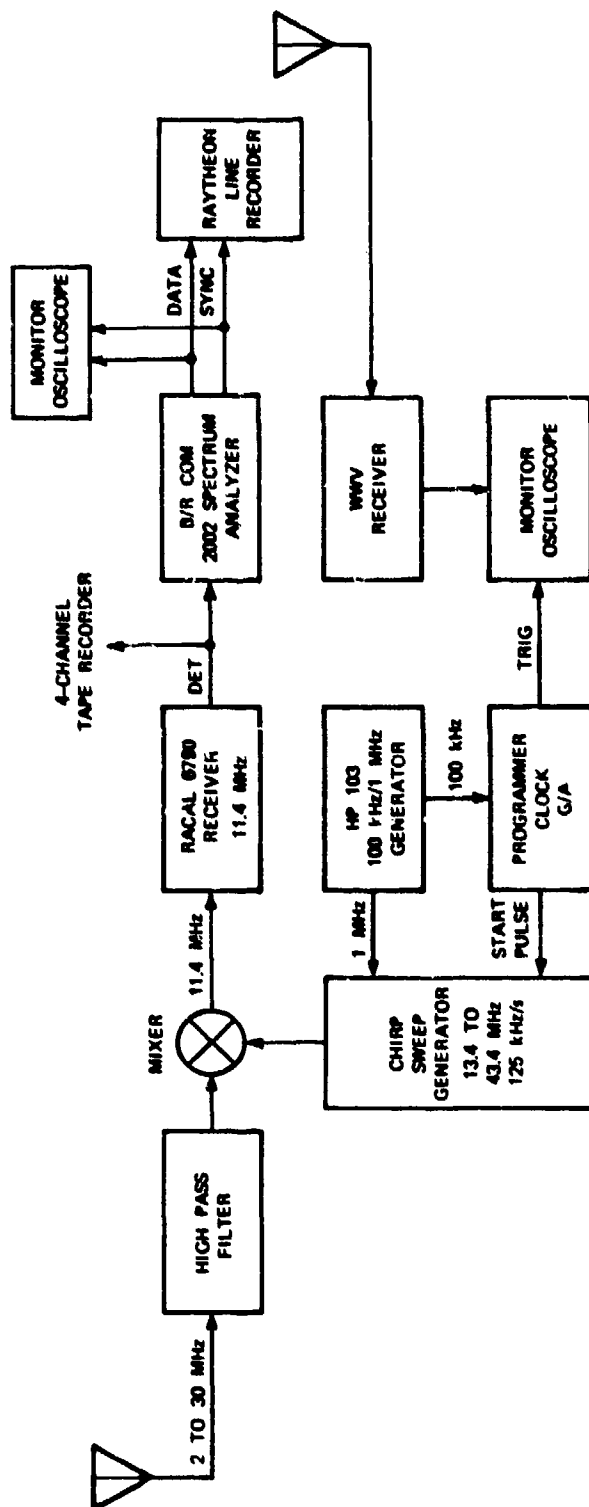


FIGURE 5 CHIRP RECEIVER AND RECORDER

of 100-W nominal output power. Both receiver and transmitter operated with the experimental antennas described above. The antennas were switched between the sounders and the SELSCAN/ARC-190. The sounder receiver detects the deramped sweep in a spectrum analyzer having spectral cell bandwidth of approximately 1 Hz, giving it about 30 dB more sensitivity than that of a system of the same power performing detection in a normal voice bandwidth.

4.2.2 SELSCAN

SELSCAN is a technique for controlling HF transceivers, not a radio in itself. For this test, the SELSCAN equipment controlled an Air Force/Collins AN/ARC-190 400-W transceiver. The radios were obtained on loan from the Air Force, and the SELSCAN equipment was provided by Collins. The ARC-190 is intended for use in aircraft. It must be provided with 400 Hz, 3-phase power. The interconnections provided normally by the aircraft wiring, junction boxes, and circuit breakers must be provided by a special junction box as illustrated in Figure 6. The normal antenna coupler supplied with Air Force ARC-190s is designed specifically for use with an aircraft probe antenna and will not work with conventional antennas more or less matched to 50 Ω . A few special couplers, called "long-wire" couplers, were procured by the Air Force for operation into more conventional antennas; one of these was made available to us for this test. The output of the long-wire coupler is a large unbalanced terminal post, for which we built an adapter so that it could be connected to coaxial cable. The SELSCAN/ARC-190 combination contains its own frequency standard, which puts the radios within a few hertz of each other, close enough that no additional tuning is needed to operate in a single-sideband (SSB) voice mode. No internal or external time reference is required for the SELSCAN.

In addition to the basic two-rate scanning-calling process that is described briefly in the introduction and that is an approach which has long been advocated by designers familiar with the problems of establishing HF links, SELSCAN performs a unique procedure that potentially enhances both its efficiency in linking and the quality of the links

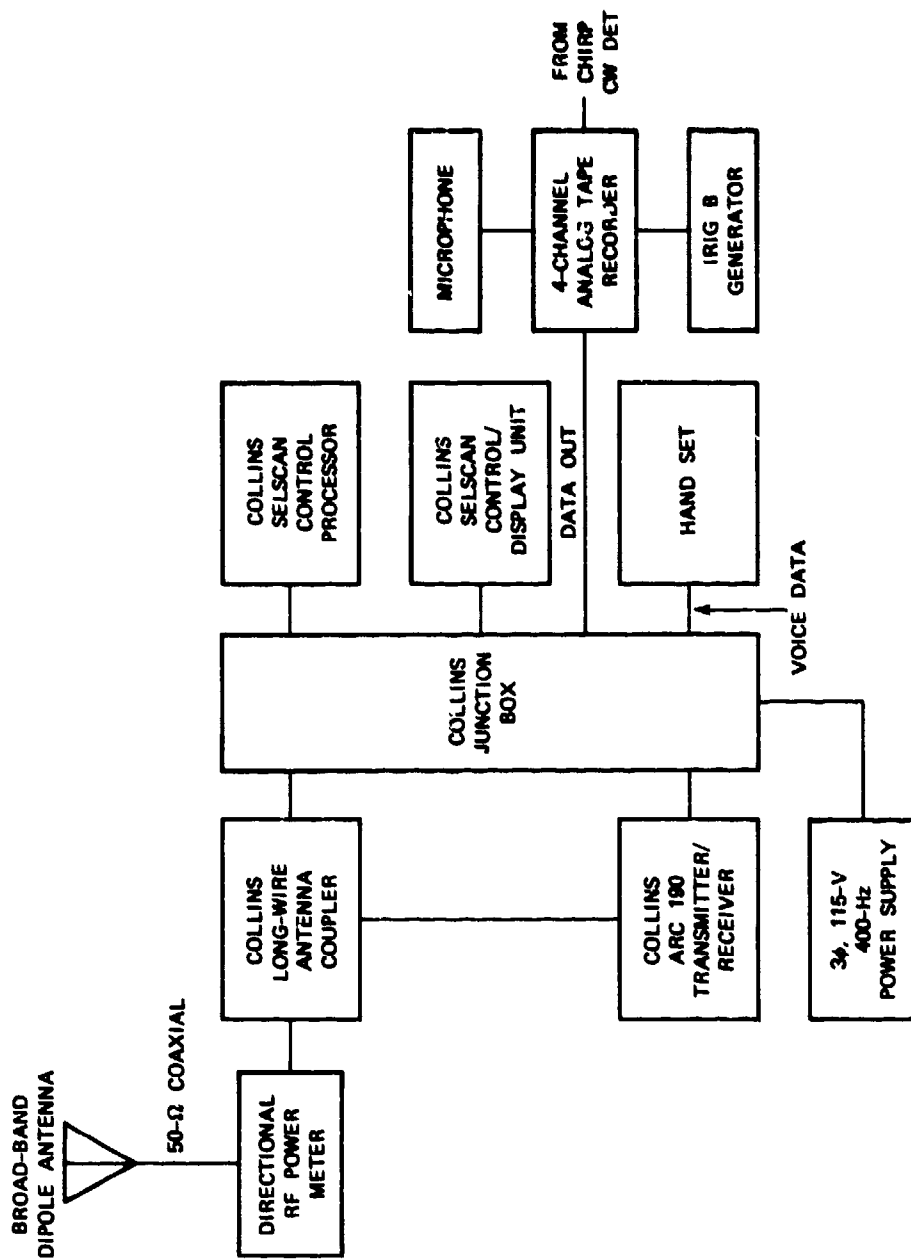


FIGURE 6 SELSCAN/ARC-190 EXPERIMENTAL SYSTEM

established. The SELSCAN controller maintains a file of the signal quality observed from all other similar stations on all frequencies scanned by the receiver. This information is termed a link quality array (LQA). In normal network operation, as in an air traffic control or military operational situation, each node will make operational transmissions from time to time. The receivers at scanning nodes take note of the signal quality observed, and put the observations in their LQA. When a request to contact a particular node is received (as an operator input) the controller scans its transmitter over the assigned channels in descending order of link quality. The link is likely to be established on the best channel available, rather than on the first one encountered in a simple sequential sweep, which may be just marginally acceptable. The information in the LQA is, of course, perishable and must be renewed frequently. If the network is active enough with operational traffic, this happens more-or-less automatically. Each entry in the LQA is tagged with the time of its observation. The controller forces the values in the LQA to decay with a time constant of tens of minutes. If a node has not been received in some time, the controller can initiate an automatic call to it to renew the values in the LQA for both.

If a SELSCAN radio is intended for backup use, in which it and the other nodes in a network are not operated until a primary system becomes unavailable, the LQA file will not contain useful information. Initiating a call in this situation will result in the radio simply scanning from highest to lowest frequency. Although this approach will eventually result in a link-up, the channel selected may not be optimum. A possible and practical modification to the software would cause the calling radio in this circumstance to request a scan by the called station to update the LQA as soon as the initial link is established, and before the link is turned over to the user, possibly on a better channel than the one originally found.

Normally, an operator would not be concerned with the LQA; he simply enters the call letters of the station to be called and talks when the control unit tells him that the link is established. For the tests,

however, the operator caused the SELSCAN controller at each end of the path to scan through the assigned channels once each half hour to provide signals to update the LQA at the other end of the link. A special operator command to the control/display unit causes the LQA to be read out on the digital display, from which it was manually recorded for the tests.

The primary measure of the operational quality of the link was the voice contact between the two operators. As a supplement, we also transmitted a pulsed audio code, from an IRIG-B time-code generator, from Cedar Rapids to Menlo Park on the regular audio channel of the ARC-190, which was recorded. A local IRIG time code, the detected audio of the sounder receiver, and a local logging microphone were also recorded on a four-channel tape. All observations can, therefore, be recovered for additional analysis if necessary.

SECTION 5

OBSERVATIONS

Approximately forty attempts to establish a link with SELSCAN were made during four experimental sessions in a period of twelve days during June 1984. A link was always established, usually in less than a minute, but sometimes taking several minutes. The quality was generally good. Once an experimental routine was established, a data run was conducted each half hour. First, an ionogram transmission would be made from Cedar Rapids and recorded at Menlo Park. Next, the operators would each in turn transmit a special scan of the SELSCAN to reestablish the LQA. Then the Cedar Rapids operator would initiate a SELSCAN link attempt. (For the first few runs, the Menlo Park operator initiated the link attempt, but this was changed early in the test to allow the Cedar Rapids operator to coordinate potential interference with other users of the same frequencies at Collins.) When linked, the operators would exchange short voice tests to obtain one measurement of link quality; then the Cedar Rapids operator transmitted a minute of IRIG tones for another measurement. Finally, the Menlo Park operator transmitted a short period of special tones to test an experimental "Advanced Link Quality Analysis" (ALQA) technique.

The results will be presented as a sequence of observations over a 24-hour day, though the actual observations spanned several days. The results, in terms of available propagating frequencies and channels selected by SELSCAN, are summarized in Figure 7. Here we have abstracted the data from the ionograms to indicate "strong" and "weak" signals on the basis of density of the recorded trace. This distinction will become more evident as the ionograms are reviewed. Although it is not quantitative, it is more informative than a simple indication of presence or absence of signal. The data here show that SELSCAN prefers the highest propagating frequency, but often selects a much lower one.

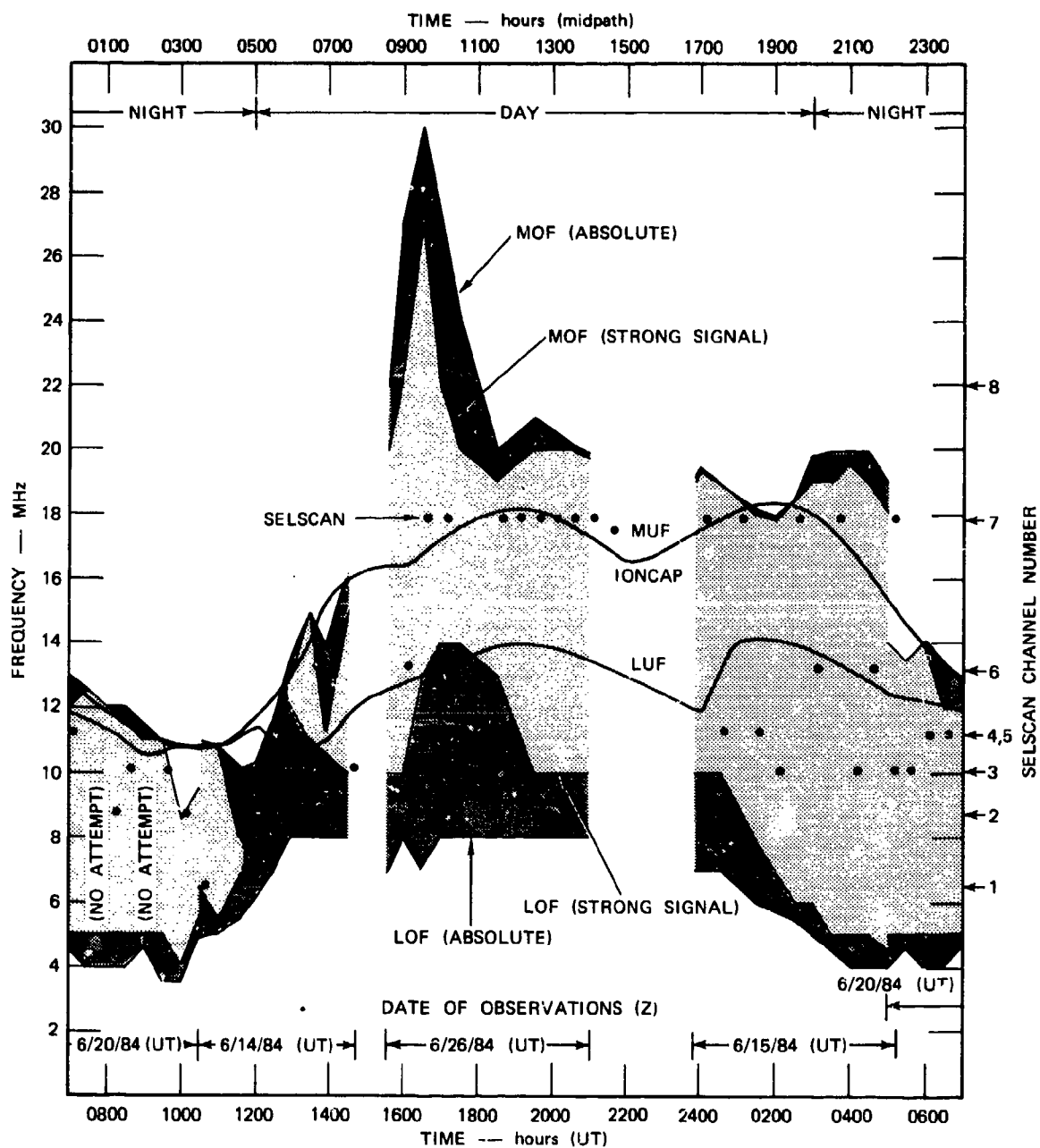


FIGURE 7 SUMMARY OF PROPAGATION AND SELSCAN CHANNEL SELECTION

The reasons for some of these choices will be seen as we examine some of the individual data sets. The figure also shows the predictions made for the conditions of the tests by IONCAP, a widely available HF propagation code. In common with many other experiments, this one shows that the predictions of maximum usable frequency (MUF) are generally consistent with maximum observed frequency (MOF) but differ in detail on any given day. (MUF is the frequency that should be exceeded by MOF on 50 percent of the days of a month. The MOF should fall below 85 percent of the MUF on only a few percent of the days of a month.)

We start our examination of the individual observations with the middle of the day, when conditions are stable and favorable.

The observations at noon on the path (1930 UT) are shown in Figure 8. The ionogram, Figure 8(a), shows propagation that is probably mostly one-hop F_2 layer ($1F_2$), but which may include a one-hop F_1 or E mode as well. The F_2 trace is identified by the upper ray that forms a fishhook at the MOF. Its main, lower, ray is more straight, and increases slightly in delay with frequency. Which of the two such traces is the F_2 , and which the F_1 or E is not clear. The isolated mode at 11 MHz and 1 ms more delay than the first mode may be a fragment of $2F_2$ or an off-great-circle mode. The gaps in the traces that extend more-or-less continuously vertically are caused by strong interference, which activates the receiver automatic gain control, thus suppressing the signal. The interference itself is not visible, because it does not remain stationary in the FMCW analysis filters. The automatic gain control (AGC), this time under control of the sounder signal, also causes the change in character of the noise seen above the MOF. The very thin traces that appear to be echoes of the main trace are believed to be artifacts of the sounder receiver spectral analysis process. The frequencies available to the SELSCAN are numbered 1 through 8 and indicated on the frequency scale. The channel selected by SELSCAN is indicated by a filled arrow below the channel frequency.

The values in the LQA are shown along the top of the ionogram for each terminal. The LQA values vary from 1, which represents no observed

signal, to 18 for the maximum measurable signal quality. This example is typical in that the LQA values at Menlo Park (MP) are often larger than at Cedar Rapids (CR). This is evidently because Cedar Rapids radiated some 6 to 7 dB more power and possibly because of differences in local noise and interference. In this instance, both terminals show the maximum value on the same channel, Number 7, which is 17.964 MHz. Communication would also have been possible on Channels 4, 5, and 6, though at a lower quality.

The operators judged the voice signal quality as Q-5, which is excellent, at Menlo Park, and Q-4, or good, at Cedar Rapids. (See Table 1 for complete definitions of voice channel quality ratings.) This

Table 1. Overall Rating for Telephony (from ITU Radio Regulations, Geneva; 1959).

Symbol	Condition
5 Excellent	Signal quality unaffected
4 Good	Signal quality slightly affected
3 Fair	Signal quality seriously affected. Usable by operators or experienced subscribers
2 Poor	Channel just usable by operators
1 Unusable	Channel unusable by operators

difference, which occurs throughout the experiment, is consistent with the difference in LQA values, and is believed to be caused by the difference in radiated power and in local noise.

The signal-to-noise-ratio (SNR) density, that is, the SNR in a 1-Hz bandwidth, SNR_0 , was measured by the experimental ALQA algorithm at Cedar Rapids as 42.1 dB, which corresponds to a 7.3-dB SNR in a 3-kHz bandwidth. This measure is probably pessimistic, or the operators were overly generous with the voice quality.

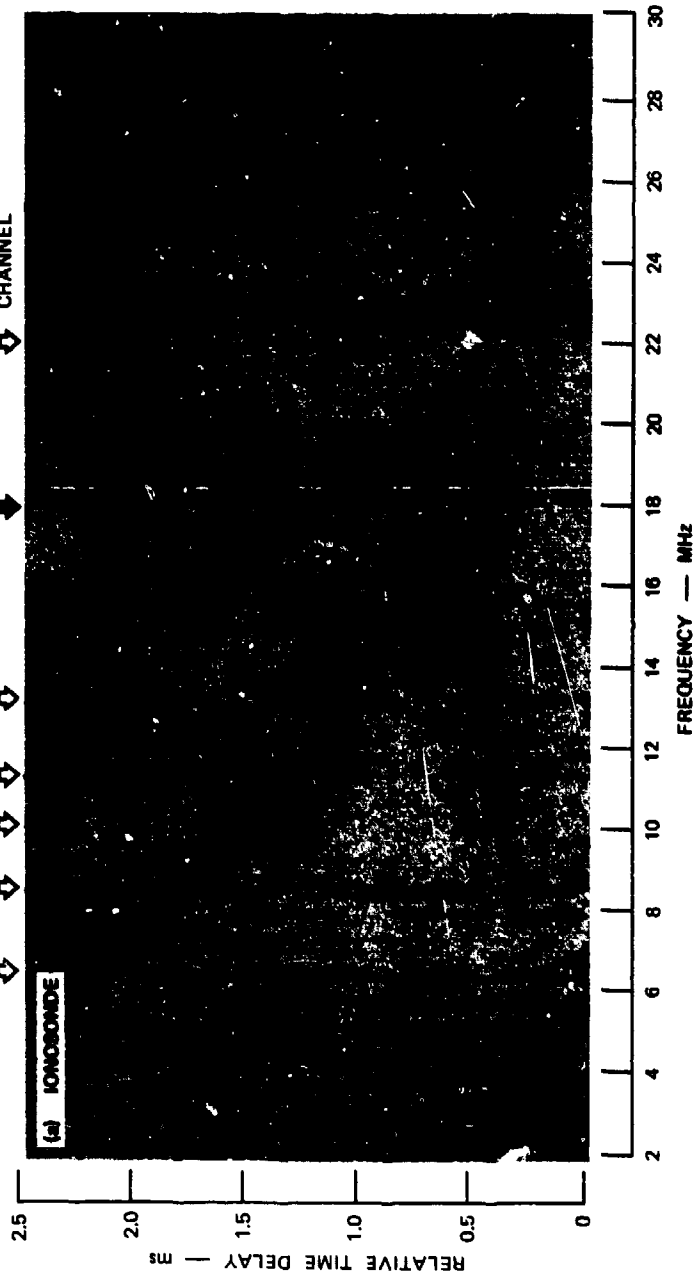
The experimental ALQA system also measured the apparent time delay spread of the signal, showing 0.2 ms on the selected channel. This value corresponds well with the spread observed on the ionogram at Channel 7 and generally throughout the data.

As a supplementary measure of the quality of the channels selected by SELSCAN, a minute of IRIG audio time code was transmitted during each data session. The results for 1930 UT are shown in Figure 8(b). The signal consists of an audio tone that is pulsed upward in amplitude, at a 10-ms (100 baud) rate, to convey digital data in a special code. When an oscilloscope is synchronized to the code, a pattern like that in Figure 8(b) appears. The background steady tone continues across the trace, with the modulation superimposed. The signal seen here is essentially the same as is observed directly, without the intervening radio path, and represents a good data channel, at least for signals with a similar pulse rate, which is comparable to that of conventional 75 baud RTTY.

The propagation and results shown in Figure 8 represent relatively good conditions typical of midday on a path of this length and latitude. Note, however, that of the eight frequencies available to the system, only one was very high quality at one end of the link. An operator might or might not have found it.

The next three data sets, Figures 9 through 11, represent typical daytime conditions over a period of several hours, into the early evening. Substantial multipath appears below about 14 MHz, some of it apparently spread from distinct modes. SELSCAN continues to select a frequency near the MOF, so is not affected. The quality of the selected channel remains high. By early evening, 2030 hr on the path (0330 UT), the MOF is starting to decrease. Multiple modes become more visible because of the decreasing D-layer absorption as the daylight recedes. SELSCAN again selects 18 MHz, but took seven minutes, much longer than normal, to link. The channel, when established, was very high quality, with the operators assigning Q-4 and Q-5, an SNR_0 of 51.1 dB (16.3 dB in 3 kHz), and only 0.1 ms of multipath. The channel is quite close to the

1	1	2	1,8	7	17	1	CR LOA
1	1	1	17,17	17	18	1	MP LOA
1	2	3	4,5	6	7	8	SESCAN CHANNEL



QUALITY OF SELECTED CHANNEL

ALOA: $SNR_0 = 36.4 \text{ dB}$
 $\Delta T = 0.3 \text{ ms}$

VOICE: CR O4
 MP O4

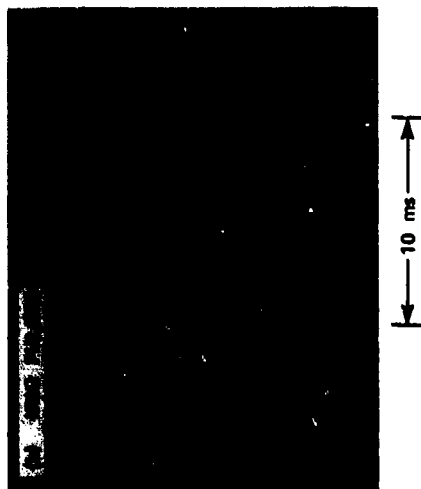
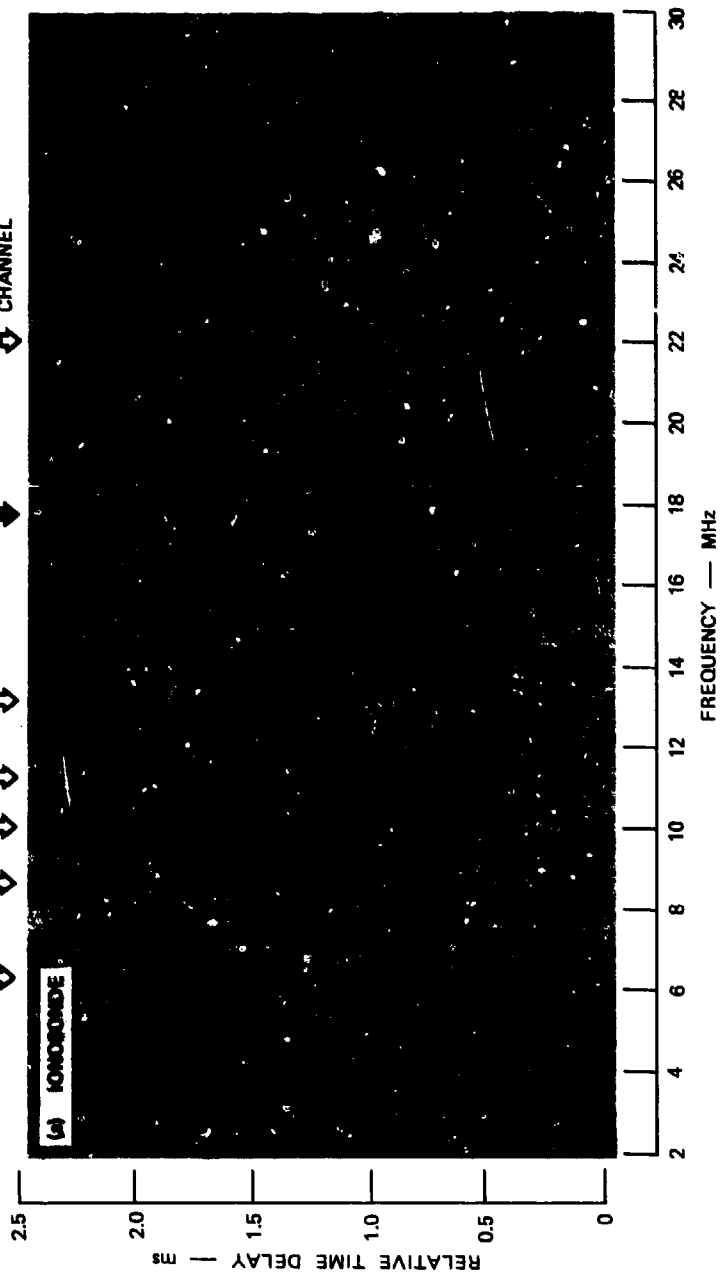


FIGURE 9 DATA FOR 2100 UT (1400-hr MIDPATH), 25 JUNE 1984

1	1	4	6,7	13	17	1	CR LOA
2	1	17	1,17	18	18	1	MP LOA
1	2	3	4,5	6	7	8	SESCAN CHANNEL



QUALITY OF SELECTED CHANNEL

ALGA: $SNR_0 = 41.8 \text{ dB}$
 $\Delta T = 0.2 \text{ ms}$

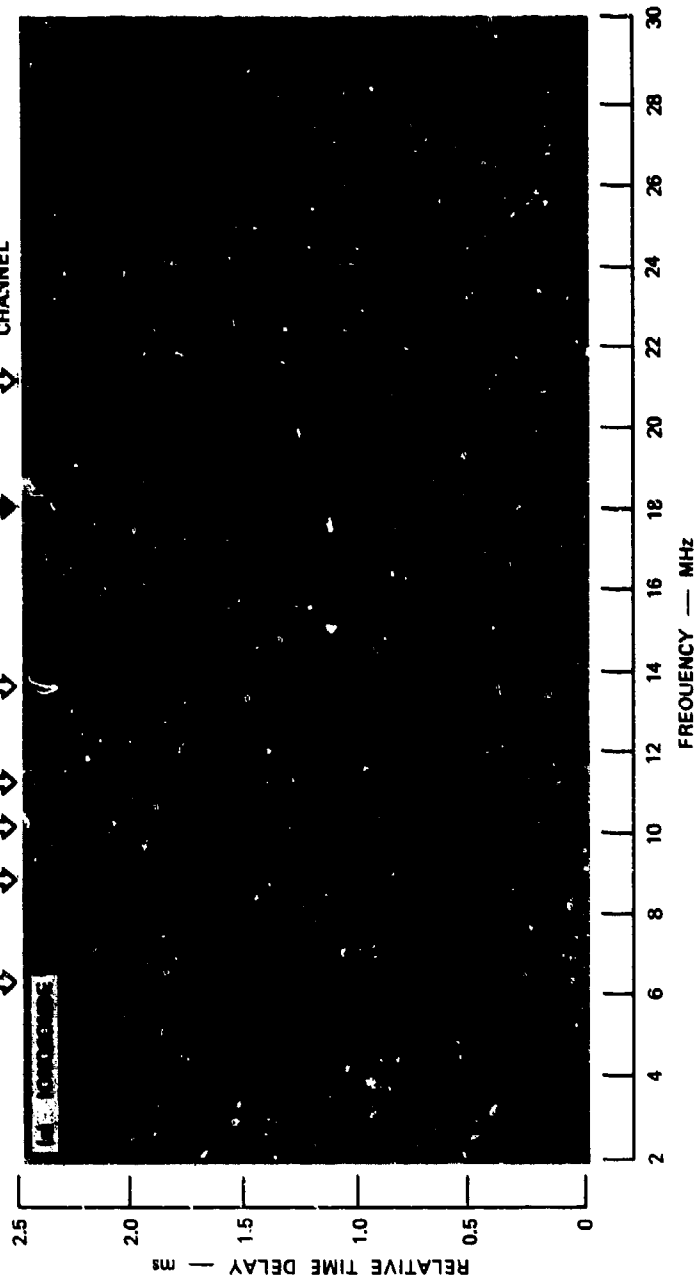
VOICE: O4
 CR
 MP O5



10 ms

FIGURE 10 DATA FOR 0000 UT (1700-hr MIDPATH), 15 JUNE 1984

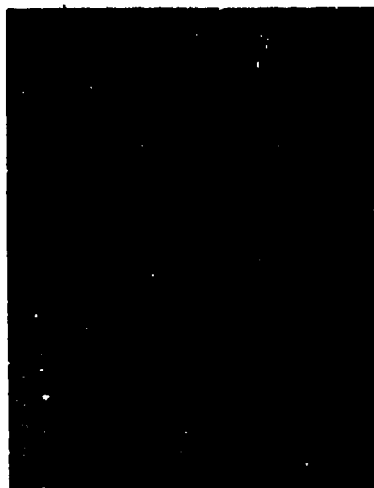
12	17	16	9.6	8		17	1	CR LOA
13	1	14	6,14	15		14	1	MP LOA
	2	3	4.5	6		7	8	SELSKAN
1	↕	↕	↕	↕		↕		CHANNEL



QUALITY OF SELECTED CHANNEL

ALOA: $SNR_0 = 51.1 \text{ dB}$
 $\Delta T = 0.1 \text{ ms}$

VOICE: 04
 CR
 MP 05



10 ms

FIGURE 11 DATA FOR 0330 UT (2030-hr MIDPATH), 15 JUNE 1984

MOF and so is subject to deep, slow fades, which may explain the problem in linking. Also, substantial interference was experienced at Cedar Rapids at this time. Data transmission, as measured by the IRIG signal, was good throughout the period.

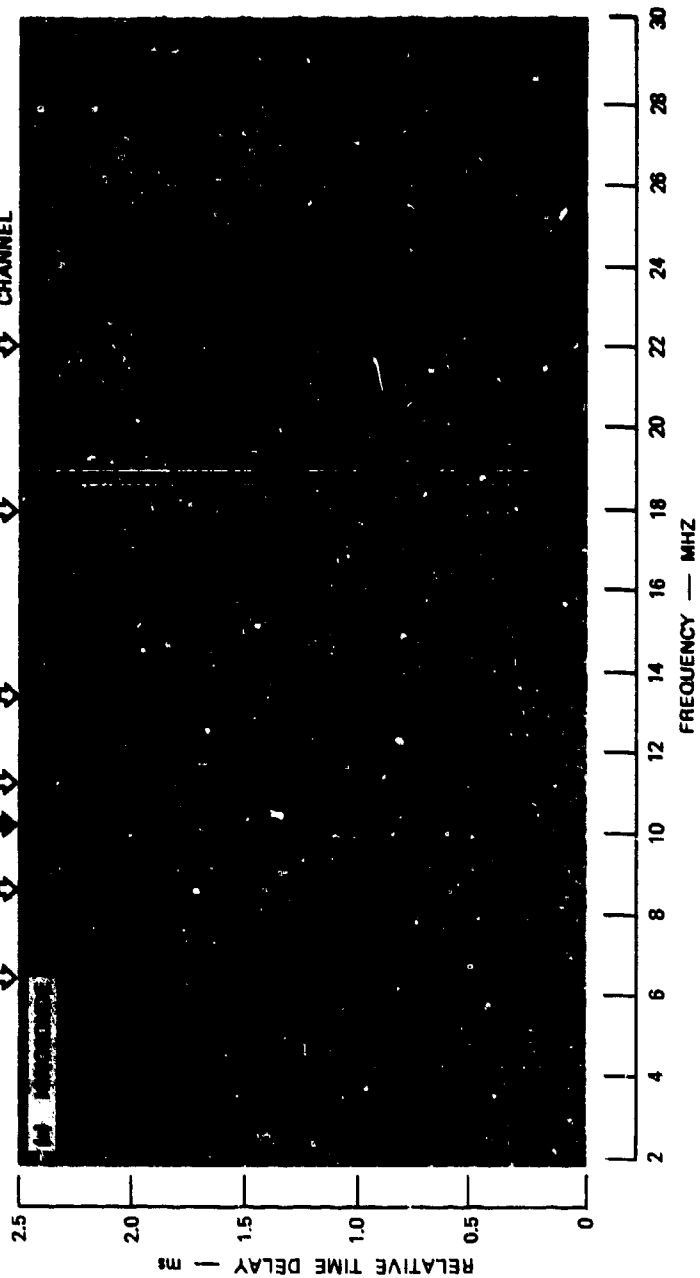
Two hours later, at 2230 hr on the path (0530 UT), in Figure 12, late evening conditions prevail. The MOF has dropped from its daytime value around 20 MHz to 14 MHz, and SELSCAN selects 10 MHz, with generally good results. Note that two channels, Numbers 2 and 4, are unusable at Menlo Park, because of interference, as noted by the operators, while they show good at Cedar Rapids.

The operating LQA shows a quality 14 at 18 MHz at Cedar Rapids, while nothing shows on the ionogram this high in frequency, and the ALQA measures a relative time delay of 0.9 ms at 10 MHz, while again the ionogram indicates no multipath at this frequency at all. These indications suggest that possibly a mode with much different path length than the normal, and therefore not displayed on the ionogram, is present at this time. This effect is just a curiosity at this time because we do not have the data to analyze it; however, it serves as a reminder that anomalous propagation is possible and should be considered in the design of system timing and modulation. SELSCAN was not affected one way or another. The IRIG signal was essentially perfect at this time, suggesting that whatever caused the high multipath measurement by the ALQA was at a very low level.

At midnight (Figure 13), SELSCAN again selects the highest frequency that is propagating well. Substantial magnetoionic fading, which manifests itself as polarization fading, is present, as evidenced by the split in the upper ray of the $1F_2$ mode and the severe fading on the IRIG tones, which, however, delivered good data to the time code reader. The ALQA measured a 0.3-ms spread on the selected channel for reasons not evident. The IRIG signal is badly distorted, probably by the polarization fading.

As the night progresses (Figures 14 and 15), the MOF drops and SELSCAN follows it. At 0300 hr on the path, the MOF has dropped to

4	17	18	15,17	16	14	1	CR LOA
17	1	18	1,18	18	1	1	MP LOA
1	2	3	4,5	6	7	8	SELSKAN CHANNEL



QUALITY OF SELECTED CHANNEL

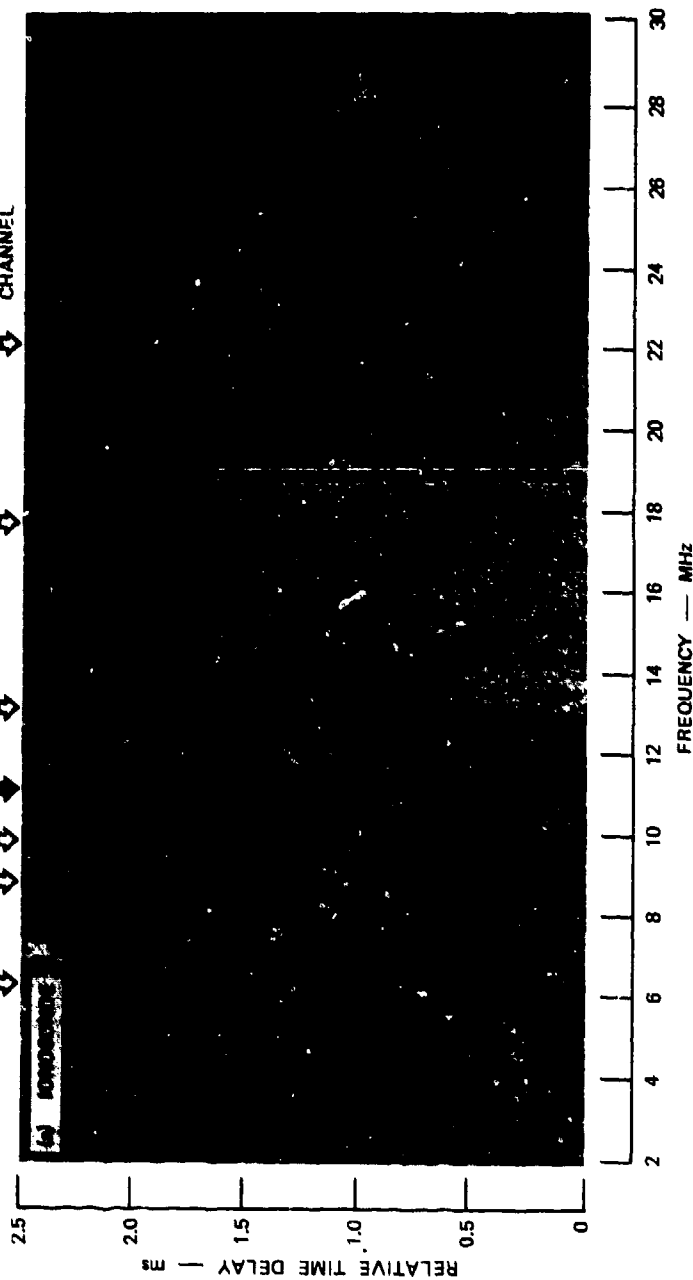
ALO: $SNR_0 = 39.8 \text{ dB}$
 $\Delta T = 0.9 \text{ ms}$

VOICE: CR 05
 MP 04

10 ms

FIGURE 12 DATA FOR 0530 UT (2230-hr MIDPATH), 20 JUNE 1984

1	18	18	11,18	1	6	1	CR LOA
16	1	18	11,18	6	1	1	MP LOA
1	2	3	4,5	6	7	8	SESCAN CHANNEL



QUALITY OF SELECTED CHANNEL

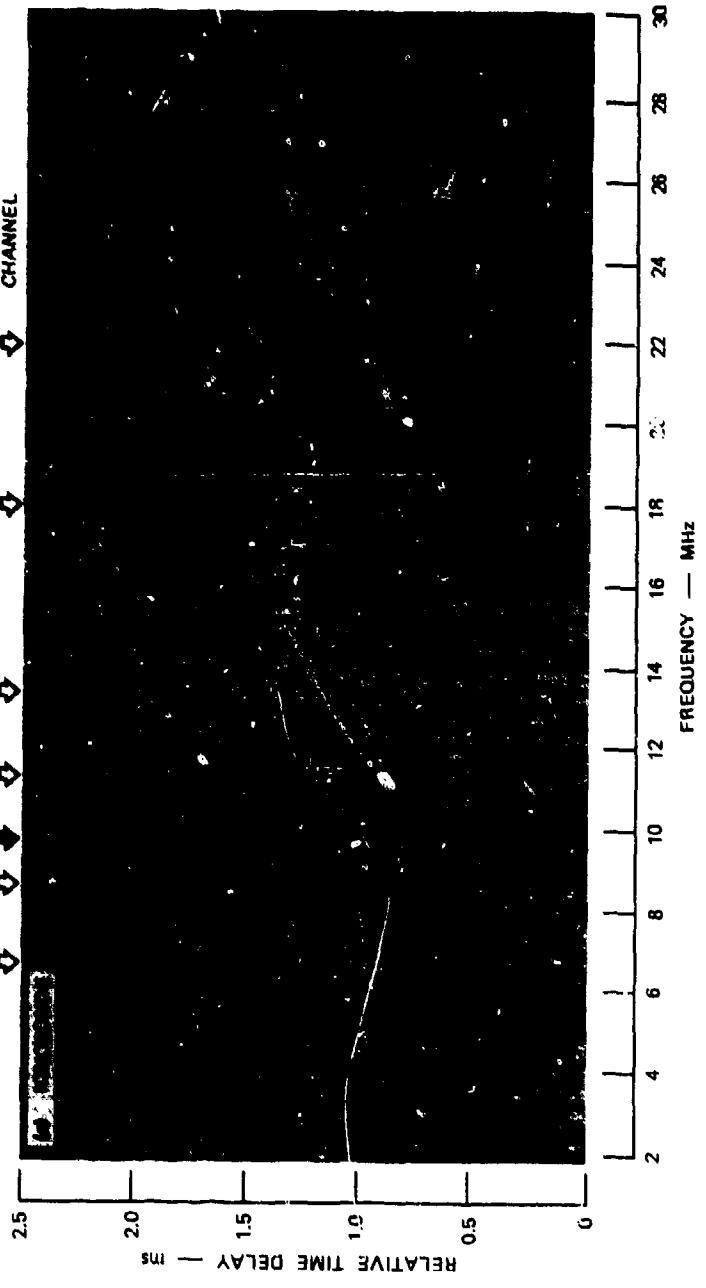
ALOA: $SNR_0 = 51.5 \text{ dB}$
 $\Delta T = 0.3 \text{ ms}$

VOICE: CR O4
 MP O4



FIGURE 13 DATA FOR 0700 UT (MIDNIGHT MIDPATH), 20 JUNE 1984

8	17	17	17	12,1	1	1	1	1	CR LOA
17	17	17	18	1,1	1	1	1	1	MP LOA
1	2	3	4,5	6	7	8	8	8	SESCAN CHANNEL



QUALITY OF SELECTED CHANNEL

ALOA: $SNR_o = 31.7 \text{ dB}$
 $\Delta T = 2.3 \text{ ms}$

VOICE: CR 03
 MP 04

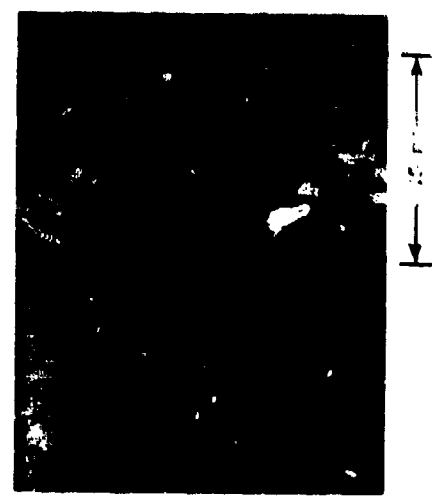
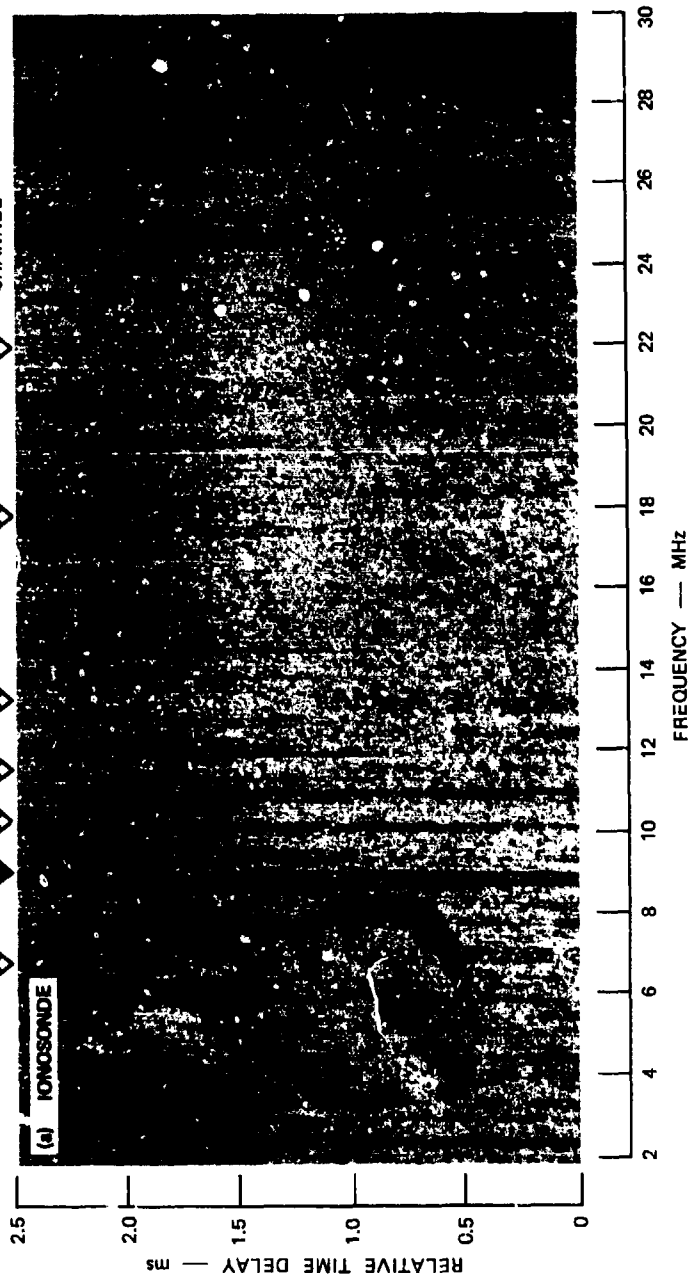


FIGURE 14 DATA FOR 0930 UT (0230-hr MIDPATH), 20 JUNE 1984

7	15	4	9,1	1	1	1	CR LOA
14	18	1	1,1	1	1	1	MP LOA
1	2	3	4,5	6	7	8	SESCAN CHANNEL



QUALITY OF SELECTED CHANNEL

ALOA: $SNR_0 = 51.9 \text{ dB}$
 $\Delta T = 0.2 \text{ ms}$

VOICE: CR Q3
 MP Q3



10 ms

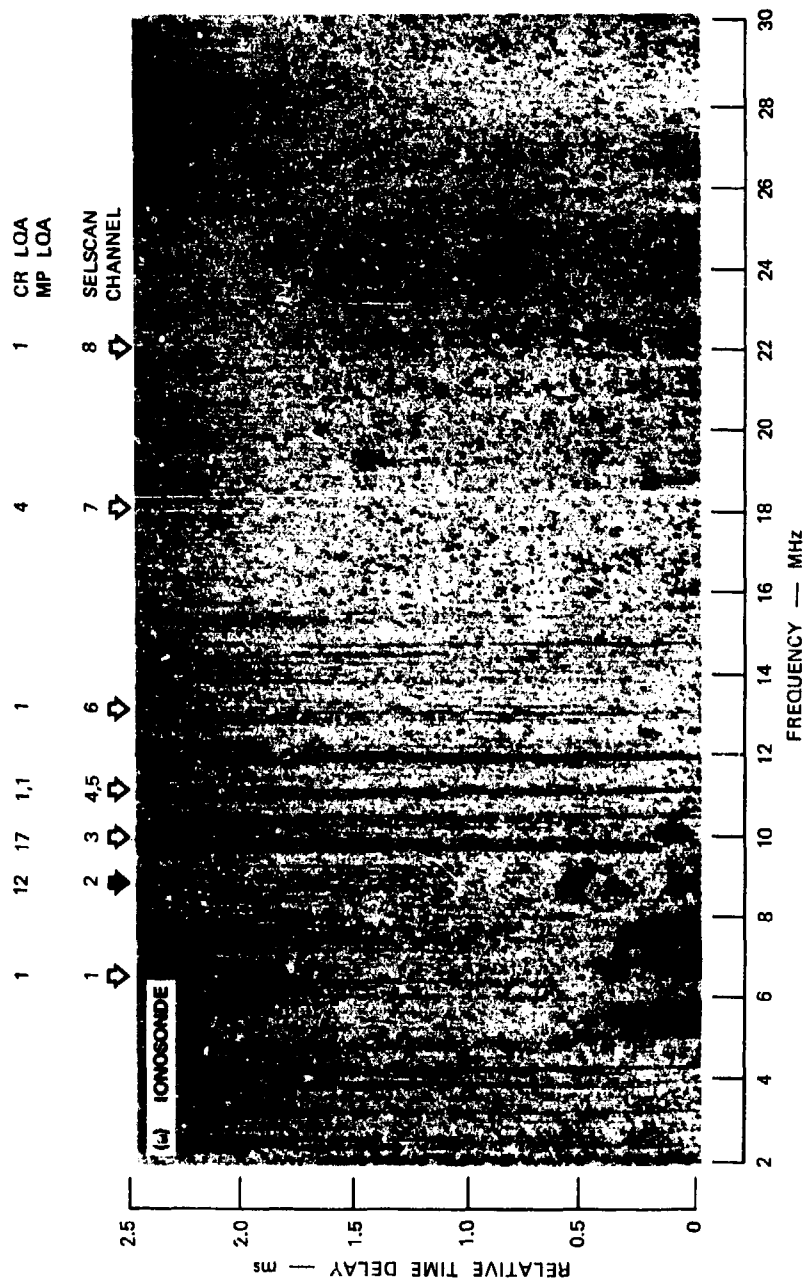
FIGURE 15 DATA FOR 1000 UT (0300-hr MIDPATH), 20 JUNE 1984

about 8.5 MHz as indicated by the ionogram, and SELSCAN found a fair channel at 8.822 MHz. It is interesting to note that the Cedar Rapids SELSCAN also found marginal channels at 10 and 11 MHz, while the Menlo Park unit found nothing at these frequencies. The operators examined these frequencies by locking out Channels 1 and 2 and attempting to relink. They could hear voice, but the units would not link reliably. One link was established on 10.045 MHz but dropped out after 30 s. We do not know if these results were caused by the general quality of the channel or by the apparent nonreciprocity in which Cedar Rapids could hear and measure the Menlo Park signal, but not the reverse, as evidenced by both the MP LQA and the ionogram. The IRIG signals were completely different on these two runs, illustrating the variability of channel characteristics at frequencies very near the MOF. Experienced operators prefer to operate about 10 percent below the MOF, partly for this reason. The other reason is that small fluctuations in MOF can cause a circuit at the MOF to drop in and out.

The predawn period is represented by Figure 16 at 0440 hr on the path. Conditions are about as bad as were observed at any time during the tests, as is normally expected. Unfortunately, during this period, the ionogram display drifted to the point that the signal appears at one edge of the time window, with the result that we can not be sure of the total mode structure. The Cedar Rapids LQA, in this case, is the best indication of propagation. The Menlo Park LQA was not recorded. During this first day of routine operation, the links were being initiated from Menlo Park, which explains the selection of the second best channel as observed at Cedar Rapids. The resulting channel was only fair, but usable.

With the coming of dawn, Figure 17, 0630 hr on the path, the MOF starts to rise, and SELSCAN follows it, finding an excellent channel.

By 0900 hr on the path, Figure 18, the daytime pattern has reestablished itself. The earliest arriving mode is possibly sporadic E, as suggested by its gradual disappearance without an upper ray with increasing frequency, or a reflection from the F_1 layer. SELSCAN



QUALITY OF SELECTED CHANNEL

ALQA: $SNR_0 = 33.0 \text{ dB}$
 $\Delta T = 1.0 \text{ ms}$

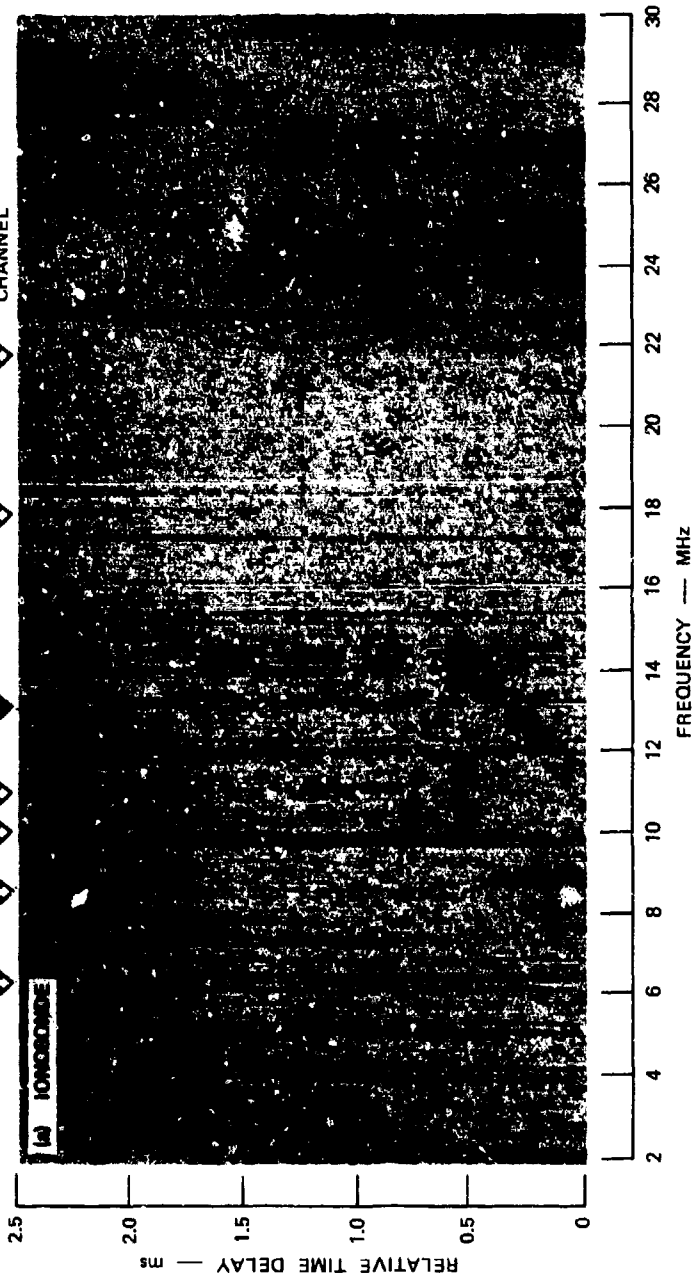
VOICE: CR Q4
 MP Q3-4

(b) IRIG PULSES

NO DATA

FIGURE 16 DATA FOR 1140 UT (0440-hr MIDPATH), 14 JUNE 1984

1	4	12	17,18	17	1	1	CR LOA
1	8	17	1,17	18	1	1	MP LOA
1	2	3	4,5	6	7	8	SELSKAN CHANNEL



QUALITY OF SELECTED CHANNEL

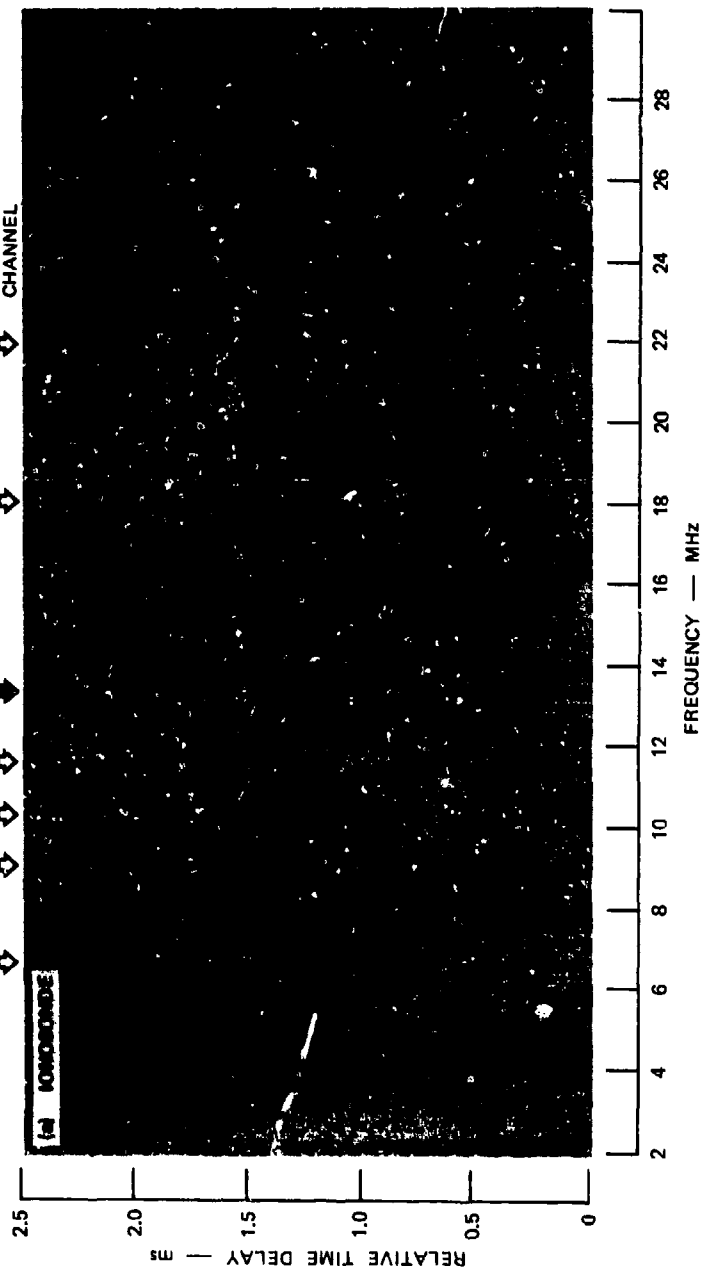
ALQA: SNR₀ = 49.3 dB
 ΔT = 0.2 ms

VOICE: CR Q5
 MP Q5



FIGURE 17 DATA FOR 1330 UT (0630-hr MIDPATH), 14 JUNE 1984

1	5	1	6,9	16	5	9	CR LOA
1	16	12	15,17	18	18	2	MP LOA
1	2	3	4,5	6	7	8	SESCAN CHANNEL



QUALITY OF SELECTED CHANNEL

ALOA: $SNR_0 = 37.6 \text{ dB}$
 $\Delta T = 0.6 \text{ ms}$

VOICE: CR Q4
 MP Q5



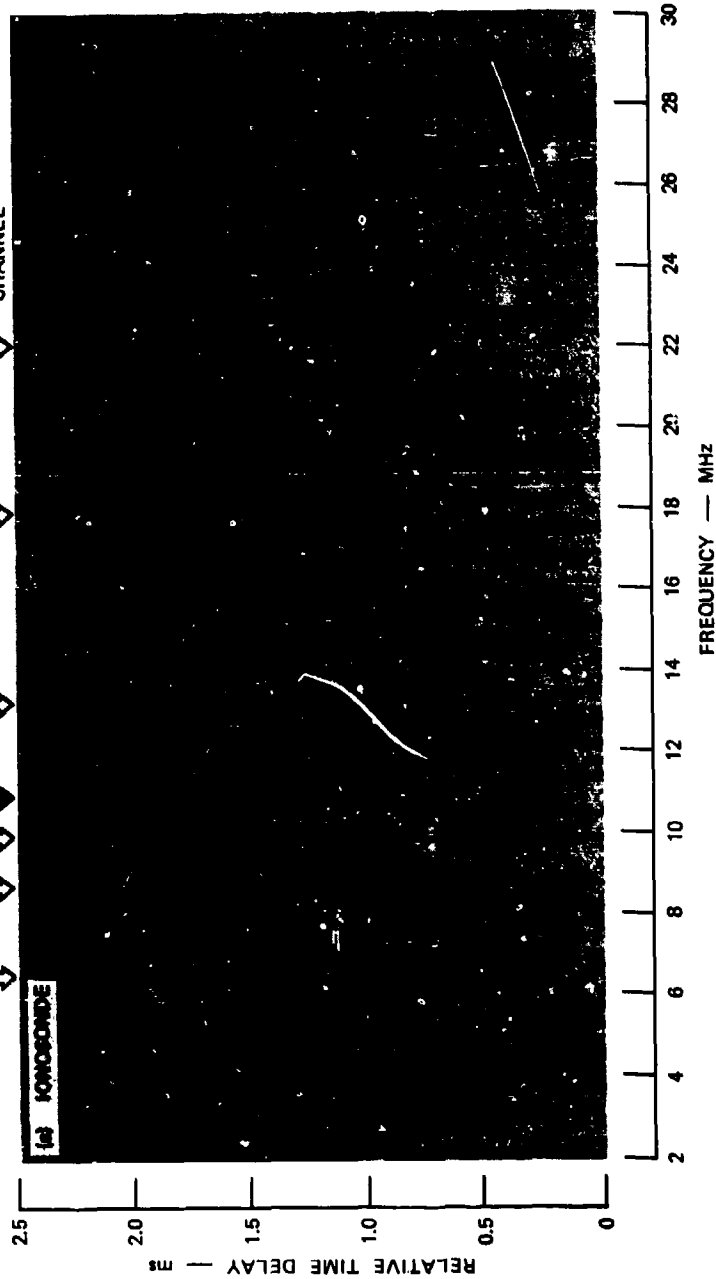
10 ms

FIGURE 18 DATA FOR 1600 UT (0900-hr MIDPATH), 26 JUNE 1984

selects 13 MHz, which seems from the ionogram to emphasize the F_2 mode. The resulting channel is good to excellent. The ALQA multipath measurement, of 0.6 ms, agrees with the ionogram, as is usually the case.

At 1030 hr on the path, Figure 19, the same two daytime modes as before are present, with what looks like good propagation at 18 MHz, Channel 7. SELSCAN, however, rates that frequency only 10 at Cedar Rapids, possibly because of interference. The same channel was rated at 18, the highest possible value, at Menlo Park. The system, under direction of the Cedar Rapids terminal, selected Channel 5, at 11.3 MHz. This channel was rated in the LQA as 17, which is very good, at both ends, but the operator's assessment of the voice quality was only Q3 at both ends. The IRIG tones were badly distorted as well. This is one of the few instances in which an operator viewing the ionogram would probably have selected a different frequency from that selected by SELSCAN. Without having tried one of these alternate frequencies, it is impossible to say whether such a choice would have been better.

1	1	3	17,17	4	10	1	CR LOA
1	8	15	17,17	18	18	12	MP LOA
1	2	3	4.5	6	7	8	SESCAN CHANNEL



QUALITY OF SELECTED CHANNEL

ALOA: $SNR_0 = 34.1 \text{ dB}$
 $\Delta T = 0.7 \text{ ms}$

VOICE: CR O3
 MP O3



10 ms

FIGURE 19 DATA FOR 1730 UT (1030-hr MIDPATH), 26 JUNE 1984

SECTION 6

CONCLUSIONS FROM THE EXPERIMENT

The first conclusion that can be drawn from the SELSCAN tests is that SELSCAN works well, even with limited propagation. In addition to always finding a frequency that provided generally good communication, it was usually able to measure the quality of all the assigned frequencies that the ionogram showed as potentially usable. Its performance in conditions of severe distortion, however, has not been explored. The SELSCAN hardware, even though developmental, worked without any problems.

The necessity of transmitting an LQA-update scan from each end of the link before making a regular call suggests that the performance of the present implementation of SELSCAN is better than it would be if it were operated in a mode in which the radios remained silent for long periods. In such a case, SELSCAN would probably simply start scanning at the lowest frequency in its list, and stop on the first channel on which a link was possible. The results of this test indicate that a channel selected this way would not always be the best one possible. This is not a serious problem because a simple addition to the software that recognized the condition of the LQA being out of date could cause an LQA update scan to be made automatically as part of the linkup process, once a workable frequency is found, with a subsequent shift to the optimum frequency. The operators would not need to be aware of this process.

The greatest difficulty in establishing the link was a series of problems not related to the SELSCAN itself, but to the remaining rf hardware, which would be a necessary part of any operational system. Setting up the link took several days in which a faulty power amplifier, excessively lossy coaxial cable, and a misdirected antenna had to be found and fixed. The hardest part of this problem was for everyone

concerned to realize that very poor performance was caused by equipment, not by propagation. This difficulty is mentioned not in accusation, but to recognize that similar problems will afflict any radio system that is nominally automatic, and that is left in a standby condition for use principally in an emergency. In our case, a link using the test radios at one end of the path, and the test radios and an independent set in an A-to-B comparison at the other, was used to locate the problems.

To generalize from our experience, we can say that an automatic adaptive radio, such as SELSCAN, can provide a valuable service as an order wire or for substantive communications, but means for verifying and troubleshooting the entire end-to-end link must be provided, especially in applications in which the radios are not used often or by professional communicators. Built-in test equipment (BITE), as specified in modern military equipment, is necessary but is not sufficient. Current standards for BITE incorporate only radio boxes as individual units. The ARC-190 is an example. Even here, there is room for improvement; one of the ARC-190s was delivering low output power for some time before the operator became aware of the fact. However, even if the box BITE were perfect, there would still be a need to confirm proper operation of the remainder of the RF chain.

SECTION 7

APPROACHES TO MITIGATING PROPAGATION DISTURBANCES

Three fundamentally different kinds of propagation disturbance must be addressed in planning an HF system to be used during nuclear warfare. These are as follows:

- Absorption
- Rapid changes in frequency support
- Distortion.

Channel congestion and jamming may also be factors, but constitute a separate, nonpropagation category.

Of the three propagation disturbances, absorption is best understood and modeled. Programs such as NUCOM can predict absorption to much better accuracy than the uncertainty inherent in the possible range of attack scenarios. In a nutshell, absorption from attacks that include high-altitude weapons can impose hundreds of decibel of loss on HF paths. The loss will persist longest in areas subject to intense but localized debris radiation and at relatively lower frequencies. The most effective approach to overcoming such absorption is to provide a network that is as widely dispersed geographically and as adaptive in frequency and routing as is affordable. Absorption, particularly of the long-lasting kind, is expected to be highly variable in location, and the effect of absorption is least at higher frequencies. Links that avoid patches of high loss, and that are operated on the highest frequency that will propagate, will, therefore, provide service hours or days before paths that traverse these areas and attempt to use lower frequencies. The implication is that flexible connectivity and routing that permits use of roundabout circuits is an important mitigating technique. Adaptive radios of the frequency-finding kind will be especially helpful in this regard. A consequence of use of such flexible, indirect

routing is that a given network of equipment will probably be used rather inefficiently compared to its capacity when routing is more direct. The design of network access and traffic loading must take this into account.

Aside from the fact that absorption is worse at low frequencies, traveling waves from a nuclear explosion cause compression and expansion of the ionosphere with periods of several tens of minutes, or less. When these waves are strong, the ionospheric support frequency can change by factors of two or more. For a radio link to be effective when absorption is higher than normal, it must follow these changes as closely as possible. Our experience with the SELSCAN, and by implication any similar frequency-finding technique, suggests that it is marginally adequate to follow the faster traveling disturbances. SELSCAN is probably an optimum economic approach to all but the most demanding applications. An approach that would respond faster would be to operate oblique sounders, such as the AN/TRQ-35, continuously on a five-minute scan both ways on all links. A computer would have to analyze the ionograms and make and execute decisions to change frequency. Although there is no question that such a system could be built, and perhaps should be for some applications, it will certainly be much more expensive than the SELSCAN type of link and will require much more extensive network coordination.

An alternative approach to mitigating the effects of traveling waves and the frequency variable nature of absorption is to, in effect, use all frequencies all the time. When the criterion is to provide connectivity, without much regard for capacity, this is clearly the optimum approach. It will deliver a short message if any propagation is possible at all, and without explicit coordination of frequency use. The cost, of course, is in efficiency. The ITT NEW LOOK and the B/R CHIRPCOM are examples of this approach. For delivering very short messages, or serving as order wires for higher capacity links, they are close to optimum, especially when provided with powerful error detection and correction techniques.

The final category of nuclear-induced disturbance is signal distortion. This effect is usually considered last and is scarcely modeled at all. The kinds of distortion expected to be encountered include excess discrete multipath caused by off-great-circle reflections from nuclear-induced ionization, and spread multipath and spread Doppler shift from reflections from or through excess ionization concentrated along magnetic field lines, both on and off the direct path. The magnitude and degree of occurrence of these effects are not well known at all. The amount of mitigation that is economically justified for a communication signal is therefore also not well definable. For design of frequency-finding adaptive radios, there is the additional problem, discussed in Appendix C, of whether to make the probing signal as robust as possible, or make it mimic the susceptibilities of the communication signal that will ultimately use the channel. Simply using the communication signal itself is not a good approach because it will seldom have the rapid synchronizing or unique identifying capabilities needed for a rapidly scanning probe.

Without depreciating the importance of developing effective and economical channel equalizing techniques, it is worth remembering that substantial benefit is often available from avoiding distortion by using a different frequency. Frequency-finding AHF can therefore contribute indirectly to improving channel quality.

SECTION 8

CONCLUSIONS

The basic conclusion from this investigation is that adaptive HF radios of the frequency-finding kind exemplified by SELSCAN are quite effective in accomplishing their intended function. Though we were unable to stress the system under test in respect to multipath and Doppler shift as much as necessary to predict performance in nuclear, or even auroral, conditions, nor to experiment with a range of waveforms, the performance of the SELSCAN in periods of very limited propagation leads to the conclusion that as it is, it should contribute significantly to connectivity of dispersed forces following nuclear attack. Although improvements to the frequency-finding technique are undoubtedly possible and should be pursued, the presently available techniques appear to be so much better than manual methods and should be so much less expensive than approaches based on full-scale sounding and computer control that they should be seriously considered for immediate deployment.

REFERENCES

1. N. F. Chang, J. W. Ames, and G. Smith, "An Adaptive Automatic HF Radio," Final Report, DNA 5507F, Contract DNA001-79-C-0364, SRI Project 8710, SRI International, Menlo Park, CA (December 1980).
2. HFDM: AN/USQ-83(XH-1)(V), The High Frequency Digital Modem, Operation and Maintenance Manual, Sylvania Systems Group, Needham Heights, MA. (See also NAVELEX document, High-Frequency Digital Modem, Technical Objectives and Goals, April 1979, or later issues.)
3. A. W. Rihaczek, Principles of High Resolution Radar (McGraw Hill Book Company, New York, New York, 1969).
4. "Performance Specification for the ANDVT Tactical Terminal," Specification No. TT-B1-4210-0087B, Joint Tactical Communications Office, Fort Monmouth, NJ (30 January 1981).
5. K. Klemba, D. Nielson, J. Tornow, "Packet Radio Network--Executive Summary," Report IPTO-83-7, DARPA, Arlington, VA (July 1983).
6. V. Ellins, P. Anderson, and M. Sandler, "HF Wideband Modem," GTE Sylvania Final Technical Report, RADC-TR-82-85, prepared for Rome Air Development Center, Griffiss Air Force Base, New York (April 1982).

Appendix A

ENCODER-DECODER-CONTROLLER DESIGN FOR THE ADAPTIVE AUTOMATIC HF RADIO N. J. F. Chang

1. Introduction

This appendix documents the design of the major functional modules for use in the adaptive high-frequency (HF) radio. The design is in the form of schematic diagrams, detailed block diagrams, timing diagrams, and software flow charts. The objective of this design effort is to specify the principal components, interfaces, and software functions needed to produce a test bed for the adaptive concept described in Chang et al.¹ Because two of the program's objectives are to evaluate various signaling waveforms and different processing algorithms, the design relies on programmed logic to implement many signal-processing functions, logic functions, and the signaling waveforms. Although this approach may not produce an optimum operating system in terms of hardware cost and operational speed, it offers advantages over realizing the various functions with discrete electronic components. First, the construction cost is less because the time-consuming task of designing and building breadboards is largely replaced by programming, which is more cost effective. Second, because program changes can easily be made, design modifications are accomplished with a minimum of time and cost.

a. General Description of Functional Modules

The overall system block diagram of the adaptive HF radio in its original form is shown in Figure A-1. Transmitter, receiver, and T/R switching functions are provided by a Collins KWM-380 transceiver modified to accept an external digital modulation and to provide AGC and IF outputs. Although the prototype radio uses PSK modulation, other types of modulation like FSK, or chirp can also be used to test propagation effects on the different waveforms.

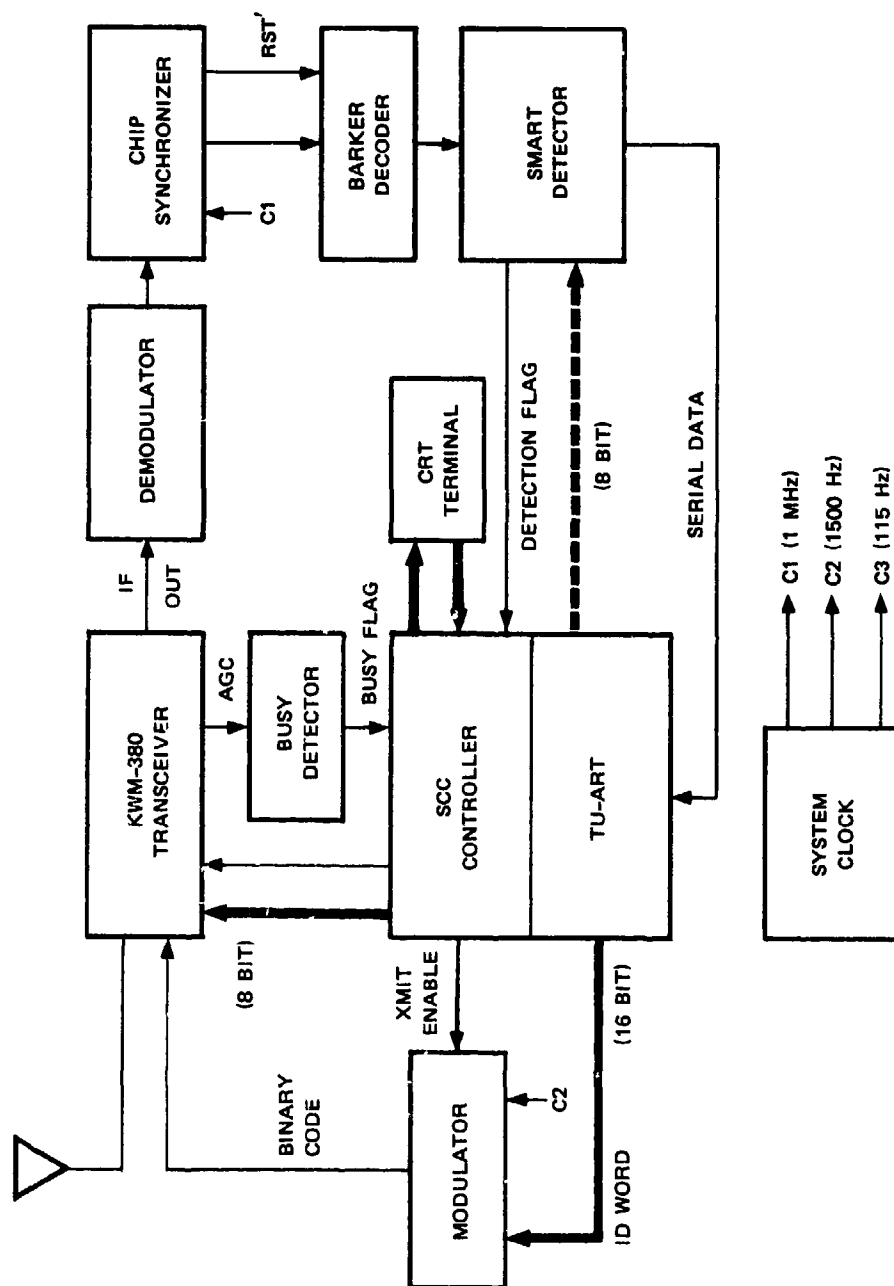


FIGURE A-1 SYSTEM BLOCK DIAGRAM OF THE ADAPTIVE HF RADIO

The Collins KWM-380 is equipped with an interface that permits the unit to be externally controlled. The controller is a CROMEMCO single-card computer (SCC), which is a Z80A-based, S-100-bus microcomputer subsystem. The single-card computer contains interrupt inputs and both parallel and serial I/O ports. The bus structure of the SCC allows other cards to be easily added to the system to expand its capability.

Additional parallel and serial I/O ports are provided by a CROMEMCO twin universal-asynchronous receiver/transmitter (TU-ART) digital interface card. This card provides the necessary I/O ports and handshaking lines to translate between parallel and serial data streams. In particular, the TU-ART card handles generating and decoding the 6-bit ASCII data words used for signaling.

The Barker decoder and the smart detector are each implemented with separate INTEL 2920 signal processors. Software coding of a 13-bit Barker correlator requires only 56 steps of code. Because 192 steps are available, the correlator function is well within the capability of the INTEL 2920. The availability of excess steps provides increased flexibility in implementing additional functions and, more importantly, provides a hedge against the necessity of adding more lines of code for program refinement.

The algorithm used in the smart detector module ignores all signals below a given threshold and outputs a mark or space only if two consecutive inputs (separated by an intersymbol period) are above the threshold. The detector also contains logic to resolve the mark-space ambiguity by a preamble. Coding of the smart detector software requires slightly more than a hundred instruction steps for the INTEL 2920.

The Costas demodulator, the modulator, and chip synchronizer are all realized with discrete integrated circuits although it is likely that a single-card microprocessor can also be used for the last two modules. System timing is provided by clock signals from a crystal oscillator. The basic clock signals are C1, a 1.0-MHz output; C2, the chip rate of the spreading modulation (1500 Hz); and C3, the bit rate of the data word (115 Hz).

b. Major Signal and Control Lines

Major signal and control lines for the adaptive radio are also shown in Figure A-1. In the prototype radio, the CRT terminal provides the principal interface between man and computer; it will be replaced with switches and visual indicators in an operational radio.

Data transfer between the controller and modulator is provided by two 8-bit parallel lines. The number enclosed in parentheses signifies the total number of bits carried by that line. Operating frequencies stored in memory are provided to the Collins KWM-380 through an 8-bit parallel port. In addition an XMIT/REC' line is used to change between transmit and receive. (The prime identifies a function that is true when the line is low. Correspondingly, no prime identifies a function that is true when the line is high. Thus, REC' is active when the line is low, and XMIT is active when the line is high.) The AGC line from the Collins KWM-380 is used to determine whether a particular channel is available or busy. For initial testing of the signaling technique, the busy detector module is a threshold detector, but a more sophisticated method will likely be needed to determine channel availability in later system testing.

The flag provided by the smart detector indicates successful correlation between a received signal and the code stored in the Barker decoder. The noise threshold against which the signal is detected will vary with frequency and time of day. The busy detector, therefore, determines the noise level and passes it to the SCC, which uses these values to establish a threshold for each channel. These threshold values are provided to the detection logic module through a parallel output port as shown.

System timing for the CALL sequence is shown in Figure A-1. When the ID of the desired station is entered in the CRT terminal and the CALL button pressed, the CALL/LISTEN line goes high (Logic 1). After an allotted delay for transmitter tuning, the AGC level is checked to ensure that the channel is clear. If the channel is clear, the XMIT-enable line goes high for the transmission of N two-character ID words.

The radio then reverts to the QUERY mode during the interval that the QUERY-enable line is high. If there is no response, the above sequence is repeated on the next channel and so on until either a response is obtained, or until all assigned channels are exhausted. In the latter case the entire cycle is repeated indefinitely until contact is established, or until the attempt is aborted.

Three counters are indicated in Figure A-2. One counter provides a delay for transmitter tuning, the second counts the number of ID words transmitted and thus establishes the duration of the XMIT-enable control signal. The third counter sets the duration of the QUERY mode. In general, counters can be implemented either through hardware or software. When timing is critical, digital hardware counters with interrupts are generally required, but for less critical applications, software timers are attractive because of implementation ease. Although the timers in Figure A-2 can probably be implemented with software, the intimate interaction of hardware and software in a real-time system, such as the adaptive radio, prevents a final choice at this time.

A flow chart for the LISTEN mode software is shown in Figure A-3. This sequence is enabled when the CALL/LISTEN line of Figure A-2 is low. The LISTEN mode of the adaptive radio is not the same as the QUERY period in the CALL sequence: during this latter period, a response is sought in only one channel at a time. In the LISTEN mode all assigned channels are interrogated for the presence of call letters unique to that station. Because this LISTEN cycle of the receiver is less than the XMIT duration of the caller (Figure A-2) contact will generally be established within one signal CALL cycle--propagation conditions permitting.

2. Major Functional Modules

The major functional modules comprising the adaptive HF radio are described in this section. Because many of the modules consist of LSI components connected in a standard configuration, and because the functions are implemented by software, the details of these modules are

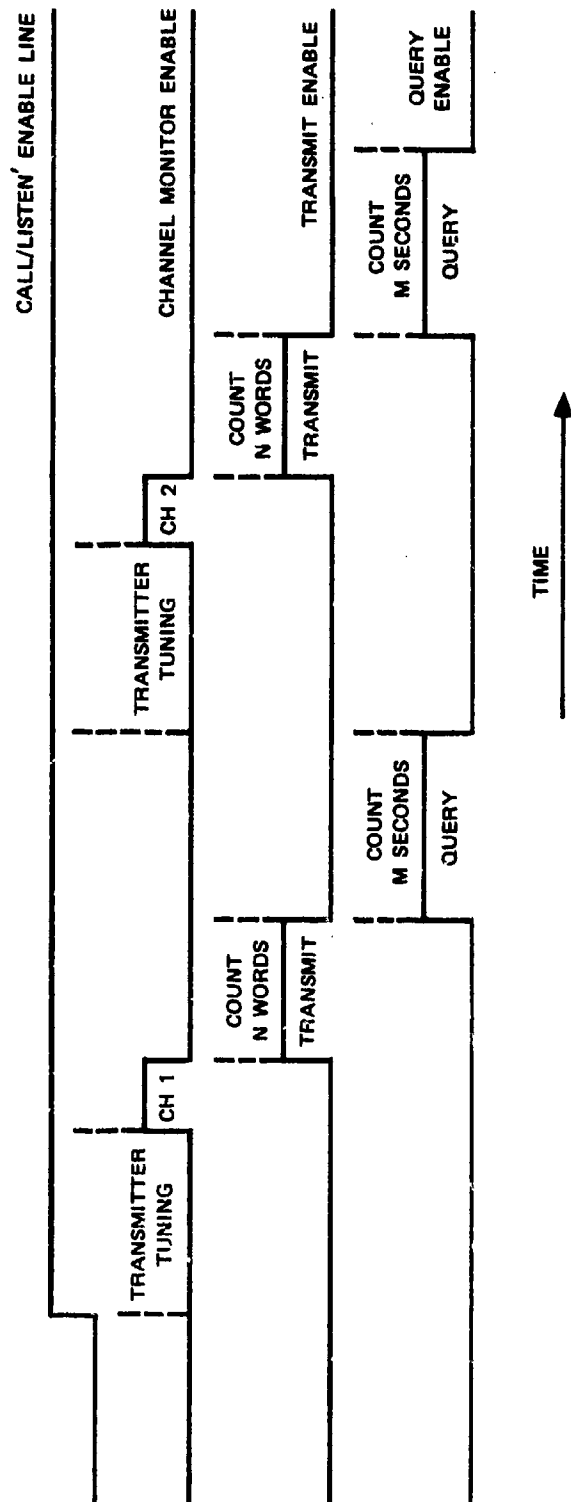


FIGURE A-2 TIMING FOR CALL SEQUENCE SHOWING TRANSMISSION OF N ID WORD GROUPS IN TWO CHANNELS

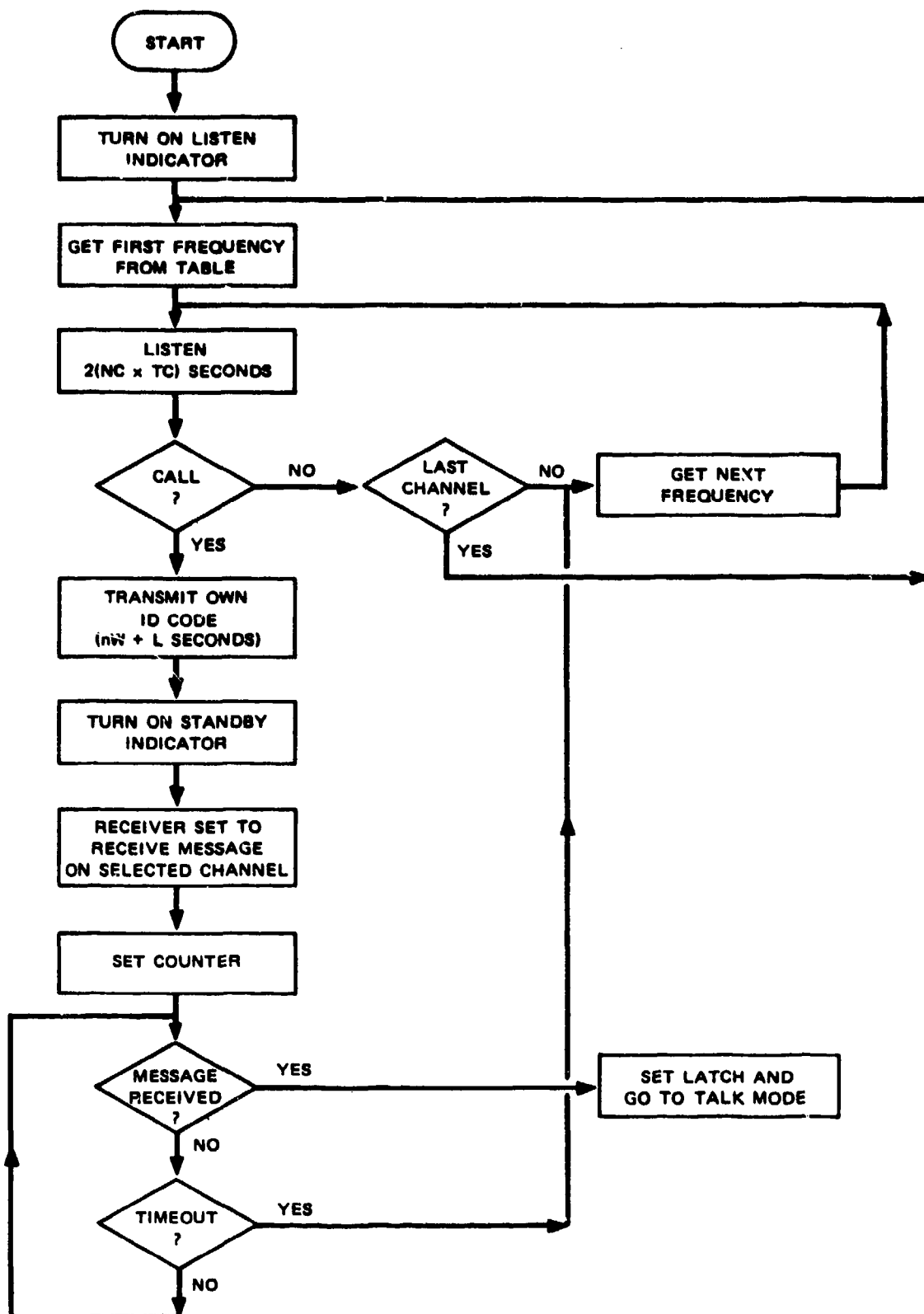


FIGURE A-3 FLOWCHART FOR LISTEN MODE

given in block-diagram form with detail timing diagrams where appropriate. The principal exceptions are the synchronous modulator, the demodulator, and the chip synchronizer, which are described at the component level. The functional requirements for these modules are contained in the Chang et al.¹ Reference to the pertinent report section is made where appropriate.

a. Microprocessor Controller

The heart of the adaptive HF radio is the microprocessor controller. The prototype radio will utilize a CROMEMCO SCC, along with a TU-ART card. These units were chosen because of their availability (DNA owned), and because the available parallel and serial I/O ports on the cards, plus existing firmware (CROMEMCO's Z80 monitor and 3K BASIC), provide the necessary hardware and software to assemble a test bed in the most economical manner.

A functional block diagram for the SCC is shown in Figure A-4. The SCC consists of three independent 8-bit parallel output ports and three independent 8-bit parallel input ports with the necessary handshake lines. The card also provides one RS-232 serial I/O port that will be used for a CRT terminal. The SCC also has five independent interval timers that can be used for various system timing. These timers will be used whenever possible to replace hardware timers.

The TU-ART card, shown as part of the controller in Figure A-1, provides two serial and two parallel input/output ports with interrupt capability. This card is the principal signal interface between the controller and the modulator and detection logic module.

b. Modulator

Implementation of the PSK modulation using TTL logic, shown in Figure A-5 (Chang et al.¹), contains further details on the modulator and waveform format. The 13-bit Barker code is parallel loaded into a recirculating shift register (74LS166) through a series of switches and Modulo 2 added to the ID data word through an exclusive OR gate (7486).

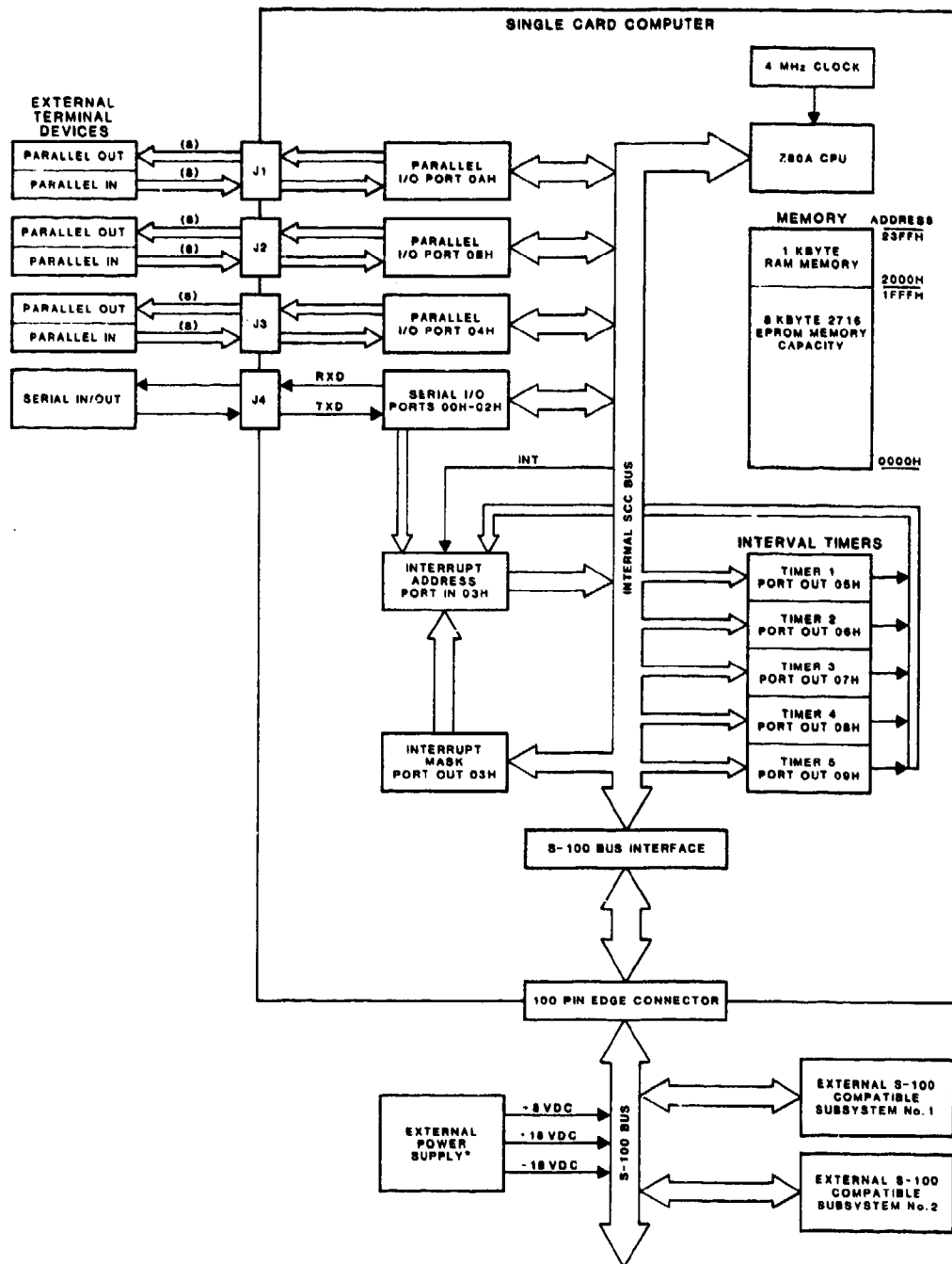


FIGURE A-4 SCC FUNCTIONAL BLOCK DIAGRAM

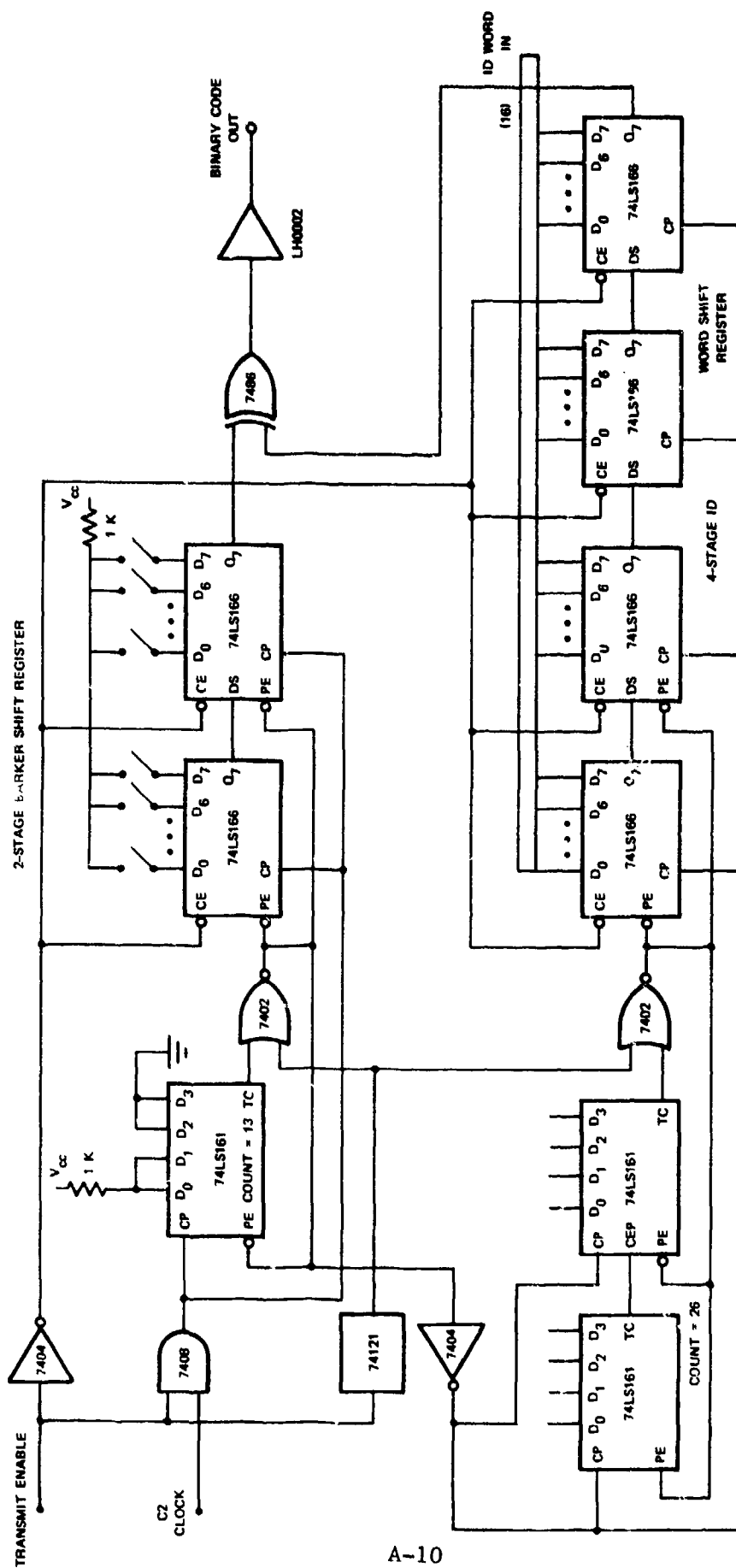


FIGURE A-5 PSK MODULATOR

The two-character ID word to be transmitted is brought into the modulator through two parallel output lines of the TU-ART card in the CROMEMCO controller. An ID word consists of an 8-bit preamble, two 6-bit ASCII characters with parity, start, and stop bits--a total of 26 bits. The preamble, start, and stop bits are loaded into the 4-stage shift register by means of "hardwire" lines (not shown in the schematic diagram).

Two 4-bit binary counters (74LS161) are used to provide the reload command for the two character ID word at a count of 26 clock cycles. The Barker code and the data word are loaded into their respective shift registers when the XMIT enable line goes high. This line also enables the C2 clock, which provides the timing for all subsequent operations. A single 4-bit binary counter (74LS161) reloads the spreading code at the conclusion of its count. Thus, the spreading code is continually cycled and synchronously loaded with the start of each data bit.

The output of the PSK modulator is shown as a binary code in Figure A-5. This signal is used to modulate the KWM-380 through a double balanced mixer installed in the transceiver.

c. Synchronous Demodulator

The function of the demodulator is to recover the modulation imposed on the received signal by the 1500-bps binary data. To recover this information in an optimum manner, coherent demodulation of the carrier signal is necessary, using a phase-coherent reference. This is accomplished in the Costas loop synchronous demodulator shown in Figure A-6. The characteristics of the loop in terms of its tracking accuracy and acquisition time are determined by the two low pass filters, the loop filter, and the gain of the amplifier preceding it. These parameters were set initially based on timing described in the Chang et al.¹ and then were optimized in response to experimental results.

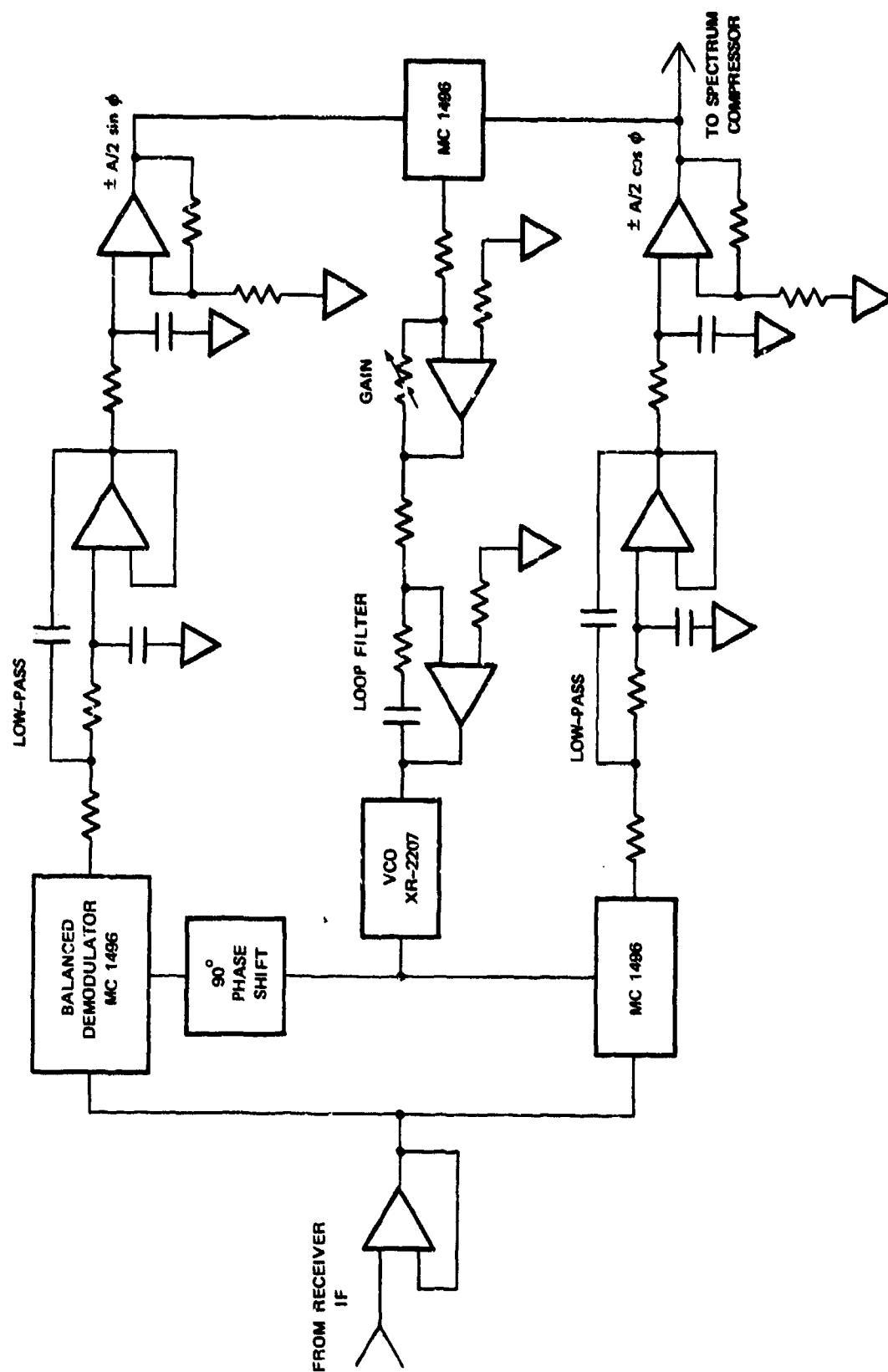


FIGURE A-6 SYNCHRONOUS DEMODULATOR

d. Chip Synchronizer

The chip synchronizer is used to synchronize the Barker decoder with the received signal. The output of this unit is a series of pulses closely matched with the received signal in both frequency and phase. The basic process is described in Chang et al., Section 6.4.3.¹

Hardware implementation of the chip synchronizer using a Burr-Brown 4085 peak detector is shown in Figure A-7. The input to the chip synchronizer is first detected by an absolute value circuit consisting of two operational amplifiers. This type of circuit is used to improve the accuracy of the detection for low-level signals. In normal detector circuits using diodes, detection will be inaccurate because of the voltage drop across the forward-bias diodes. When the diodes are placed in the feedback loop of the operational amplifier, this signal loss is reduced by the high gain of the amplifier.

The applied signal will consist of well defined peaks, or transitions, 30 percent of the time when a 13-bit Barker code is used. The peak detector will operate in the conventional manner and output a low-to-high transition at the occurrence of each peak (transition). This output transition triggers a one-shot multivibrator (74123), which in turn resets the peak detector through its Q and Q' outputs. The peak detector outputs a sampling pulse, which also resets the divide-by-m counter. When there is no phase change (transitions) in the PSK waveform for two or more consecutive chips, a peak will not occur within a chip interval and the sampling pulse will be generated by the divide-by-m counter.

To illustrate the operation and timing, assume that the 13-bit Barker code is derived from a 1500-Hz clock. Two consecutive peaks detected with the peak detector should be separated by very nearly the clock period or 0.667 ms. A clock started at the occurrence of one of these peaks will take m microseconds to count m cycles of the 1.0 MHz clock. Thus, if $m = 668$ and a peak is not detected, the divide-by-m counter will complete its count and output a pulse in 0.668 ms. Once a peak is detected, the divide-by-m counter will provide the sampling

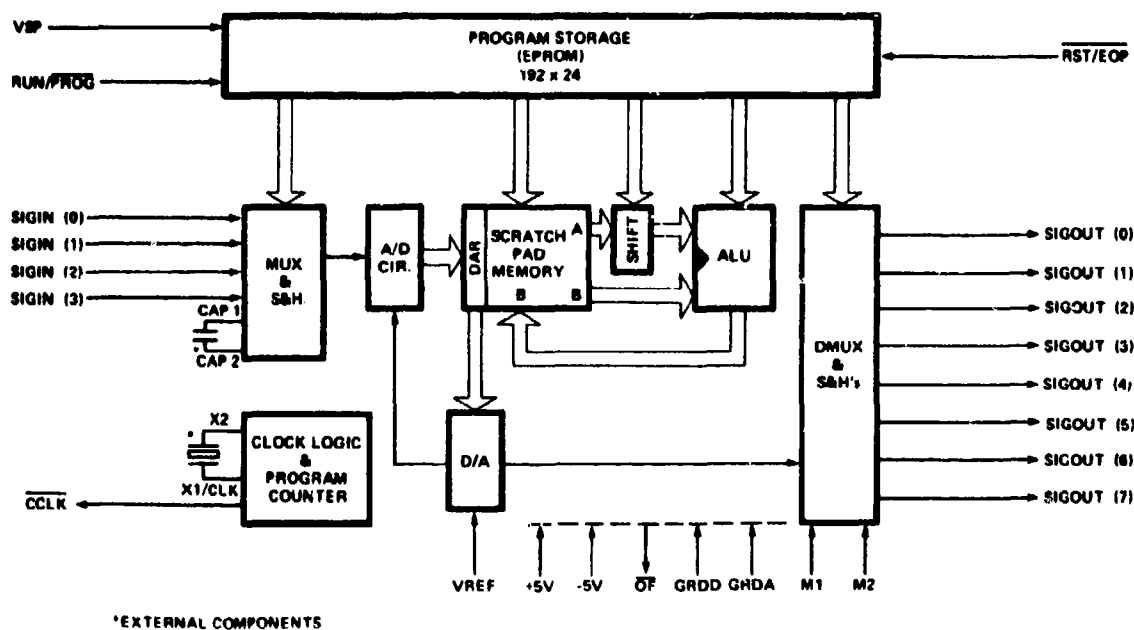
pulse unless it is overridden by the peak detector. The exact value of m will depend on the amount of hysteresis added to the Burr-Brown peak detector.

e. Barker Decoder

Figure A-8(a) shows a functional block diagram of the INTEL 2920 signal processor. The INTEL 2920 is divided into three major sections: (1) a program storage area implemented with an EPROM, (2) the arithmetic unit with RAM data memory, and (3) the analog I/O section.

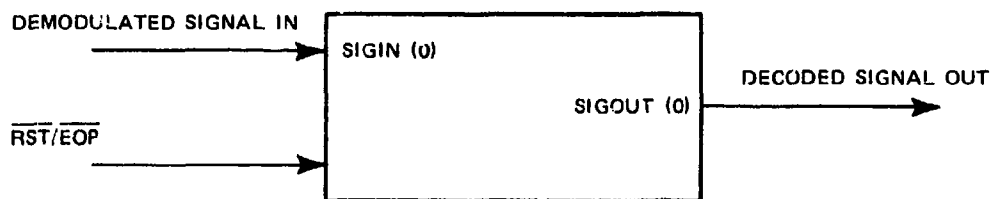
The analog section performs analog-to-digital (A/D) and digital-to-analog (D/A) conversions upon commands from instructions stored in the EPROM. The analog section includes: (1) an input multiplexer with four inputs, (2) an input sample-and-hold circuit and an A/D converter, (3) a D/A converter, and (4) an output multiplexer with eight output sample-and-hold circuits. A special register, called the digital/analog register (DAR), acts as an interface between the digital and analog sections.

The basic signal and control lines that are necessary in the Barker decoder are shown in Figure A-8(b). The demodulated signal will be sampled at a time determined by the RST^*/EOP^* input. (A low RST^* input initializes the program counter to the first location. An output EOP^* signifies an end of program instruction preset.) The sampling rate of this line is approximately equal to the chip rate of the PSK modulation (1500 Hz), which means that the INTEL 2920 must complete all calculations on each sample and output the results within 0.667 ms. The rate is well within the capability of the INTEL 2920 even if all 192 instructions are used. Although the INTEL 2920 can be operated synchronously by means of an external clock, current plans are to use an internal clock and provide synchronization with the RST^*/EOP^* input. Additional details on the Barker decoder can be found in Chang et al.¹



(a) INTL 2920 SIGNAL PROCESSOR (RUN MODE)

Source: INTEL 2920 Data Sheet



(b) SIGNAL AND CONTROL LINES FOR THE BARKER DECODER

FIGURE A-8 FUNCTIONAL BLOCK DIAGRAM

f. Smart Detector

The logic to recognize a valid signal is performed by the smart detector. The algorithm is based on the assumption that the ray paths constituting an HF path will not change appreciably in an intersymbol period.¹ Only signals above a given threshold are considered, and these, in turn, must correlate with an earlier sample, separated by an intersymbol period. The smart detector is implemented in a separate INTEL 2920 signal processor. This device is particularly attractive because it can be easily changed to test different algorithms.

Appendix B

CURRENT STATUS OF THE HARDWARE AND SOFTWARE OF THE AHF TEST BED
N. J. F. Chang1. System Description

A block diagram of the adaptive radio is shown in Figure B-1. The radio is similar to that described in Chang, Ames, and Smith,¹ except that the Costas loop demodulator is replaced by an I & Q demodulator as shown in Figure B-2. This change was necessary because the nonlinear transfer function of the Costas loop caused the phase-lock loop to track the strongest received signal. Under strong fading condition, this causes time discontinuities in the received signals. The linear transfer function of the I & Q demodulator preserves the received waveforms and allows the detection software to contend with multimodes as discrete signals, provided that the system bandwidth is sufficient to resolve them.

As shown in Figure B-2, the 455 RCVD IF is converted to an in-phase component (I) and a quadrature component (Q). The quadrature channel of the Barker decoder is combined with the I channel to form an output that is related to the sum of the magnitude of the two decoded quadrature channels. (The magnitude of the signal is equal to the magnitude of the largest channel plus one-half the magnitude of the smaller channel.) This output is digitized and passed to the CROMEMCO computer as a 6-bit word.

a. PSK Modulator

The PSK modulator shown in Figure B-2 generates the PSK waveform that is routed to the Collins for transmission. The two character ID (Symbol 1 and 2) are passed from the CROMEMCO to the modulator and loaded in 2 8-bit buffers. The buffers are in turn loaded into shift

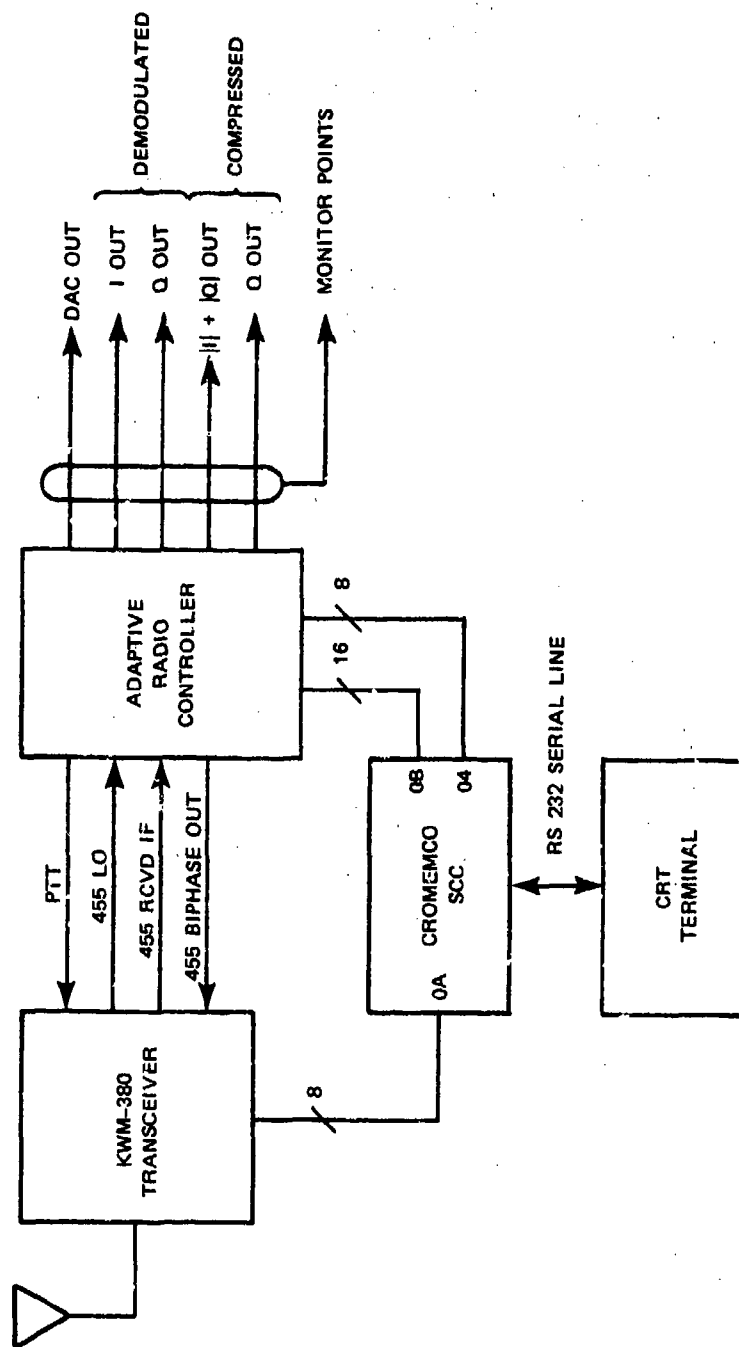


FIGURE 8-1 BLOCK DIAGRAM OF THE ADAPTIVE RADIO SYSTEM

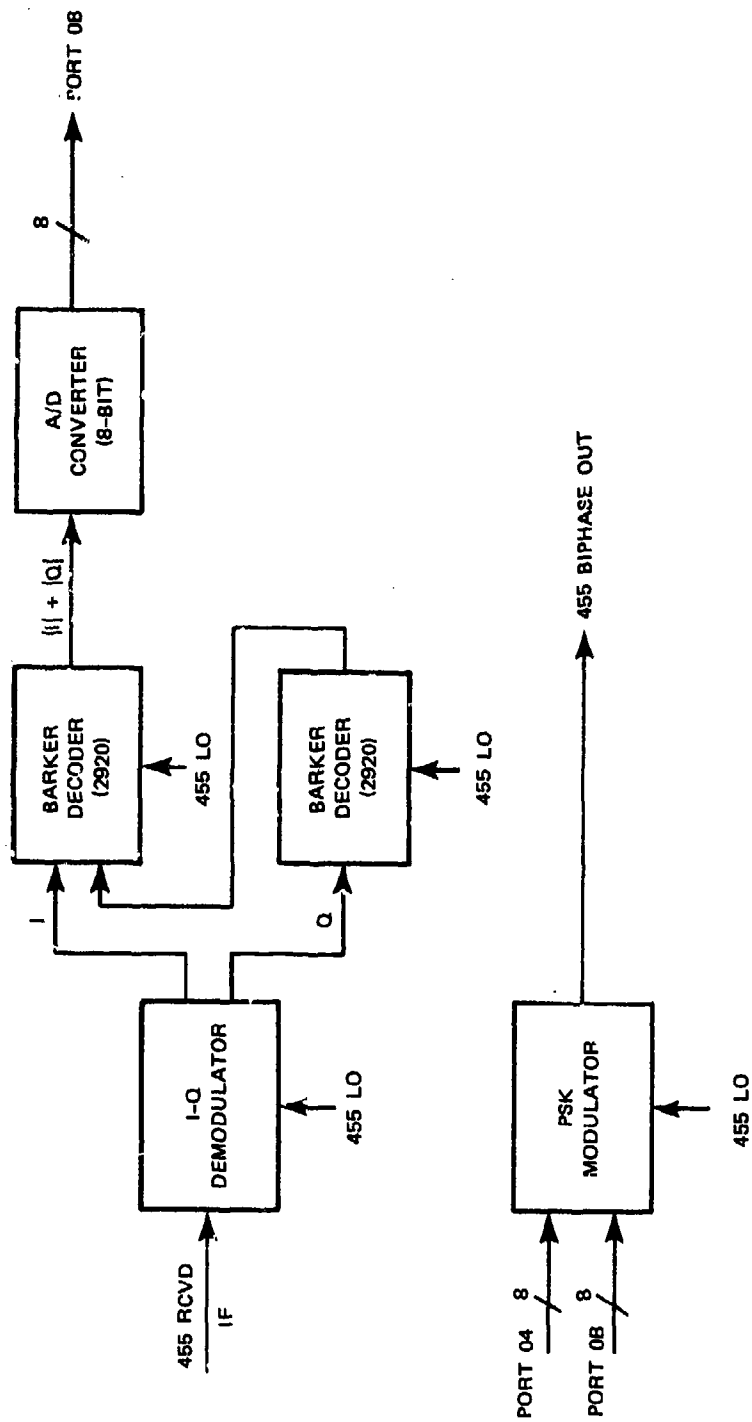


FIGURE B-2 BLOCK DIAGRAM OF THE ADAPTIVE RADIO CONTROLLER

registers along with an 8-bit preamble plus switch selectable start and stop bits. The length of this serial string is determined by an 8-bit counter. In the present configuration, a complete word (a two symbol ID) consists of 26 bits: an 8-bit preamble, 2 start bits, 2 stop bits, and 2 7-bit ASCII words.

b. I & Q Demodulator

The demodulator is constructed from two SL640 modulators connected to form a pair of double-balanced mixers. The quadrature phase shift between I & Q is provided by phase shifting the 455 kHz LO by means of an LC and an RC network.

c. Barker Decoder

1. Hardware Description--The decoder is based on a pair of 2920 analog signal processors. Externally these devices are analog (analog input and output), but the major internal functions are digital under control of an on-board microprocessor. The 2920 consists of program memory, scratch-pad memory, D/A circuitry, A/D circuitry, digital processor, and I/O circuitry. The 2920 is controlled by a program entered by means of an on-board EPROM. This is particularly convenient because changes in the operation of the Barker detector are easily made in software and reprogrammed on the 2920.

The clock for the 2920s is derived from the 455-kHz LO; hence, the precise chip rates of the received PSK signal depend on any frequency shifts introduced by the propagation media and on the accuracy and stability of the crystal in the KWM-380s. In actual operation, the frequencies of the received signals were not adversely affected by passage through the ionosphere nor by the translation process in the receiver. Hence, we conclude that the frequency accuracy and stability of the KWM-380 were adequate, and that Doppler shifts introduced by the ionosphere over the paths used were negligible.

Because the transmitter and the receiver operate asynchronously, the decoded output of the Barker decoder is sampled at twice the chip

rate in order to preserve signal fidelity. The decoded signal is digitized, and 6 bits of the digital output is made available to the CROMEMCO.

ii. Software Description--The program used for control of the 2920 analog signal processor in the quadrature channel consists of an input section, a digital processing section, and an output section. The input section of the program provides the code to convert the analog signal into an 8-bit digital word by means of the on-board sample/hold and comparator circuits. Because each bit at the transmitter is represented by a 13-bit Barker code and the decoded signal at the receiver is oversampled by a factor of two, each bit is represented by 26 contiguous samples. The input section of the 2920 provides these samples to the digital processor in a continuous stream at twice the chip rate.

Each unique, contiguous 26 samples is treated by the digital processor as two 13-bit Barker sequences. The odd samples form one set, and the even samples form the other set. Each of these sets is decoded by numerical correlation with a 13-bit Barker code, and the two decoded outputs are combined by adding the magnitude of the largest to one-half the magnitude of the smallest. The digital result is converted into an analog voltage by the output section and routed to the direct channel (I) to be combined with the decoded direct channel.

The 2920 control program used for the direct channel is very similar to the program used for the quadrature channel except that in the direct channel additional coding is provided to combine the magnitude of the decoded Barker signal with the magnitude of the decoded quadrature signal. The resultant digital signal represents the magnitude of the received signal and is converted into an analog signal by the output section. This signal is digitized and passed on to the CROMEMCO as a 6-bit digital word.

d. Software Implementation

The CROMEMCO Z80-based, S-100 bus computer was chosen as the CPU for the adaptive radio because it was available from a previous Defense Nuclear Agency (DNA) project. Although an STD-bus computer was considered, we chose the CROMEMCO because of past experience with it and because of the availability of driver software written for it on past projects.

1. CROMEMCO Computer--The CROMEMCO Computer, as implemented for the adaptive radio, consists of 2 S-100 cards, an SCC card, and a 32K memory card. The SCC card provides 8K of on-board program storage; 4K for firmware program storage, and the remaining 4K for the system monitor/control basic firmware. The system monitor provides a convenient tool for simple debugging and program patches, but is not suitable for program development. Four I/O ports (three parallel and one serial) are provided by the SCC card as shown in Figure B-1. The serial port was used to connect a standard RS-232 terminal to the adaptive radio. All user interface to the system was done through this terminal. Two parallel ports provided the interface with the adaptive radio controller. The third parallel port was used to communicate with the Collins KWM-380 transceiver.

Although the CROMEMCO hardware was adequate for the adaptive radio, its major deficiency was the lack of a disk-drive for mass storage. Hence, developmental tools, like an editor, assembler, and a debugger, were not available on the CROMEMCO.

Software development was initially done on an STD BUS Z80 computer and later on an APPLE IIe computer with a Z80 plug in card. The software development cycle consisted of three steps: (1) the program was written and assembled on one of the disk-based development systems; (2) the object code was programmed (burned) on two 2716(2K) EPROMs and the EPROMs inserted into the SCC card for final testing; and (3) if the software did not work, debugging was done on the adaptive radio system with the CROMEMCO monitor.

The debugging stage is generally the most time consuming and difficult in any hardware/software development. The difficulty was compounded because the proper tools and utilities were not available on the CROMEMCO.

ii. Adaptive Radio Software--The adaptive radio software consists of nine Z80 assembly subroutines. The compiled code is slightly under 4K in length. The major components of the software are Main, Radio, Smart, and the I/O Driver routines.

Main provides control of the two major operational modes of the adaptive radio: CALL and LISTEN. When one of the two modes is selected, control passes to Radio. This routine manages the frequency selection, transmission of the call letters in CALL mode, and listening for a response. In the LISTEN mode, Radio handles stepping through each of the assigned frequencies and listening for a call.

Both CALL and LISTEN modes utilize Smart for processing of the received signals and correlating the processed signals with the station's call letters. Smart accepts digital data from the Barker decoder, processes the data, and decides whether a call has been received. The original version of Smart had the following major features:

- (1) Mark/space decisions were made on the basis of strength. If either of these values exceeded a threshold calculated from the 26 samples that formed one data bit, the bit was called a mark, otherwise it was a space.
- (2) Integration was done bit-by-bit using a decaying average algorithm.
- (3) The preamble was used for synchronization.
- (4) The calculations done in Smart were time critical because averaging and calculation of the maximum and thresholds were done between samples. In addition, the time allocated to listening at each frequency was interrupt driven so that if too much time was spent in "finding" the preamble, or in doing the calculations prior to actual correlation of the received signal with the station's ID, timeout could occur before the process was completed.

The original Smart detector routine was written without benefit of real data and was recognized as the weak link in the system. Some of the limitations of the original Smart detection software was overcome by careful selection of the thresholds and ID word. On a benign path, like Los Banos to Menlo Park, the system worked fairly well. The system, however, proved unworkable over the Churchill-to-Los Banos path because of fading.

2. Experiments With the AHF Test Bed

Operational verification of the adaptive radio was done in three phases: bench test, local test, and long-distance test.

a. Bench Test

Bench test of the adaptive radio system was accomplished by connecting both systems together through a two wire link as shown in Figure B-3. The low-level output (Xmtr Out) of each radio was connected to

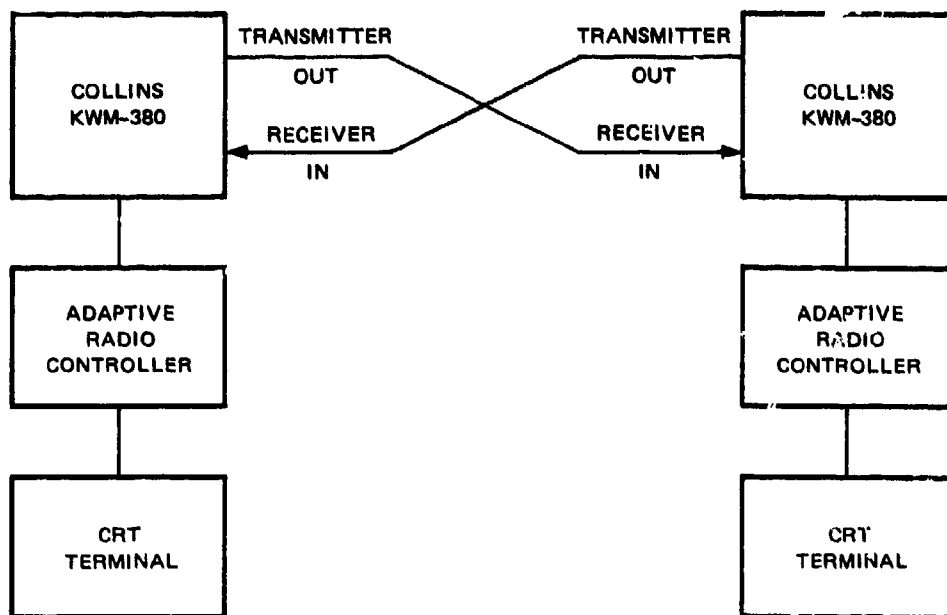


FIGURE B-3 BENCH TEST CONNECTIONS

the RCVR Input of the respective transceiver through appropriate attenuators. Noise could be introduced by means of directional couplers. This arrangement allowed operational testing of the entire system from the linking protocol through the detection algorithm.

Most of the testing of the adaptive radio was done on the bench to avoid the logistics involved in running the stations over a bistatic path. The setup provided a convenient means of testing operations in a realistic manner. The test setup, however, could not account for the effects of fading or multimodes.

b. Local Test (Menlo Park to Los Banos)

The Los Banos-to-Menlo Park path was used to test the system under actual propagation conditions. The sites were separated by approximately 115 km. After the threshold settings in the smart detector were adjusted to account for the noise background, the radios were successfully tested over several days.

Local noise was quite severe at the Menlo Park site, and on the frequencies that the radio successfully linked up, there was no evidence of multimode or fading. In effect, for the few frequencies that supported propagation, the local tests were no more stressful on the system than the bench tests. Based on these results, we decided that a long-distance path was necessary to properly stress the system under a variety of propagation conditions.

Although it was recognized that the use of fixed thresholds in the smart detector algorithm was a major weakness of the system, revision of the algorithm and verification of proper operation would have caused at least a month delay. Because this delay would have meant conducting the Churchill test in the October/November period in which we would have had to contend with severe weather conditions, and because we felt that the proper thresholds could be set in the field, we decided to use the existing system.

c. Churchill, Manitoba to Los Banos

Operation of the Churchill site began on 12 September 1983, and the first ionogram was received on 13 September. The antenna was a modified TCI, the details of which are given in Figure 4 of this report. The boresight of the antenna was directed due south to optimize transmissions with both Los Banos and GTE in Needham, Massachusetts.

Initially, Menlo Park was used as one end of the path to avoid the logistical problems in operating the Los Banos site. It soon became apparent, however, that the Menlo Park site was not suitable, probably because of the poor on-site antenna. Although an LPA was available at the Stanford field site, preliminary checks revealed that the noise environment there would probably preclude successful reception of the Churchill signals.

After several unsuccessful days of attempting to link up the adaptive radio, it became apparent that the fixed threshold settings could not contend with the dynamics of the noise background and the received signal. In the original design of the radio, an audio tone, related to the channel number, would be recorded along with time of day to provide a log of successful linkups. Although this type of data would be useful in evaluating how well the system worked in choosing a particular frequency over the set of possible frequencies (as revealed by the oblique ionogram), it provides no information on data quality and, in particular, no data to qualitatively assess the detection algorithm.

The objective of the AHF experiments over the Churchill/Los Banos path was to demonstrate the automatic link-up capability of the radios over a path that would stress the system. This was a highly ambitious goal because the adaptive radio was never tested under strong fading conditions. Although the adaptive radio could have been made to work over the Churchill to Los Banos path by carefully selecting the thresholds, we decided that the detection algorithm needed complete revision, and that merely getting the radios to link would not provide data to improve the algorithm or to test alternative ones.

During the last three days of the experiment, an IBM PC was used in place of the "dumb" terminal to communicate with the adaptive radio. The IBM provided all the capabilities of the terminal, but in addition could record on a floppy disk everything that appeared on the screen. The adaptive radio software was modified to allow 10 s of data to fill 6760 bytes of memory. The CROMEMCO monitor was then used to dump the memory contents to the screen, which was in turn recorded by the IBM. Nearly seventy 10-s blocks of data were collected over a variety of frequencies and times-of-day.

Figure 2 of the main report shows a sample of the recorded data. A complete ID word group, consisting of an 8-bit preamble, 2 start bits, 2 stop bits, and 2 7-bit ASCII words, is contained in each line. Each line contains 26 bits, and each bit consists of 26 chips or samples for a total of 676 samples. The preamble can be identified by the group of ten consecutive bits (the 8-bit preamble, one start bit, and one stop bit). The word transmitted in this example was "5V."

The new smart detector, written with these data as a guide, has the following features:

- (1) Processing is applied to two consecutive words consisting of 1352 samples so that a complete word is processed regardless of the starting time. This eliminates the need for synchronization.
- (2) Integration is done over 4 double words; thus 10 seconds of data is processed at each frequency. The processing is independent of time, and all results are left in memory for ease in debugging and in verifying the calculations.
- (3) Although the preamble is no longer required in the present smart detector algorithm, it was retained to avoid hardware changes.
- (4) For each "bit," the maximum value and its location are calculated and saved.
- (5) The noise in two double words (2704 samples) is found by summing all samples with the exception of the maximum and the two samples adjacent to it.
- (6) The threshold is calculated to be approximately three times the mean noise level.
- (7) Mark/space decision is based on the magnitude of the maximum compared to the threshold.

- (8) The resulting 52 bits (2 ID words) is correlated against the station's ID by correlating each 16-bit segment against the station's ID. The 52-bit word is broken into 16-bit segments by means of a circulating software shift register.

The present Smart detector software has been successfully tested on the computer using a few data sets recorded over the Churchill to Los Banos path. The new Smart detector needs to be tested further with the data already collected, but current indications are that the algorithm used in the detection software is more robust than the old scheme.

3. Conclusions

The adaptive radio was conceived and developed over approximately a three-year period. During this time the microcomputer industry, in terms of software and hardware, reached levels of performance that were undreamt of when the design of the adaptive radio was started in late 1979. By present standards, the CROMEMCO ca. easily be surpassed both in hardware, software developmental tools, and cost by several other systems. The experience and the techniques that have been developed with the present system, along with the data that have been collected over the Churchill/Los Banos path should be invaluable in any future efforts. Detailed full-size engineering schematic diagrams of the hardware developed for the test bed are available on request to the authors.

Appendix C
THEORETICAL ANALYSIS OF PROBING SIGNAL
T. Magill

1. Functions of the Automatic Link Establishment Signal

The calling signal should (1) identify the calling party (source); (2) identify the called party(ies) (destination); and (3) characterize the channel. Under most circumstances, a unique address will suffice to identify the calling party; however, for the destination several classes of addresses are required: (1) we may wish to call a unique address; (2) we may wish to call (or broadcast to) a group of addresses corresponding to a particular subset of the network; and (3) we may wish to broadcast to the entire network. Consequently, in general, there are more destination addresses than there are network members; therefore, the size of the destination word needs to be larger than the size of the source word. The difference in size will depend on the network organization and function.

Channel characterization entails measurement of (1) channel error rate, (2) time spread, and possibly (3) frequency spread. Ideally, the channel error rate should be measured at the desired data rate and with the desired modulation format; however, in many cases we may wish to adapt the data rate, or even the modulation format, to match the channel. Thus, if feasible, it is desirable to measure or estimate the bit or symbol error rate at a range of rates and for different modulation formats. Measurement of error rate for different modulation formats clearly requires transmission of these different modulation formats. Changing of modulation formats is operationally undesirable and, consequently, it becomes necessary to estimate the performance of other modulation formats. The two best indicators are time spread and frequency spread. Frequency spread can be estimated from the rate of change of the channel impulse response. Consequently, it is not necessary to measure frequency spread directly.

Owing to the very rapid change of symbol error rate with E_b/N_0 , it is relatively difficult to predict the bit error rate (BER) at other bit rates.* Thus, in a short word the absence of errors may be difficult to interpret. For example, it might be possible to signal eight times faster without errors. On the other hand, it may not be possible to double the signaling rate without producing an excessive BER. For these reasons it may be desirable to also directly estimate the detector signal-to-noise ratio. Unfortunately, this can lead to considerable receiver complexity. Nevertheless, it is operationally preferable to overly long calling sequences designed to estimate BER accurately over a wide range of data rates.

Returning to the error detection concept, we must have a method of detecting errors. This can be accomplished in two fundamental fashions. First, we can transmit a known test signal so that the receiver could recognize bit errors and count them to calculate the BER. Second, we can encode an unknown signal by the addition of some parity bits to detect the presence of error(s) and perhaps even count the errors.

Use of a channel sounding signal that is known to the receiver permits the detection of errors in this signal. Thus, for the present system, it is possible to measure the chip errors in a 13-chip Barker sequence signaled at a 1.5-kchips/s rate. This rate is quite high considering that many applications will require only 75 bits/s data rate. The BER for these lower rates may be better estimated by error-detection encoding the call signs. Chip error detection will require chip synchronization and chip detection at the chipping rate in addition to the normally required bit detection. Thus, two sets of synchronization and detection equipment will be required if the approach is followed.

*For low BERs, the BER versus E_b/N_0 (receiver operating characteristic or ROC) is very steep, assuming Gaussian noise. That is, a small change in E_b/N_0 produces a very large change in BER. For non-Gaussian noise, for example, intersymbol interference created by time spread, the BER may be very insensitive to E_b/N_0 . Similarly, for Gaussian noise at high BER, the BER is relatively insensitive to E_b/N_0 .

The alternative approach, which is suitable for the estimation of BER at lower data rates, encodes the source and destination call signs with parity bits so that bit errors occurring at a 115.3-bits/s rate can be detected. A CRC code is commonly used to detect errors in blocks of data and might usefully provide a crude assignment of link quality at 115 bits/s. If more precision were required, an error correction code can be used. Either a Hamming code or a Golay code can be used to detect the existence of two errors in a block of bits. A greater number of errors could result in failure to detect errors.

2. FSK Channel Sounding

Some existing automatic link establishment (ALE) techniques use binary FSK modulation for channel sounding. SELSCAN uses binary FSK at a rate of 300 bits/s. Assuming random data for call signs, the 6-dB time resolution is ± 1.67 ms or five times poorer than that of the AHF test-bed signal. With the proper reception techniques, channel time-spreads greater than a few milliseconds can be readily identified as a source of degradation (as opposed to interference or noise) by SELSCAN. Owing to the relatively high data rate of 300 bits/s, the ability to resolve frequency spread easily is quite limited. In fact, the Kineplex or multitone QPSK format is much more sensitive to frequency spread than FSK. As a result, successful transmission with FSK does not prove that transmission will be successful in the Kineplex format.

In summary, 300 bits/s FSK channel sounding provides a limited time resolution capability while requiring additional receiver circuitry to identify this spread. The principal advantage of this sounding signal is that BER can be measured at a nominal data rate representative of presently acceptable rates in a presently popular modulation format. Little may be inferred about the ability to signal at much higher rates over that channel or how well multitone formats will perform in a frequency spread channel. Consequently, it is desirable to investigate other channel sounding signal formats. Before doing so, let us consider the data modulation formats that may be used in conjunction with the channel sounding signal.

3. Modulation Formats

Different modulation formats have different sensitivities to the different types of channel distortions. For example, FSK is much more tolerant of frequency spread than PSK.* Consequently, depending on the modulation format the channel sounding signal needs to extract different information. Of course, this raises the issue as to whether a common sounding waveform can extract all the information required by each modulation format, or whether separate sounding signals should be used. Conceptually, a single sounding waveform is desirable because its output may suggest the modulation format and rate to be used for the transmission of information. Furthermore, this concept of operation is compatible with the use of programmable signal processors to implement the HF modems. The Navy has developed the HF digital modem (HFDm)² that permits implementing of different modulation formats simply by changing the program code. The sounding signal can readily determine which modulation (and coding) format to implement.

For those cases in which the modulation is restricted by the data modem available, it may be desirable to use that modulation format for the sounding signal. In this case, there is no need to infer the quality of channel for one modulation format from measurements in another format. The bit error rate of the sounding signal will be a direct measurement of the bit error of the data signal, assuming that the same data rate was used for sounding as was intended for transmission.

Several modulation formats are popular for HF use. For lower data rates, FSK and differentially detected binary PSK are common. The FSK format at 75 bits/s commonly uses narrow shifting (85 Hz); for some applications, such as aeronautical, it uses wide shifting (850 Hz).

The BDPSK system uses differential encoding and phase comparison detection. This detection process loses about 1 dB with respect to quasi-coherent detection (Costas loop) but is less sensitive to rapid phase jitter.

*Appendix D demonstrates the greater sensitivity of BDPSK to frequency spread.

For high data rates, the most common modulation format uses multiple tones, each of which is modulated with differential quadrature phase shift keying. The number of tones ranges from 16 to 39.* Use of parallel tones creates long symbols which are less vulnerable to multipath-induced intersymbol interference. Further, insensitivity to multipath, which is achieved at the cost of reduced bandwidth efficiency, is obtained by the use of guard times in which no energy is transmitted and the receiver detector is blanked. The ANDVT⁴ is a classic example of a multiple tone QPSK modem. Operation at 2400 bits/s uses a 16-tone format, while secure voice, operating at approximately 3500 bits/s (after error correction encoding), uses 39 tones with an intersymbol duration the size of the vocoder analysis frame (22.5 ms).

Lower data rates are commonly achieved through redundant transmission (in band diversity) and the use of rate one-half,[†] one-quarter, one-eighth, and so on, coding. Time interleaving is frequently employed to provide protection against long duration fades across the full 3-kHz passband.

Owing to the long symbol duration employed by the multiple tone format, these modems are relatively insensitive to multipath effects, but they are quite sensitive to frequency spread such as might be caused by auroral scatter or nuclear disturbance. Thus, for such modems it is important that the sounding signal be able to identify the presence of frequency spread.

An in-band sounding signal will have its resolution limited to approximately 0.5 ms. Thus, in general, it will not be possible to identify fine detail of the path structure. For the nominal Kineplex format, the intersymbol duration is 13.3 ms with a symbol duration of

*Use of 16 tones is by far more common and, in fact, there are at least two noninteroperable 2400-bits/s formats using 16 tones.

[†]The (24,12) Golay code is the most popular rate one-half code. Lower rate codes are usually obtained by redundantly transmitting the same information on two or more frequency channels frequently with time displacement between these channels.

8 or 9 ms and a guard time of 5 or 4 ms, respectively. In-band sounding signals are capable of resolving multipath responses in the 0.5 ms and above range. In particular, for multipath responses greater than 4- or 5-ms, in-band sounding is clearly capable of resolving these returns. As a result, in-band sounding is capable of identifying those circumstances when the Kineplex format performance will be degraded by the multipath.

Other modulation formats are planned for HF use. 8-ary FSK will be used with frequency-hopping modes of operation but at reasonably low signaling rates.* The sensitivity to channel distortions of 8-ary and binary FSK are roughly the same except for the following effects. For a given F_b/N_0 , 8-ary FSK offers a lower BER than binary FSK. Because the 8-ary FSK symbols are three times longer than binary FSK symbols, 8-ary FSK is less sensitive to multipath delay spread. On the other hand, the 8-ary FSK detection filters, being three times narrower than binary detection filters, are more sensitive to frequency spread.

It is noteworthy that M-ary FSK offers relatively poor bandwidth efficiency and cannot support data at 2400 bits/s or digitized voice in a standard 3-kHz voice channel. Furthermore, the Kineplex format, which can support data at 2400 bits/s, cannot operate with frequency hopping. The phase discontinuities created by frequency hopping of independent oscillators cause bursts of errors at each hopping instance for phase modulation techniques. Multiple tones simply compound the problem. That is, a 16-tone system has 16 times the error rate of a single tone system.

As a result, there is considerable on-going research into 2400-bits/s single-tone modems. Differential phase modulation is one good way to accommodate the FH phase hits (the first symbol per hop acts as a phase reference) and provide the required bandwidth efficiency. High symbol-rate phase modulation requires the use of equalization to

*Frequency hopping is desirable since the same encoded information is transmitted redundantly over several channels, thereby reducing the impact of serious degradations, e.g., complete fades, on any single channel.

combat multipath-induced intersymbol interference. Ideally, the channel sounding signal should measure the channel impulse response in such a fashion that the measurements are directly transferable to the equalizer tap settings. Thus, after establishing a link connection using the sounding signals, the equalizer can be initialized with the impulse response measurements, and communications can commence at 2400 bits/s. Ideally, the equalizer should adapt to changing channel characteristics without requiring additional channel soundings. However, periodic channel sounding may be desired for other reasons and offers the advantages discussed in Section 6 of this appendix.

The preceding discussion has demonstrated that a variety of modulation formats are in use or are planned for use in the HF band. These modulation formats have different sensitivities to frequency and time spread. That is, some modulation formats such as FSK are relatively tolerant of frequency spread, while others such as multitone DPSK are tolerant of time spread. Thus, it is desirable to sound with a waveform capable of identifying both forms of spread.

At present, the sounding waveform is a 13-chip Barker sequence signaling at a 1.5-kchips/s rate. This waveform provides relatively good time resolution (although improvements are possible as discussed in Section 5 of this appendix) but may not provide the desired frequency resolution to characterize in detail the frequency spread. Ideally, a single sinusoidal line component provides infinitely accurate frequency resolution. In practice, the resolution is limited by the length of observation interval.

If the Barker word is repeated sufficiently often, it presents, in effect, a line component that may be used for frequency spread measurements. The 13-chip Barker sequence has a bias of +5 (that is, there are 5 more plus ones than minus ones). As a result, a carrier component down 8.3 dB with respect to the total sounding signal power exists. If we observe this component for one sequence length, its first-null-to-first-null bandwidth is 230 Hz. Each doubling of the number of Barker words observed halves this bandwidth. Thus, for example, observing eight successive Barker words permits a resolution of 28.8 Hz.

Use of such a carrier component* can identify the frequency spread, but the carrier component will not be helpful in combating the degradation. Equalization is based on time spread, and time-variant time-spread concepts. Thus, frequency spread is regarded as more useful than time-variant time spread. The only real issue is how quickly the sounding waveform can measure the time spread because this will determine our ability to identify frequency spread. For our purposes, however, we need only to identify the existence of frequency spread rather than perfectly measure it. Thus, if our sampling rate produces aliasing in the frequency or time-spread measurements, we can still detect their existence, if not accurately estimate their magnitude, and this may be sufficient for many circumstances.

For the present system, the sounding performance is set by the chipping rate and the code length. Table C-1 lists the 6-dB time

Table C-1. Present System Sounding Characteristics.

Characteristic	Performance
6 dB Time	$\pm 333 \mu s$
Maximum Unambiguous Delay	8.67 ms
Maximum Measurement Frequency	115 Hz

resolution and maximum unambiguous delay that can be measured with the present system. System limitations, such as restricted bandwidth and group delay distortion, if any, will degrade the cited value. The table also lists the maximum rate at which the impulse response may be gathered.

The maximum measurement frequency of 115 Hz means that frequency spreads, i.e., time variations in the multipath pattern occurring at a

*In the present system, no carrier component exists owing to the data modulation reversing randomly the polarity of the Barker sequence.

57.5-Hz rate, can be measured unambiguously. Actually, this number is somewhat misleading for the present system, which uses on-off keying (OOK) to represent data marks and spaces. Depending on the data pattern, there may be substantial periods without a sounding signal. As a result, the frequency of measurement may be considerably lower than 115 Hz, implying a much reduced ability to track rapidly changing multipath. For this reason, we do not advocate OOK data modulation but rather recommend phase reversal keying (PRK).

It should be noted that with OOK modulation, the absence of a sounding signal, although harmful in measuring frequency spread, is helpful with respect to unambiguous maximum delay. That is, depending on the data pattern, the maximum unambiguous delay may be 17.3 ms or even longer. However, 8.67 ms cited in Table C-1 is adequate for almost any envisioned circumstance so that little, if anything, is gained by this feature of OOK.

4. Code Choice

For accurate channel impulse response measurement, it is desirable to use a code with good autocorrelation function. For binary code applications, the Barker codes are known to offer optimum autocorrelation functions in that the magnitude of the maximum side lobe is +1. Unfortunately, the maximum length Barker code is only 13 chips. This code is being used in the present hardware implementation. The signaling rate is 1.5 kchips/s so that the bit rate associated with this code is 115.3 bits/s. If we desired to measure BER at a lower bit rate directly, we would have to find a longer channel sounding code. For example, a code of length 20 would be required for measurements at 75 bits/s. Thus, some alternative longer codes appear desirable for some sounding applications.

The Barker code of length 13 has an undesirable bias characteristic. That is, there are five more plus ones than minus ones; thus, when it is correlated with a dc level, a very substantial cross correlation exists. At rf, this means that the Barker code offers negligible

processing gain against an unmodulated carrier. Ideally, the sounding code should have zero (or near-zero) bias and offer full processing gain against unmodulated carriers because this enables successful operation under the most difficult circumstances. However, the presence of bias is representative of nonspread BPSK data signaling, and thus measurements with a biased code are more indicative of the performance of this common form of modulation in the presence of interference.

Table C-2 lists the known Barker sequences, their bias, and their maximum relative side-lobe level in decibels below the maximum

Table C-2. The Known Barker Sequences and Their Characteristics.

Length (Chips)	Sequence	Bias	Maximum Side-Lobe Level (-dB)
1	+	+1	∞
2	++	+2	6
2	+-	0	6
3	++-	+1	9.5
4	+++-	+2	12
4	++-+	+2	12
5	+++--	+3	14
7	+++---	+1	16.9
11	+++---+---	-1	20.8
13	+++++---++---	+5	22.3

autocorrelation level. Other Barker sequences can be generated by complementing or/and time reversing the codes shown.³ The Barker sequence of length 11 is attractive owing to its low bias. It correlates very poorly with unmodulated carriers. Assuming a 1.5-kchips/s signaling rate, the maximum unambiguous delay is 7.3 ms, which is still quite adequate, and the maximum sampling rate is 136 Hz. Thus, changes in channel impulse response occurring at rates as high as 68 Hz can be measured.

If the signaling and sounding format includes call signs (as it does at present) by complementing or not complementing the Barker codes, then the Barker code bias may not be very significant. Assuming random

(zero-bias) call signs, the bias of the Barker code is not present on the transmitted signal. However, if we cannot assure zero bias call signs, then the 11-chip Barker sequence is preferable to the 13-chip sequence. Owing to the emphasis on keeping call signs as short as possible, they will not have zero bias, in general.

5. Choice of PN Code Rate

The present system uses a chipping rate of 1.5 kchips/s such that the first-null-to-first-null bandwidth is ± 1.5 kHz or the nominal HF channel bandwidth of 3 kHz. Little is to be gained with a lower chipping rate because this would only degrade the time resolution. It does make sense to consider the use of higher chipping rates.

Higher rates offer better time resolution and increased processing gain against interference. Of course, the higher rates require proportionally greater bandwidth and, on the average, encounter proportionally greater interference.* Consequently, proportionally increased processing gain is required on the average to maintain the SNR ratio of the present system. Consequently, the only time advantage of a higher chipping rate is improved time resolution.

Higher chipping rates may require more complex circuitry and more extensive modifications of the HF transceiver. In addition, assuming that we desire the same unambiguous time range, a higher chipping rate implies the need for a longer code. Unfortunately, no Barker codes longer than length 13 are known and, consequently, a longer code will have a higher side-lobe level. Depending on the length, the performance may, nevertheless, be adequate.

The principal disadvantage with higher chipping rates is the state of HF frequency management. Channels are commonly assigned in 3-kHz

* HF interference on the long-term average basis may be regarded to have a uniform distribution in the frequency domain. However, on the short term, localized basis it will be very lumpy. Thus, we might substantially increase the bandwidth with luck, with no increase in the interference level. On the other hand, a very slight increase could very well produce a dramatic increase in the interference power.

increments. There is little need to characterize more than a 3-kHz passband because the modems will be restricted to operate in this bandwidth. Furthermore, a signal occupying 3 kHz is sufficient to characterize a 3-kHz bandwidth. Use of a wider bandwidth sounding signal creates a situation in which the sounding signal is likely to encounter interference that is out-of-band with respect to the data signal.

In summary, we recommend that the ALE signal use the existing chipping rate of 1.5 kHz. Slower rates will degrade time resolution while higher rates are too likely to encounter misleading (with respect to data signal BER) out-of-band interference.

6. Time Resolution

If we assume signaling at a rate of 1500 chips/s, the time resolution corresponds to approximately one or two chips in duration or 0.67 to 1.3 ms. The larger value corresponds to essentially the side-lobe level, and the smaller value corresponds to the 6-dB down-correlation level. The above calculations were performed assuming an infinite bandwidth—that is, perfectly rectangular chips. If ideal rectangular filtering at the first spectral null is employed to restrict the occupied bandwidth, then the time resolution will be somewhat degraded, principally because of the 0.5-dB degradation in the main peak of the autocorrelation. The resulting autocorrelation function will be the convolution of the PN triangular autocorrelation and a $(\sin x)/x$ function. Thus, the PN code side-lobe levels will be increased by the side lobes of the $(\sin x)/x$ function. The $(\sin x)/x$ side lobes fall off very slowly, and other forms of filtering, e.g., raised cosine, are preferable.

The time resolution can be improved if more high-frequency content is present in the power spectrum than for an ideal low-pass filtered sinc^2 function. Too little power is present at the band edge. One approach would use ideal low-pass filtering of white noise. In this case, the autocorrelation function consists of a sinc function. For comparison purposes, the sinc function is plotted in Figure C-1 along

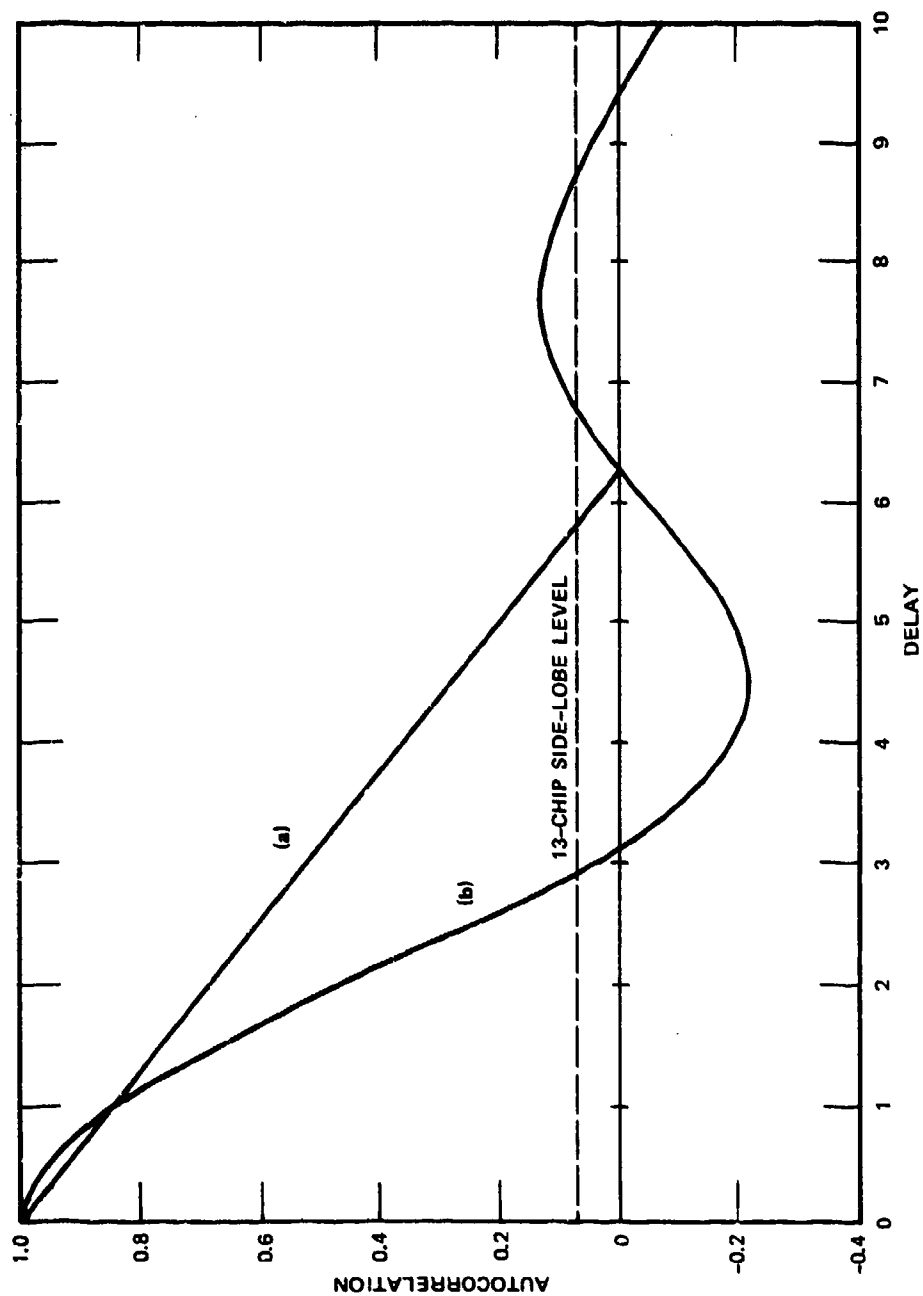


FIGURE C-1 AUTOCORRELATION FUNCTIONS OF (a) IDEAL PN SEQUENCE AND (b) IDEAL BAND-LIMITED WHITE NOISE

with the ideal triangular function for a Barker sequence of length 13. As can be seen from Figure C-1, the ideal band-limited noise autocorrelation function has a main lobe that is considerably narrower than that of the ideal PN sequence. The latter's first zero crossing is twice as wide as for the former signal. The ratio of the 6-dB points is 1.65 in favor of the band-limited white noise.

However, as can be seen from Figure C-1, the side-lobe level of the band-limited noise sinc function is considerably higher than that of the PN sequence. The first side lobe, which lies within the main lobe of the PN sequence, is slightly smaller (about 1.5 dB) than the corresponding offset value for the PN sequence. The higher order side lobes of the sinc function fall off very slowly. Thus, far-out resolution of the PN sequence will generally exceed that of the band-limited white noise. For illustrative purposes, the envelope of the side-lobe level for a 13-chip Barker sequence is shown as a dotted line in Figure C-1.

This figure suggests that the use of raised-cosine pulse shaping in the frequency domain (which requires some modest additional bandwidth) could be used to obtain the best of both worlds. That is, the main lobe width would remain narrow while the side-lobe levels would be reduced. Unfortunately, such an approach requires the use of a considerable amount of nonbinary signal processing. For example, the matched filters would require more than one-bit coefficients and be considerably more complex to implement than the present system.

Use of ideal low-pass filtered noise is difficult for two reasons: (1) a true noise waveform is harder to store and reproduce than a binary PN sequence, and (2) the amplitudes are continuously distributed, requiring analog rather than digital transmission techniques. Multi-level digital techniques can be used to approximate an ideal band-limited noise process. It is relatively easy to generate a 4-level PN sequence with an autocorrelation function that approximates the sinc function. This is done by taking the binary PN sequence (with a triangular autocorrelation function) delaying and weighting it appropriately and subtracting it from the original sequence. The resulting four-level

sequence is easy to store and generate and only somewhat more difficult to modulate than the original binary sequence.

Figure C-2 illustrates the autocorrelation functions that result for a delay of three-fourths with weightings of one-half and one-quarter. Figure C-3 illustrates the autocorrelation function for a delay of one-half chip with weightings of one-half and one-quarter. Figure C-4 presents the same information for a delay of one-quarter chip. The autocorrelation function for the original binary sequence is also presented for comparative purposes. Table C-3 summarizes the resolution and side-lobe performance of these modified signals. Clearly, other sequences are possible and will offer somewhat different characteristics. The examples presented here illustrate that four-level sequences can substantially improve time resolution.

A weighting factor of 0.5 produces four levels that are equally spaced with a 10-dB amplitude fluctuation. The weighting of 0.25 more closely spaces the amplitude levels of the same polarity and has a reduced amplitude fluctuation of 4.4 dB. Because most HF receivers are designed for analog voice communication, these amplitude variations are acceptable. However, the weighting factor of 0.25 results in a higher average power. From an implementation viewpoint, the weighting factor of 0.5 is preferable because a 2-bit word size is adequate to represent the tap weighting in a matched filter.

7. Channel Equalization

One means of mitigating the distorting effects of nuclear-induced multipath and Doppler spread is to measure the channel transfer function adaptively and continuously, then set the parameters of a filter automatically with the inverse characteristics. This approach has been known for some time, but is only now becoming practical.⁶ Even now, however, channel equalization represents a quantum increase in the complexity of an HF transceiver, even if we compare it to the SELSCAN control unit. Because the approach depends on cooperative probing between terminals, it is evidently practical only for circuits that have already been established, not as a selective calling, channel-finding signal.

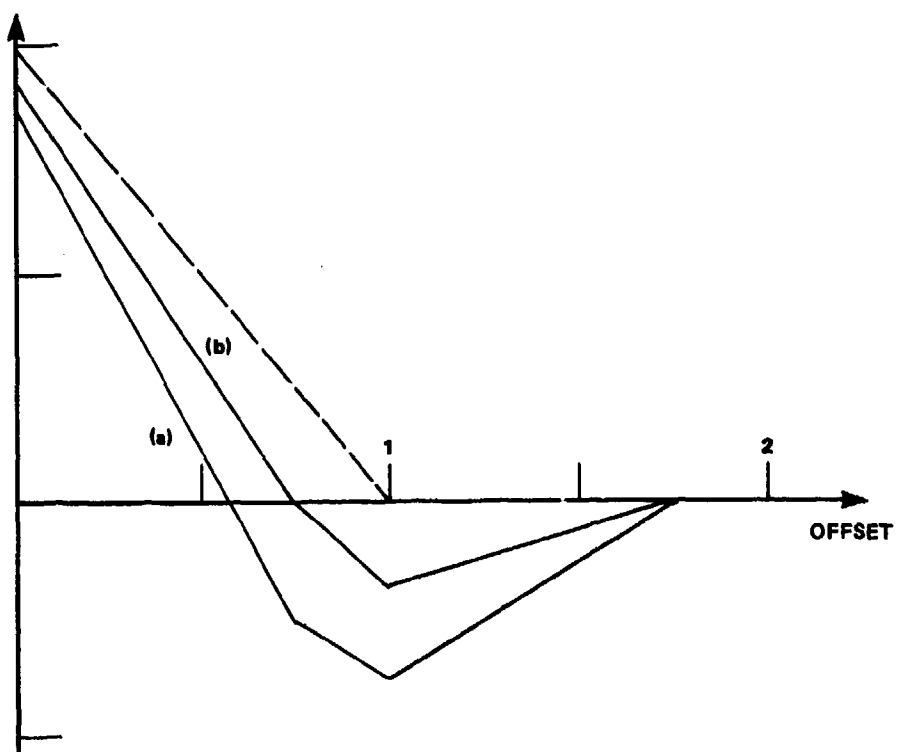


FIGURE C-2 AUTOCORRELATION FUNCTION FOR FOUR-LEVEL PN SEQUENCE WITH DELAY OF THREE-QUARTER CHIP FOR WEIGHTING FACTORS OF (a) 0.5 AND (b) 0.25

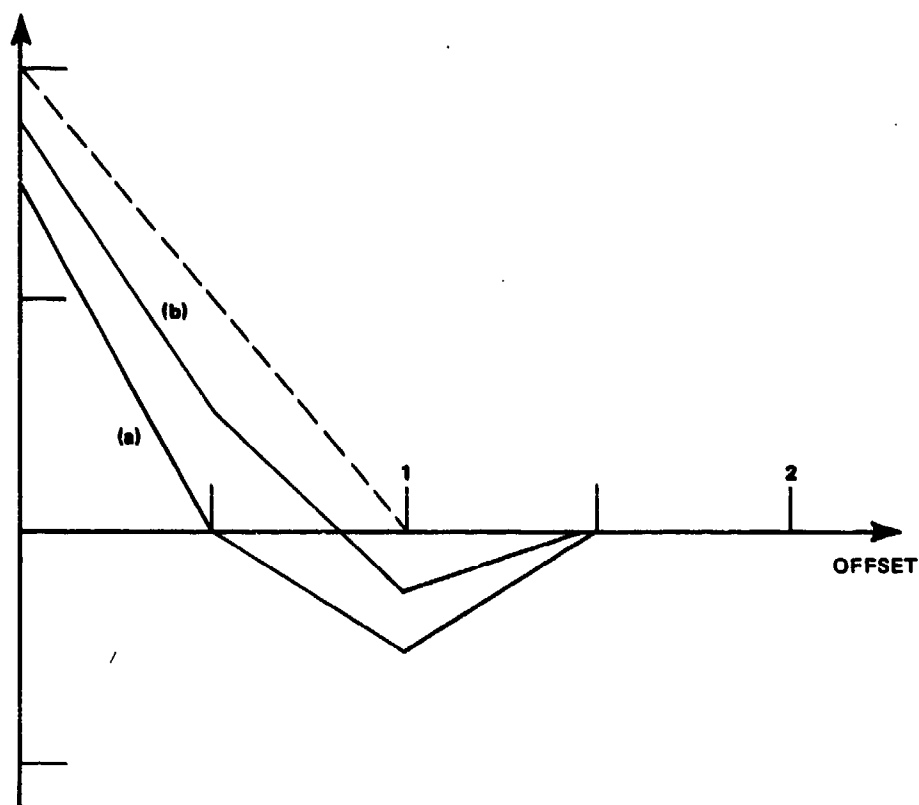


FIGURE C-3 AUTOCORRELATION FUNCTION FOR FOUR-LEVEL PN SEQUENCE WITH DELAY OF ONE-HALF CHIP FOR WEIGHTING FACTORS OF (a) 0.5 AND (b) 0.25

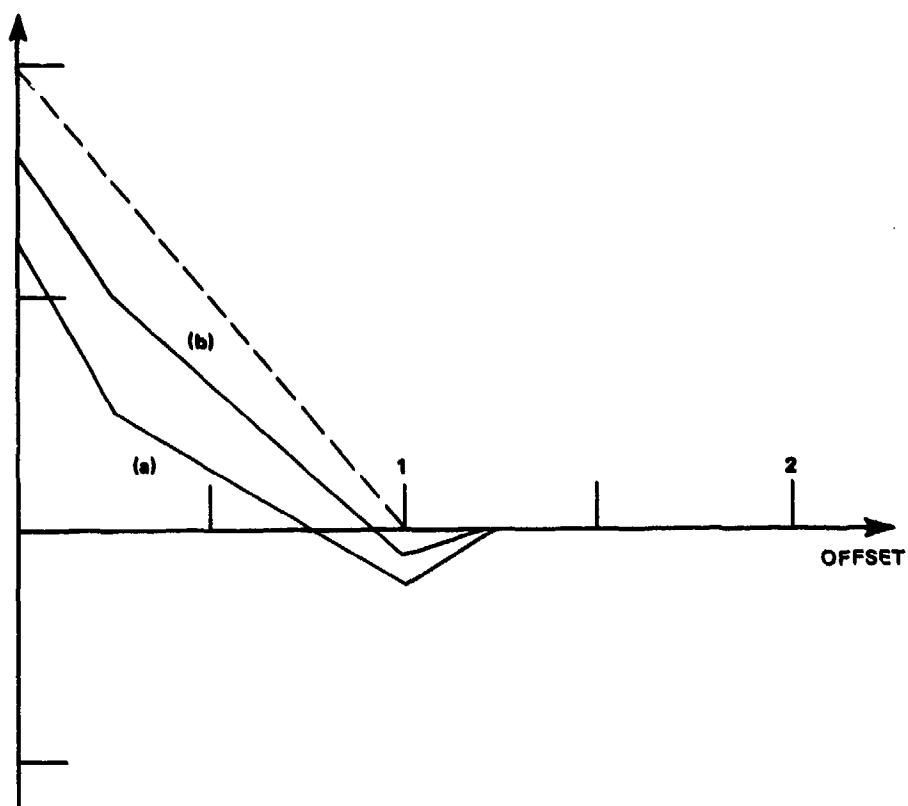


FIGURE C-4 AUTOCORRELATION FUNCTION FOR FOUR-LEVEL PN SEQUENCE WITH DELAY OF ONE-QUARTER CHIP FOR WEIGHTING FACTORS OF (a) 0.5 AND (b) 0.25

Table C-3. Autocorrelation Characteristics of Six Four-Level PN Sequences.

Offset (Chips)	Weighting Factor	Width (Chips)	Maximum Side-lobe (-dB)
3/4	0.5	0.3	7.4
3/4	0.25	0.375	13.6
1/2	0.5	0.25	9.5
1/2	0.25	0.33	16.9
1/4	0.5	0.21	14.0
1/4	0.25	0.38	22.3

Knowledge of the channel impulse response permits equalization. The amount of computation necessary for conversion of the impulse response to equalizer tap coefficients depends on the form of the equalizer. For decision feedback equalizers, the measured impulse response can be used directly as tap coefficients. Transversal equalizers require processing of the measured impulse response to obtain the required tap coefficients.

The decision feedback equalizer (DFE) is relatively simple to implement but does not offer optimum performance for channels with weak early responses. The DFE will tend to select the first arriving component and cancel the responses from later stronger components. Consequently, the DFE can offer poorer noise performance than equalizers that use stronger components.

For either equalizer type, the results of measuring channel-impulse response can be used to initiate the equalizer and permit rapid acquisition. Furthermore, if the channel sounding signal is transmitted periodically and at a high enough rate, it may not be necessary to construct a data-adaptive equalizer. In addition to more rapid acquisition, use of the sounding signals avoids relying on the randomness of the data that is assumed in all data-adaptive equalizers. (In fact, for most data-adaptive equalizer systems, a scrambling operation is performed to ensure data randomness.)

Furthermore, the channel-impulse response is measured with the greatest resolution possible within the channel bandwidth with the proposed approach. The actual data rates and modulation format may not provide the same degree of time resolution.

8. Coherent Demodulation

Use of efficient PRK modulation for the call signs requires either the use of differential phase comparison detection or quasi-coherent detection such as occurs with Costas loops. For multipath channels, there is a basic problem with quasi-coherent detection: How do we know to which signal we should phase lock? Phase-locking to some weighted average value, as a conventional phase-lock, will produce a phase reference that, in general, is good for detecting no path's signal. One potential solution is to identify the desired path and gate only that signal into the phase-lock loop. Of course, this is possible only if the signals do not overlap in time so that gating is ineffective.

The best approach to the phase-reference problem is to use spread spectrum processing before the phase-locking operation. Spread-spectrum processing will reduce the effect of interference and consequently improve the accuracy of the phase reference. In addition, spread-spectrum processing can separate the various multipath components in time, making possible the time-gated phase-reference concept described above. The separation capability is limited to the time resolution inherent in the transmitted waveform (see Section 6 in this appendix). The time separation is most easily achieved through the use of matched-filter rather than cross-correlation detection. The channel impulse response can be observed directly at the output of a matched-filter detector.

Figure C-5 is a block diagram of one approach to implementing a system for reconstructing a phase reference selectively for individual paths. The most critical element of this system is the bit synchronizer. It must recognize the strongest path in a time-variant

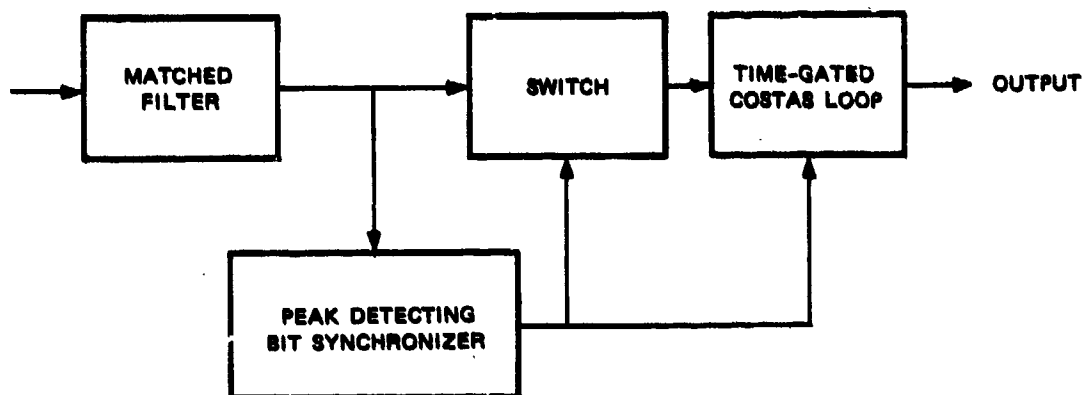


FIGURE C-5 BLOCK DIAGRAM OF QUASI-COHERENT MULTIPATH PHASE-REFERENCE RECONSTRUCTION SYSTEM AND DETECTOR

situation. This problem can be severe under conditions of rapid change.* Rapidly-changing strongest paths will present problems in acquiring phase lock.

It is preferable to adopt a different detection philosophy rather than attempt to deal with the problems in acquiring phase lock. Phase comparison detection nicely avoids the problems in acquiring phase lock. Figure C-6 is a block diagram of the recommended approach. Note that either two matched filters are required as illustrated or alternatively the analog output of the (single) matched filter must be stored for one bit duration (i.e., 13 chips in the present system). The output of the phase detector is a series of impulses (all of the same polarity--the bit polarity) corresponding to the channel impulse response. The peak detecting bit synchronizer selects the maximum peak within the bit duration and gates that value through the switch to the polarity detector, which produces the detected output bit stream.

As illustrated, the system selects a single multipath component for detection. However, a relatively trivial modification can greatly

*Rapid changes may occur as the result of several slowly changing unsolvable components.

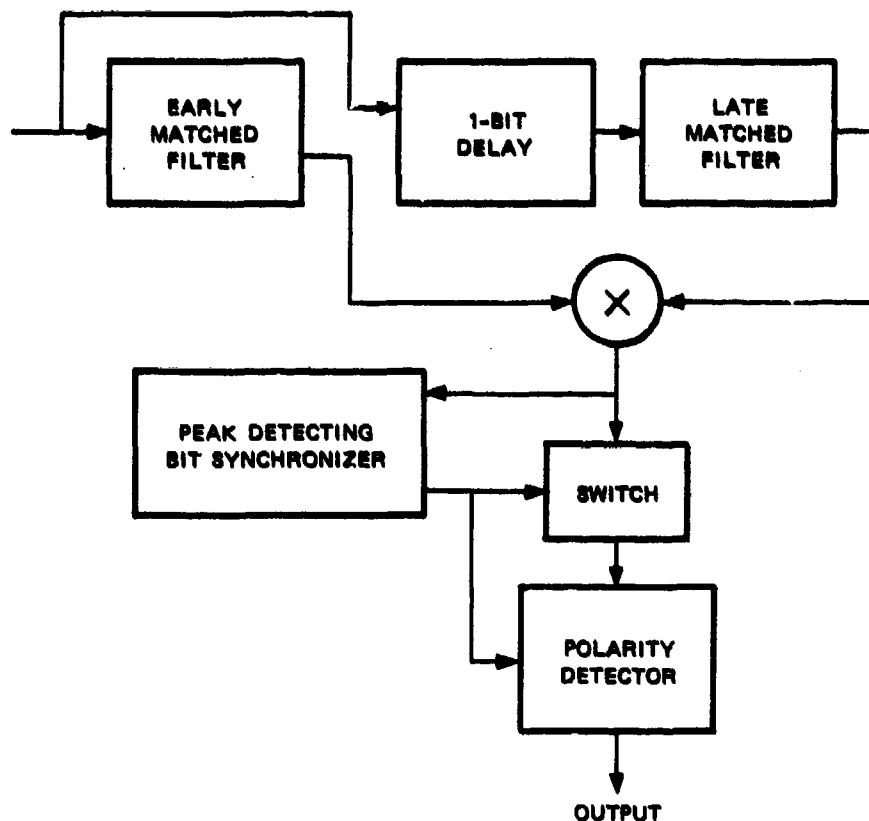


FIGURE C-6 BLOCK DIAGRAM OF PHASE-COMPARISON SYSTEM

enhance performance in multipath channels. Owing to the differential nature of the detector, each multipath component produces the same polarity output but with an amplitude proportional to the strength of that path. Thus, the signal-to-noise ratio can be increased by integration over these responses. The optimal detector will perform a weighted integration with the weighting factor proportional to the strength of the path. Implementing this optimal detector entails accurately learning the multipath structure and performing a relatively large number of multiplications per second. Usually this design is considered excessively complex, and a simple approximation, known as the postdetection integrator (PDI) is employed.

The PDI uses uniform weighting over a fixed window that is optimized for the long-term average distribution of multipath components. The PDI has been used in the packet radio system⁵ as a technique for enhancing system performance (by as much as 20 dB) in the presence of multipath. The packet radio system operates at 2 GHz in a LOS mode in an urban environment and at considerably higher data rates than achievable at HF. Consequently, the PDI window size at HF will be of a different size and may offer a different amount of enhancement. In fact, the window size should be optimized depending on the HF propagation mode.

Figure C-6 illustrates a conceptual block diagram of the proposed system based on the use of bandpass matched filters such as might be implemented with surface acoustic-wave (SAW) devices. The intermediate frequencies commonly used for HF receivers are too low for SAW devices. Consequently, an alternative design approach is required to make the proposed system feasible.

Figure C-7 is a conceptual block diagram of one digital implementation of the proposed system. It is quite similar to the existing system in that I and Q channels are used and that the matched filters are digitally implemented by oversampling at twice the chip rate. At certain time phasing offsets between the sampling clock and the received signal, a slight degradation in time resolution will result for a two-to-one oversampling rate. This minor degradation is acceptable and preferable to the resulting circuit complexities associated with higher sampling rates. Figure C-7 depicts the use of PDI, which may be removed by using a window width of one sample. Thus, the receiver has the capability of measuring performance in at least two modes of operation--one which has a variable parameter--the window width.

As can be seen from the block diagram, the principal difference with respect to the present system is that differential phase comparison detection is employed rather than OOK. In addition to the 3-dB theoretical power advantage that BDPSK offers, there is a significant practical advantage. There is no need to set a detection threshold for a

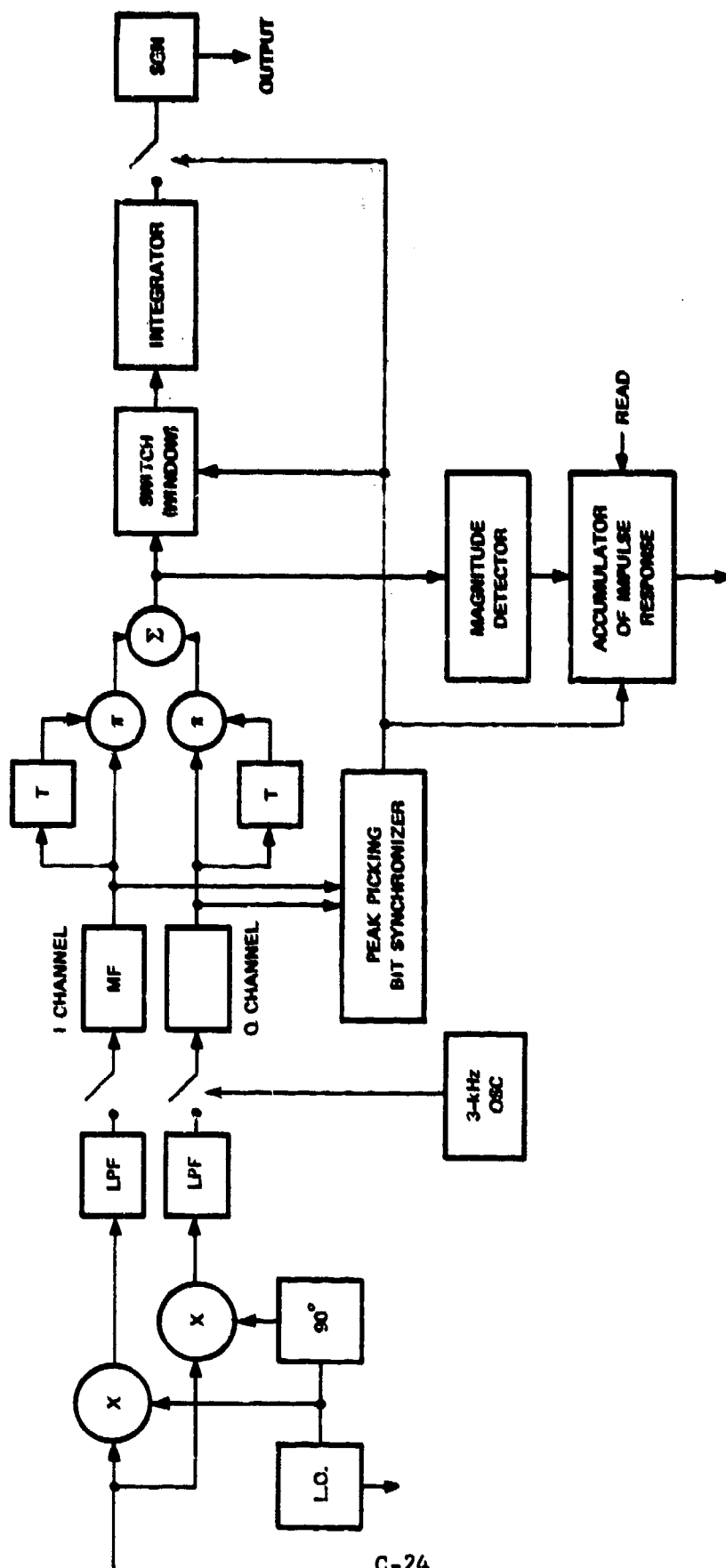


FIGURE C-7 BLOCK DIAGRAM OF DIGITALLY IMPLEMENTED PHASE-COMPARISON DETECTION SYSTEM

time-variant multipath channel. Consequently, the AGC system and threshold circuitry is considerably simplified for the BDPSK system and contributes nothing to the performance degradation.

Figure C-7 also shows some additional (optional) circuitry used to record the magnitude of the channel impulse response. This information can be read out on command by the read pulse. Presumably, this information will be processed by a microprocessor to record time spread (as a minimum, useful in setting the window size for the PDI circuit) and the rate of change of the channel impulse response. The channel impulse response can be used to adjust the data modem format and rate and might be used to adjust an equalizer. Sufficient memory should be available to store the impulse response measurements for several, if not all, channels scanned.

We recommend that the receiver shown in Figure C-7 be implemented and used for a series of experiments. Nominally a 13-chip Barker sequence at a 1.5-kchips/s rate should be used; however, we may wish to use a 10-chip Barker sequence or use a slightly lower clock rate, or both. The experiments should be performed with various modes of propagation and with various modulation formats. The objective of the experiments is to correlate the BER for the ALE signal (as a function of PDI window size) with the BER of the various modems.

9. Conclusions from Theoretical Analysis

The present AHF Test-Bed sounding system is fairly well matched to the problem of evaluating HF channels for voice and data. Nevertheless, there is room for improvement in the existing design. Perhaps the principal improvement is the replacement of OOK data modulation with PRK data modulation. There are several substantial advantages in using PRK: (1) the noise performance is improved by 3 dB, (2) it is not necessary to set threshold levels and interact with the AGC system, and (3) the sounding signal is transmitted with each bit, guaranteeing a more frequent measurement of the channel impulse response.

The principal difficulty associated with PRK data modulation is the implementation of a carrier-recovery (e.g., Costas) phase-lock loop for the multipath channel. While complex solutions exist, the whole problem is best avoided by using phase-comparison detection. The resulting 1-dB detection loss is a negligible price to pay for a much simplified detector. Furthermore, phase-comparison detection permits using PDI, if so desired.

Although PDI may not be used by the data modem, it nevertheless provides useful information about the channel's inherent capability. For many channels, the PDI detector can gain 10 to 20 dB in signal power by coherently combining the various paths. The truly optimum detector may perform better (by incorporating optimum path weighting) but is overly complex to implement for a sounding signal. Thus, the PDI represents an attractive compromise and yields a rough estimate of the channel's inherent data transmission capability.

The 13-chip Barker code is desirable because it is the longest Barker code and offers the lowest side-lobe level. However, owing to its bias of 5, it does not offer as much processing gain against a line component as we would like, to establish the channel's ultimate capability. Because of its low bias of -1, the 11-chip Barker code is preferable in this regard.

Because of the large number of modulation formats and data rates that might be used for HF channels, it is difficult to predict the best data modulation from the sounding signal accurately. This problem is best addressed by using error detection coding on the source and destination addresses and estimating the signal-to-noise ratio of the ALE signal. Appendix E addresses some issues and approaches to the BER prediction problem.

Appendix D
RELATIVE SENSITIVITY OF BFSK AND BDPSK TO FREQUENCY SPREAD
T. Magill

Binary Frequency Shift Keying (BFSK) is considerably less sensitive to frequency spread than Binary Differential Phase Shift Keying (BDPSK). This fact can be readily demonstrated by considering a simple case in which the communication channel introduces an angular frequency-shift error, $\Delta\omega$. An AFC or APC loop could track out such a fixed error and neither BFSK or BDPSK would suffer any degradation. However, frequency spread, as opposed to shift, produces a simultaneous collection of similar shifts that are impossible to remove by AFC or APC loops. Consequently, this simple analysis provides a very useful demonstration of the much greater sensitivity of BDPSK to frequency spread.

For BDPSK, the detector output power is proportional to $\sin^2 \theta / \theta^2$, where $\theta = \Delta\omega \cdot T$ and T is the symbol duration. For binary FSK, it may be shown that output power in the desired filter is proportional to $2(1 - \cos \theta) / \theta^2$ where θ has the same meaning as for BDPSK.

Table D-1 presents these loss functions for BDPSK or BFSK. Note how much more quickly BDPSK degrades with frequency error. Table D-2

Table D-1. Power Loss (dB) Versus Frequency Offset for BDPSK and BFSK.

$\theta = \Delta\omega \cdot T$	BDPSK	BFSK
$\pi/4$	0.9	0.2
$\pi/2$	3.9	0.9
$(3/4)\pi$	10.4	2.1
π	∞	3.9

Table D-2. Relative Power Requirements (dB) for a Given Bit Error Rate for BDPSK and BFSK as a Function of Frequency Offset Error.

$\Theta = \Delta\omega \cdot T$	BDPSK	BFSK
$\pi/4$	0.9	3.2
$\pi/2$	3.9	3.9
$(3/4)\pi$	10.4	5.1
π	∞	6.9

presents the same results but includes the fact that BFSK requires 3 dB more power than BDPSK.

The most common multitone signaling formats use QDPSK rather than BDPSK. Because QDPSK is much more sensitive to phase errors than BDPSK, QDPSK will be more sensitive to frequency spread than BDPSK.

Appendix E
BER MEASUREMENT
T. Magill

As noted in Appendix C, it is difficult to predict the data modem BER from the ALE signal BER. It is also difficult to measure the ALE signal BER accurately, and this appendix deals with this more limited problem.

Specifically, the difficulty is that, on the basis of a very short measurement, we wish to measure the BER in the range of one part in a thousand to perhaps one part in a million. Clearly, it is necessary to observe at least one million bits to measure BER in the latter range. It is often observed that one million bits is insufficient because a single additional error will double the observed BER. Although this is true, it is also true that we are more commonly interested in estimating the E_b/N_0 so that this value may be used to predict performance. For the typical coherent BPSK, ROC doubling the BER at 10^{-6} corresponds to only 0.25 dB change in E_b/N_0 . Thus, the situation is not as bad as it appears. Nevertheless, the envisioned ALE calling sequence will be far short of that required for accurately estimating the BER.

There are three solutions to this problem. The first involves modifying the conventional ALE protocol by adding a second BER measurement phase. A list of those channels with a measured BER of zero will be more accurately tested for BER in the second phase.

The second approach is to estimate the signal-to-noise ratio. This may be done by measuring the signal and noise levels just before the polarity detector (Figure C-7) at the bit decision sampling interval. The noise level will be measured at the same location but at a time when the channel was not occupied by the ALE sounding signal.

The third approach is also to measure the chip error rate because the signal-to-noise ratio for a chip detection is a factor of 13 lower than for a bit decision. The chip error rate (CER) may be measured within the matched filter (equivalent to setting one tap at unity and all the others at zero) and phase-comparison-detecting chips separated by 1-bit (13-chips) duration. The resulting chip sequence appearing at the output of the IQ summation device in Figure C-7 will consist of a sequence of positive-phase chips with errors being negative-phase chips. The signal levels of each detected chip can be used to estimate SNR.

Because we want to measure BER and CER simultaneously, two sets of detectors are required in concept. However, in practice, it is likely that this circuitry will be implemented on a digital signal processor. If the processor had sufficient speed, both chip- and bit phase-comparison detection functions could be performed on the same processor. Both functions operate on the same input data and perform essentially the same operations and, therefore, increase the likelihood that a single processor will suffice.

DISTRIBUTION LIST

DEPARTMENT OF DEFENSE

Command & Control Sys Organization

ATTN: G500, R. Crawford
ATTN: G510, G. Jones
ATTN: G510, P. Bird

Defense Communications Agency

ATTN: Code 230
ATTN: J300 for Yen-Sun Fu

Defense Communications Engineer Center

ATTN: Code R123, Tech Lib
ATTN: Code R410, N. Jones

Defense Intelligence Agency

ATTN: DB, A. Wise
ATTN: DB-4C
ATTN: DC-7B
ATTN: DIR
ATTN: DT-1B
ATTN: RTS-2B

Defense Nuclear Agency

ATTN: NATF
ATTN: NAWF
ATTN: RAAE, P. Lunn
ATTN: RAEF
ATTN: STNA
3 cys ATTN: RAAE
4 cys ATTN: STTI-CA

Defense Technical Information Center

12 cys ATTN: DD

Deputy Under Secy of Defense, Cmd, Contl, Comm & Intell

ATTN: DADSD(I)
ATTN: Dir of Intelligence Sys

Field Command, DNA, Det 2

Lawrence Livermore National Lab
ATTN: FC-1

Field Command, Defense Nuclear Agency

ATTN: FCPR
ATTN: FCTT, W. Summa
ATTN: FCTXE

Joint Chiefs of Staff

ATTN: C3S
ATTN: C3S Evaluation Office, HD00

Joint Data Systems Support Center

ATTN: C-312, R. Mason

Joint Strat Tgt Planning Staff

ATTN: JLK, DNA Rep
ATTN: JLKS
ATTN: JPPFD
ATTN: JPSS
ATTN: JPTM

National Security Agency

ATTN: B-43, C. Goedeke

Under Secy of Defense for Rsch & Engrg

ATTN: Strat & Space Sys (US)

DEPARTMENT OF THE ARMY

Asst Chief of Staff for Automation & Comm

ATTN: DAMO-C4, P. Kenny

Deputy Chief of Staff for Ops & Plans

ATTN: DAMO-RQC, C2 Div

Harry Diamond Laboratories

ATTN: DELHD-NW-P
ATTN: DELHD-NW-R, R. Williams, 22000

US Army Comm-Elec Engrg Instal Agency

ATTN: CC-CE-TP, W. Nair

US Army Communications R&D Command

ATTN: DRDCO-COM-RY, W. Kesselman

US Army Information Systems Command

ATTN: CC-OPS-W
ATTN: CC-OPS-WR, H. Wilson

US Army Material Command

ATTN: DRCLDC, J. Bender

US Army Nuclear & Chemical Agency

ATTN: Library

US Army TRADOC Sys Analysis Actvty

ATTN: ATAA-PL
ATTN: ATAA-TCC, F. Payan, Jr
ATTN: ATAA-TDC

DEPARTMENT OF THE NAVY

Joint Cruise Missiles Project Ofc, PM-23

ATTN: JCMG-707

Naval Air Systems Command

ATTN: PMA 271

Naval Intelligence Support Center

ATTN: NISC-50

Naval Research Laboratory

ATTN: Code 4108, P. Rodriguez
ATTN: Code 4187
ATTN: Code 4700
ATTN: Code 4720, J. Davis
ATTN: Code 4780
ATTN: Code 6700
ATTN: Code 7500, B. Wald
ATTN: Code 7950, J. Goodman

Naval Telecommunications Command

ATTN: Code 341

Office of the Deputy Chief of Naval Ops

ATTN: NOP 654, Strat Eval & Anal Br
ATTN: NOP 941D
ATTN: NOP 981N

Office of Naval Research

ATTN: Code 412, W. Condell

Strategic Systems Programs, PM-1

ATTN: NSP-2141
ATTN: NSP-2722
ATTN: NSP-43, Tech Lib

DEPARTMENT OF THE NAVY (Continued)

Space & Naval Warfare Systems Cmd
ATTN: Code 3101, T. Hughes
ATTN: Code 501A
ATTN: PDE-110-X1, B. Kruger
ATTN: PDE-110-11021, G. Brunhart
ATTN: PME 106-4, S. Kearney
ATTN: PME 117-20
ATTN: PME-106, F. Diederich

Theater Nuclear Warfare Program Office
ATTN: PMS-423, D. Smith

DEPARTMENT OF THE AIR FORCE

Air Force Wright Aeronautical Lab/AAAD
ATTN: A. Johnson
ATTN: W. Hunt

Air Logistics Command
ATTN: OO-ALC/MM

Air University Library
ATTN: AUL-LSE

Asst Chief of Staff, Studies & Analysis
ATTN: AF/SASC, C. Rightmeyer

Ballistic Missile Office/DAA
ATTN: ENSN
ATTN: ENSN, W. Wilson
ATTN: SYC, D. Kwan

Deputy Chief of Staff, Rsch, Dev, & Acq
ATTN: AF/RDQI
ATTN: AFRDS, Space Sys & C3 Dir

Electronic Systems Division
ATTN: SCS-1E
ATTN: SCS-2, G. Vinkels

Foreign Technology Division
ATTN: NIIS Library
ATTN: TQTD, B. Ballard

Rome Air Development Center
ATTN: OCS, V. Coyne
ATTN: OCSA, R. Schneible
ATTN: TSLD

Rome Air Development Center
ATTN: EEP, J. Rasmussen
ATTN: EEPS, P. Kossey

Strategic Air Command
ATTN: NRI/STINFO
ATTN: SAC/SIZ
ATTN: XPFC
ATTN: XPFS
ATTN: XPQ

OTHER GOVERNMENT AGENCIES

US Dept of State, Bureau of Politico Military Affairs
ATTN: PM/STM

Central Intelligence Agency
ATTN: OSWR/SSD, K. Feuerpfetl

Institute for Telecommunications Sciences
ATTN: A. Jean
ATTN: W. Utlaut

DEPARTMENT OF DEFENSE CONTRACTORS

Autometric, Inc
ATTN: C. Lucas

BDM Corp
ATTN: L. Jacobs
ATTN: T. Neighbors

Boeing Co
ATTN: G. Hall

Boeing Co
ATTN: MS 8K-85, Dr. S. Tashiro

BR Communications
ATTN: J. McLaughlin

University of California at San Diego
ATTN: H. Booker

Charles Stark Draper Lab, Inc
ATTN: A. Tetewski
ATTN: D. Cox
ATTN: J. Gilmore

Computer Sciences Corp
ATTN: F. Eisenbarth

EOS Technologies, Inc
ATTN: B. Gabbard
ATTN: W. Lelevier

GTE Government Systems Corp
ATTN: R. Steinoff

Honeywell, Inc
ATTN: G. Terry, Avionics Dept

IBM Corp
ATTN: H. Ulander

Institute for Defense Analyses
ATTN: E. Bauer
ATTN: H. Wolfhard
ATTN: J. Aein

Kaman Tempo
ATTN: B. Gambill
ATTN: DASIAC

Kaman Tempo
ATTN: DASIAC

M/A Com Linkabit Inc
ATTN: A. Viterbi
ATTN: H. van Trees
ATTN: I. Jacobs

Maxim Technologies, Inc
ATTN: J. Marshall
ATTN: R. Morganstern

Meteor Communications Corp
ATTN: R. Leader

Mission Research Corp
ATTN: D. Knepp
ATTN: G. McCartor
ATTN: R. Dana
ATTN: S. Gutsche
ATTN: Tech Library

DEPARTMENT OF DEFENSE CONTRACTORS (Continued)

SRI International

ATTN: A. Burns
ATTN: C. Rino
ATTN: D. Nielson
ATTN: G. Price
ATTN: G. Smith
ATTN: J. Petriceks
ATTN: M. Baron
ATTN: R. Leadabrand
ATTN: R. Livingston
ATTN: R. Tsunoda
ATTN: W. Chesnut
ATTN: W. Jaye
2 cys ATTN: N. Chang
2 cys ATTN: T. Magill
2 cys ATTN: J. Ames

DEPARTMENT OF DEFENSE CONTRACTORS (Continued)

Mitre Corp

ATTN: M. Horrocks
ATTN: W. Foster
ATTN: W. Hall

Pacifica Technology

ATTN: E. Giller

Stewart Radiance Laboratory

ATTN: R. Huppi